REGULATION OF TRANSFERRIN RECEPTOR 2 STABILITY AND TRAFFICKING IN HEPATOMA CELLS

by

Martha Browning Johnson

A DISSERTATION

Presented to the

Department of Biochemistry and Molecular Biology and the

Oregon Health & Science University School of Medicine

in partial fulfillment of

the requirements for the degree of

Doctor of Philosophy

September 2006

School of Medicine

Oregon Health & Science University

CERTIFICATE OF APPROVAL

This is to certify that the Ph.D. dissertation of

Martha Browning Johnson

has been approved.

[redacted]

Advisor [redacted]

Member and Chair [redacted]

Member [redacted]

[redacted]

Member

[redacted]

Member

TABLE OF CONTENTS

List of Figures

List of Tables

Abbreviations

AP	adaptor protein
β2m	beta-2-microglobulin
BMP	bone morphogenic protein
CAT	chloramphenicol acetyl transferase
C/EBP	CCAAT enhancer binding protein
Cp	ceruloplasmin
CME	clathrin-mediated endocytosis
DFO	desferrioxamine
DcytB	duodenal cytochrome B
DMT1	divalent metal transporter 1
EEA1	early endosome antigen 1
EGF	epidermal growth factor
EGFR	epidermal growth factor receptor
EPO	erythropoietin
FAC	ferric ammonium citrate
FACS	fluorescence activated cell sorting
FeNTA	iron nitrilotriacetic acid
Fe_2Tf	diferric transferrin
Fpn1	ferroportin1
Ft	ferritin
Hamp	hepcidin antimicrobial peptide gene name
HBS	HEPES buffered saline
HBSS	Hank's balanced salt solution
HEPES	N-2-hydroxyethylpiperazine-N'-2-ethanesulfonic acid
Hepc	hepcidin
Heph	hephaestin
HFE	the hemochromatosis protein, mutation of which causes HFE1
HFE#	OMIM disease classification for hereditary hemochromatosis
Hfe2	hemojuvelin gene name
HH	hereditary hemochromatosis

Hjv	hemojuvelin
hpx	hypotransferrinemic mouse
IL-1	interleukin-1
IL-6	interleukin-6
IRE	iron responsive element
IRP	iron regulatory protein
LAMP-1	lysosome-associated membrane protein 1
LEAP	liver-expressed antimicrobial peptide
LPS	lipopolysaccharide
mAb	monoclonal antibody
MEL	murine erythroleukemia
MEM	mininmal essential media
MHC	major histocompatibility complex
OMIM	Online Mendelian Inheritance in Man database
PBS	phosphate buffered saline
PCR	polymerase chain reaction
qRT-PCR	quantitative real-time polymerase chain reaction
RBC	red blood cell
RGM	repulsive guidance molecule
SDS-PAGE	sodium dodecyl sulfate-polyacrylamide gel electrophoresis
siRNA	small interfering ribonucleic acid
Tf	transferrin
TfR1	transferrin receptor 1
TfR2	transferrin receptor 2
Trfr2	transferrin receptor 2 mouse gene name
TTP	TfR trafficking protein
USF2	upstream stimulatory factor 2
UTR	untranslated region
WT	wild-type
YXXØ	tyrosine(Y)-based endocytic motif X represents any amino acid; Ø represents a bulky hydrophobic residue

Acknowledgements

In order to arrive at what you do not know
You must go by a way which is the way of ignorance.
In order to possess what you do not possess
You must go by the way of dispossession.
In order to arrive at what you are not
You must go through the way in which you are not.
And what you do no not know is the only thing you know
And what you own is what you do not own
And where you are is where you are not.
-T.S. Eliot, *Four Quartets*

Ω Caroline Enns, my advisor, has guided this project and my progression through graduate school. She possesses a depth and breadth of knowledge in the techniques and literature of both cell biology and iron biology that has been invaluable and is most impressive. Her dedication to science is something to aspire to.

Ω Members of the Enns lab, past and present, have provided encouragement and advice throughout the past years. I would like to thank especially Frank Green, Nicholas Murchison, and Todd Vogt for the work they contributed to this project; and An-Sheng Zhang for sharing his knowledge and showing an amused interest in my life.

Ω The members of my Thesis Advisory Committee - Drs. Svetlana Lutsenko, David Farrens, Jan Christian, and David Koeller - never wavered in their support. This project has benefitted from their scientific insights, and I have greatly enjoyed and valued our exchange of ideas over the years.

Ω The laboratories of Drs. Linda Musil, Svetlana Lutsenko, Gail Clinton, Philip Copenhaver, Melissa Wong, and Richard Magun at OHSU generously shared reagents and equipment.

Ω Drs. Richard Brennan and Maria Schumacher infused my post-seminar happy hours with food, drink, company, and conversation. I am grateful for all, especially the latter.

Ω Paige Davies was unstinting in her assistance with techniques, as well as a wonderful companion, both at the bench and at meetings.

Ω Former teachers and mentors - Cheryl Christianson, Charles Lovett and John Thoman, Roger Simon - gave me my first glimpses into biology, research, and grant writing, respectively. I still draw on their teachings and their belief in me.

Ω Steve Mansoor, my sole surviving classmate within the biochemistry department, has set a high standard since our first term, while enlivening classes, journal clubs, even the written qualifying exam with equal parts humor and zeal.

Ω Margie Borra, Ezhil Subbian, Martha Sommer, Minsun Hong, and Lara Shamieh, students in the biochemistry class ahead of me, adopted me without hesitation. I will always be grateful for their support, especially throughout the qualifying exam process, and remember their friendship. I have missed them and their companionship around the sushi table in the time between their departures and my own.

Ω Tatyana Shaw became a close friend when we were technicians in collaborating labs and has remained so, despite the often irreconcilable demands of graduate school and

medical school on our time and attention. Her efforts to maintain an expansive view of what life should hold have helped me to do the same.

Ω Cortny (Huddleston) Williams has been a friend and colleague throughout our years in graduate school. I am indebted to her for the time she spent imparting her knowledge of flow cytometry. I am deeply grateful to her for the companionship she has provided.

Courtny, Jen, Terri, Uma,

Stephen,

Dad, Mom, Anne, Adrienne, Brian:

Namaste.

And the end of all our exploring
Will be to arrive where we started
And know the place for the first time.
-T.S. Eliot, *Four Quartets*

Abstract

Transferrin receptor 2 is mutated in a rare form of the iron overload disorder, hereditary hemochromatosis. As its name suggests, transferrin receptor 2 (TfR2) is also a homolog of transferrin receptor 1 (TfR1), the protein that delivers iron to cells through receptor-mediated endocytosis of its ligand, diferric transferrin (Fe_2Tf). Consequently, TfR2 is a protein of interest to two fields: iron homeostasis and protein trafficking. Ultimately, the trafficking of TfR2 is likely to prove integral to its function in iron homeostasis. This is the case for TfR1. Whereas the role of TfR1 in iron homestasis is defined and its trafficking detailed, the function of TfR2 is unknown and its trafficking unstudied. The work described in this dissertation, therefore, investigates the function and trafficking of TfR2.

Because it is expressed principally in hepatocytes, studies of TfR2 were conducted using two human hepatoma cell lines, HepG2 and Hep3B. The expression of TfR2 in hepatocytes is significant because hepatocytes synthesize and secrete the small peptide hormone, hepcidin. Hepcidin downregulates the iron exporter ferroportin, thereby reducing the amount of iron entering the body and lowering systemic iron level. Modulation of hepcidin expression in hepatocytes, therefore, maintains iron homeostasis. Mechanisms exist to regulate hepcidin expression in accordance with systemic iron level. These mechanisms are not understood. TfR2, however, is an essential component because its mutation results in misregulation of hepcidin and, consequently, iron overload. Given that the concentration of Fe_2Tf in the serum reflects systemic iron level, TfR2 may, by responding to changes in the concentration of its

ligand, enable the hepatocyte to sense systemic iron level. The following results support this hypothesis.

TfR2, endogenously expressed by HepG2 cells and stably transfected in Hep3B cells, is regulated by Fe_2Tf. Addition of exogenous Fe_2Tf to the culture medium of cells, at concentrations found in human serum, increases the half-life of TfR2. Fe_2Tf also changes the intracellular distribution of TfR2, increasing its localization to recycling endosomes and decreasing its localization to late endosomes. Thus, Fe_2Tf stabilizes TfR2 by redirecting its trafficking from a degradative pathway to a recycling pathway. Fe_2Tf does not stabilize TfR2/G679A, a mutant unable to bind Fe_2Tf. This indicates that TfR2 is stabilized by interaction with its ligand and provides the first known example of receptor stabilization by a soluble ligand. A second mutant, TfR2/Y23A, does not efficiently internalize from the cell surface and is extremely stable in the presence or absence of Fe_2Tf, thereby implicating the tyrosine-based motif YQRV in the intracellular domain of TfR2 as an endocytic motif required for internalization and for proper regulation by Fe_2Tf.

The regulation of TfR2 by Fe_2Tf provides a mechanism by which hepatocytes might sense systemic iron level. A change in TfR2 number or localization might modulate a signal, relayed by ligand delivery, protein interaction, or a signaling cascade, that regulates the expression of hepcidin in accordance with systemic iron level.

Chapter I

Introduction

adapted and updated from:

Johnson, M.B., Enns, C.A., and Zhang, A.S. (2006)

Iron in Mammals: Pathophysiological Mechanisms of

Overload and Deficiency in Relation to Disease.

Topics in Current Genetics 14: 155-191.

Iron Homeostasis

Overview of iron transport and homeostais

Iron enters the body principally through enterocyte cells in the duodenum of the intestine (Figure 1). The iron absorbed by these cells may be in two forms, heme and non-heme. The mechanism by which heme iron enters the body is not established. For non-heme iron, duodenal cytochrome b (DcytB) or another ferrireductase, on the apical membrane of the enterocyte facing the intestinal lumen, first reduces Fe^{3+} from food to the more soluble Fe^{2+} (McKie et al., 2001). The divalent metal ion transporter (DMT1) then transports Fe^{2+} across the apical surface of the intestinal cell (Fleming et al., 1997; Gunshin et al., 1997). Once inside, either iron remains within the cell, stored in ferritin and unabsorbed by the body, until it is lost when, after several days, the cell dies (Kaplan, 2002); or iron crosses to the basolateral side where ferroportin1 (Fpn1) then transports Fe^{2+} out of the cell (Abboud and Haile, 2000; Donovan et al., 2000; McKie et al., 2000). After iron exits the enterocyte, a multicopper ferroxidase on the cell surface, hephaestin (Vulpe et al., 1999), or its soluble homolog in the circulation, ceruloplasmin (Cp) (Mukhopadhyay et al., 1998; Harris et al., 1999), re-oxidizes iron to the Fe^{3+} form. The serum protein transferrin (Tf) binds Fe^{3+} and transports it to cells throughout the body.

In most tissues iron enters cells by receptor-mediated endocytosis. Iron bound to transferrin (Fe_2Tf) binds to transferrin receptor 1 (TfR1) on the surface of cells. Endocytosis delivers the Fe_2Tf-TfR1 complex to the early endosome where the acidified environment promotes the release of iron, which is reduced to Fe^{2+} by an undetermined mechanism. The TfR1-Tf complex then recycles to the cell surface and dissociates at the neutral pH, releasing Tf into the circulation. On the endosomal membrane, a ferrous

transporter transports iron into the cytosol (Fleming et al., 1998), where it is incorporated into newly synthesized proteins or stored in ferritin (Ft) (Kaplan, 2002).

Differentiating erythrocytes in the bone marrow utilize the majority of iron in the body for heme biosynthesis. Macrophages phagocytose senescent erythrocytes, degrade their heme, and return the iron to the circulation where it is bound by Tf (Fletcher and Halliday, 2002). Efficient recycling of 20-30 mg of iron per day reduces the dietary iron requirement to 1-2 mg, a fraction of the 3-5 g found in healthy adult humans (reviewed in Andrews, 1999; Townsend and Drakesmith, 2002). To maintain a supply of iron available for erythropoiesis, hepatocytes store iron in Ft that can be released when needed (Figure 2) (Fletcher and Halliday, 2002; Pietrangelo, 2002).

The body monitors and regulates iron at the cellular and systemic levels. At the cellular level, iron regulatory proteins (IRP) bind stem-loop structures called iron responsive elements (IRE) found in the untranslated regions (UTR) of the transcripts encoding several iron related genes (Figure 3). Binding of the IRP either blocks translation of the transcript or protects the transcript from degradation, depending on the location of the IRE. The binding of IRPs to IREs when intracellular iron levels are low increases TfR1 and decreases Ft levels, thereby facilitating iron uptake and minimizing iron storage. The inhibition of IRP binding by high intracellular iron levels decreases TfR1 and increases Ft levels, thereby limiting iron uptake and increasing storage. At the systemic level, the body maintains iron at appropriate levels by controlling the absorption of dietary iron (Figure 4). When iron levels are high, hepatocytes secrete higher amounts of a small, soluble peptide called hepcidin that decreases the amount of iron absorbed into the body from the intestine. Conversely,

when iron levels are low, hepatocytes suppress hepcidin synthesis, promoting iron absorption.

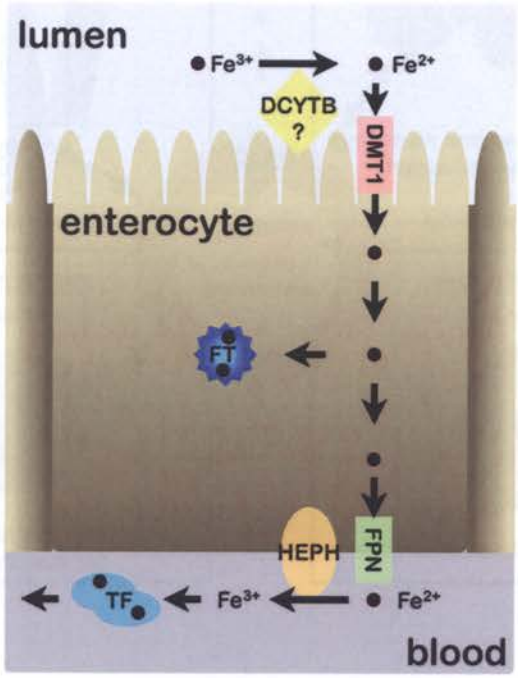

Figure 1. Absorption of non-heme iron across the enterocyte. On the apical surface of enterocytes facing the lumen of the intestine, non-heme iron from the diet is reduced to Fe^{2+} by DcytB or another ferrireductase and transported into the cell by divalent metal-ion transporter 1 (DMT1). Iron may be stored within the cell bound to ferritin (Ft) or transported across the basolateral surface of the cell by ferroportin (Fpn) into the blood, where iron is oxidized to Fe^{3+} by hephaestin (Heph), bound by transferrin (Tf), and circulated throughout the body. (adapted from: Philpott, 2002)

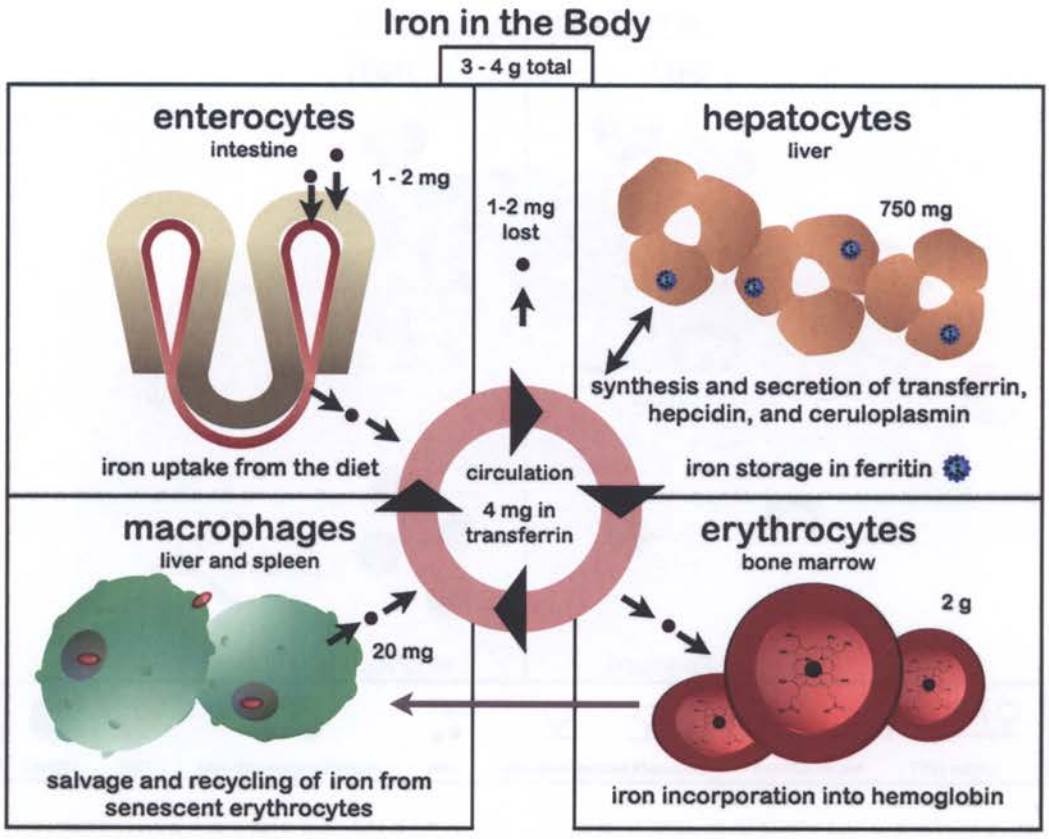

Figure 2. Iron in the body. The healthy human body maintains a total iron level of 3-5 g by absorbing iron from the diet and recycling iron from red blood cells. Enterocytes in the duodenum of the intestine absorb 1-2 mg of iron from the diet per day to replace iron that is lost in sloughed cells. Cells throughout the body utilize and store iron, but developing erythrocytes incorporate the majority of the body's iron into heme to facilitate oxygen transport, while hepatocytes in the liver serve as the principal repositories of iron. The iron within heme is recycled to the circulation by macrophages that phagocytose senescent erythrocytes. (adapted from: Andrews, 1999; Fletcher and Halliday, 2002)

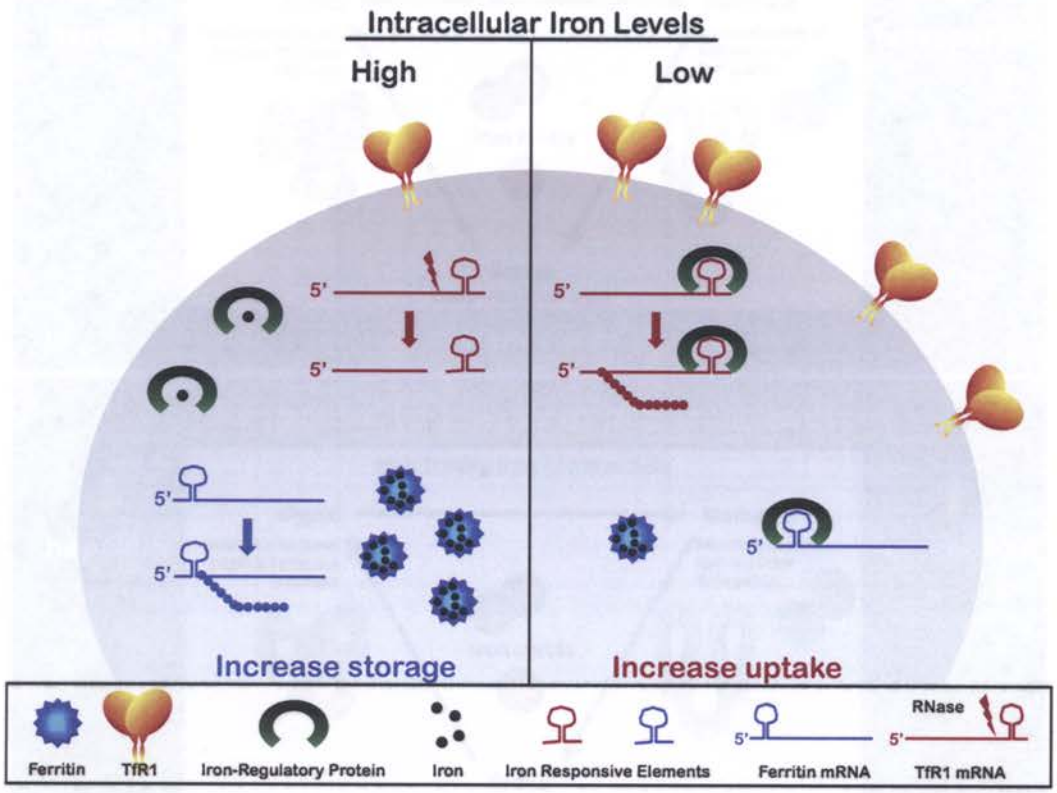

Figure 3. Cellular iron homeostasis. Cells regulate iron uptake and storage through post-transcriptional control of transferrin receptor 1 (TfR1) and ferritin (Ft). The 3' untranslated region (UTR) of TfR1 mRNA and the 5' UTR of Ft mRNA contain stem-loop structures called iron-responsive elements (IRE). When intracellular iron levels are high, iron regulatory proteins (IRPs) are unable to bind IREs. Unbound TfR1 transcript is degraded, whereas unbound Ft transcript is translated into protein, thus reducing iron uptake and increasing the capacity for iron storage. Conversely, when intracellular iron levels are low, IRPs bind IREs. Binding of IRPs to IREs protects TfR1 transcript from degradation and blocks translation of Ft transcript, thereby increasing iron uptake and decreasing the capacity for iron storage. (adapted from: Enns, 2001)

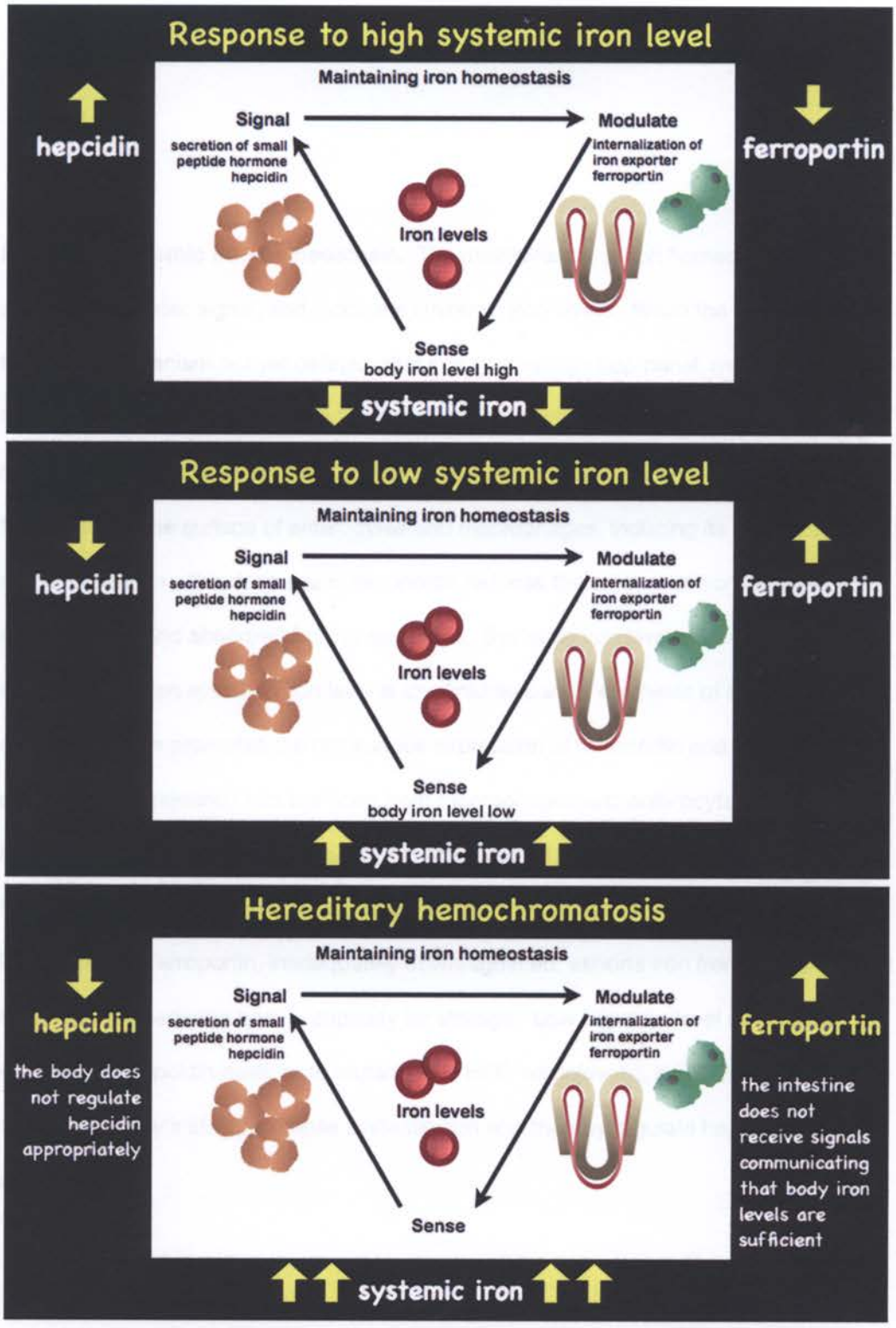

Figure 4. Systemic iron homeostasis.

Figure 4. Systemic iron homeostasis. The maintenance of iron homeostasis requires a system to sense, signal, and modulate systemic iron levels. When the body senses, though a mechanism not yet defined, that iron level is high (top panel, moving clockwise from bottom), hepatocytes in the liver increase the synthesis of the small peptide hormone hepcidin. Secreted into the circulation, hepcidin binds to the iron exporter ferroportin on the surface of enterocytes and macrophages, inducing its internalization and degradation. The decrease in ferroportin reduces the amount of iron recycled from macrophages and absorbed from enterocytes. Systemic iron level subsequently decreases. When systemic iron level is low (middle panel), synthesis of hepcidin decreases. This promotes the cell surface expression of ferroportin and increases the amount of iron released into the body from macrophages and enterocytes. Systemic iron level subsequently increases. In hereditary hemochromatosis (bottom panel), hepcidin level is inappropriately low and fails to correlate with body iron status. Consequently, ferroportin, inadequately downregulated, exports iron from enterocytes at a rate that exceeds the body's capacity for storage. Low hepcidin level may be due to mutations in hepcidin itself, or to mutations in HFE, hemojuvelin, or TfR2. The latter may disrupt the body's ability to sense systemic iron and thereby regulate hepcidin appropriately.

Hereditary hemochromatosis

When mutations disrupt the function of proteins that transport, monitor, regulate, and metabolize iron, diseases of iron overload or deficiency result. The most common iron overload disease is hereditary hemochromatosis. Mutations in five molecules, HFE, hemojuvelin, hepcidin, transferrin receptor 2, and ferroportin1, cause hereditary hemochromatosis. The five types of hemochromatosis comprise diseases with three distinct phenotypes.

Hereditary hemochromatosis type 1 (HFE1) and type 3 (HFE3), caused by mutations in *HFE* on chromososme 6p21.3 (Feder et al., 1996) and *TFR2* on chromosome 7q22 (Camaschella et al., 2000), respectively, are autosomal recessive disorders. Individuals with HFE1 or HFE3 absorb excess dietary iron. Iron slowly accumulates throughout life, depositing foremost in hepatocytes within the liver, then in other parenchymal tissues of the heart, pancreas, and thymus. Iron does not accumulate in macrophages of the liver or spleen until later stages of the disease. Serum transferrin saturation and serum ferritin levels increase and serve as diagnostic indicators. If iron levels are not reduced by frequent phlebotomy, liver cirrhosis, hepatoma, heart abnormalities, diabetes, and arthritis develop, generally beginning in the fourth decade of life. HFE1 accounts for ~80% of hereditary hemochromatosis cases (Feder et al., 1996). HFE3 is much rarer.

Hereditary hemochromatosis type 2A (HFE2A) and type 2B (HFE2B), also referred to as juvenile hemochromatosis (JH), are autosomal recessive disorders caused by mutations in genes encoding hemojuvelin (*Hfe2*) on chromosome 1q21 (Papanikolaou et al., 2004) or hepcidin (*HAMP*) on chromosome 19q13s (Krause et al., 2000; Park et al., 2001; Pigeon et al., 2001; Roetto et al., 2003), respectively. The

pathology of HFE2 is similar to that of HFE1 and HFE3, but individuals with HFE2 accumulate higher levels of iron earlier in life, generally within the first two decades. Serum transferrin saturation and serum ferritin levels are elevated. Iron accumulates in parenchymal tissues, notably the heart and liver. If not treated, death results from heart failure.

Hereditary hemochromatosis type 4 (HFE4), in contrast to the other forms of HH, is an autosomal dominant disorder. HFE4 arises from mutations in the gene *SLC40A1* (for solute carrier family 40 member 1) on chromosome 2q32 (Abboud and Haile, 2000; Montosi et al., 2001; Njajou et al., 2001) encoding the iron transporter ferroportin1 (Fpn1; (Donovan et al., 2000)). The pathology of HFE4 is often distinct from that of the other forms of hereditary hemachromatosis. Iron accumulates predominantly within macrophages of the liver and spleen. Serum ferritin levels consistently increase, while serum transferrin saturation remains normal. However, in a subset of cases, correlating with particular mutations in Fpn1, iron accumulates in hepatocytes and serum transferrin saturation increases, as in HFE1, 2, and 3.

Fpn1, hepcidin, Hjv, HFE, and TfR2 are central players in a homeostatic loop that maintains systemic iron at an appropriate level. Of the five molecules that cause hereditary hemochromatosis, the functions of two, hepcidin and ferroportin, are known. The functions of the other three proteins, HFE, TfR2, and Hjv, are unknown, but they are essential for hepcidin's regulation.

Regulation of iron export: Fpn1 and hepcidin

Ferroportin1 Fpn1 (also called Ireg1, MTP1) is a 571 amino acid protein of 63 kDa in humans (Abboud and Haile, 2000; Donovan et al., 2000; McKie et al., 2000).

Human, mouse, and rat orthologues are 90% similar and bear some homology to other metal transporters, including DMT1. Topology prediction programs indicate Fpn1 has nine, ten, or twelve transmembrane domains (Abboud and Haile, 2000; Donovan et al., 2000; McKie et al., 2000; Devalia et al., 2002). Fpn1 protein is present in hepatocytes, in macrophages within the liver, spleen and bone marrow, in the tubular cells and glomerulus of the kidney, in heart-muscle, and at the basolateral surface of enterocytes in the duodenum (Abboud and Haile, 2000; Donovan et al., 2000; Yang et al., 2002).

Fpn1 functions as an iron exporter (McKie et al., 2000). For iron homeostasis, its activity and regulation in enterocytes and macrophages is of particular importance. At the basolateral surface of enterocytes in the intestine, Fpn1 exports into the circulation approximately 1 mg of iron per day that has been absorbed from the diet. On macrophages, Fpn1 exports 20-30 mg of iron per day that has been recycled from erythrocytes.

Fpn1 mutants are autosomal dominant. They fall into two categories, whose phenotypes account for the two distinct pathologies of HFE4 described above (De Domenico et al., 2005; Schimanski et al., 2005). Mutants in the first category do not traffic to the cell surface and, thus, cannot export iron or lower intracellular iron levels. Their pathology, accumulation of iron in macrophages, could be the result of haploinsufficiency or dominant negative effects. In the former scenario, because macrophages export a greater amount of iron than enterocytes, an autosomal dominant mutation that disrupts half of the ferroportin activity severely affects macrophages, but not enterocytes. Haploinsufficiency permits normal iron export from enterocytes but limits iron export from macrophages, causing them to accumulate iron (Montosi et al., 2001). In the second scenario, dimerization of Fpn1 molecules allows Fpn1 mutants to

function in a dominant negative fashion and limit cell suface expression of wild-type Fpn1 (De Domenico et al., 2005). Loss of functional transporter limits iron export from macrophages, in particular, and enterocytes, increasing iron levels in those cells, but reducing iron levels in the body. Serum transferrin saturation does not increase. Insufficient iron for erythropoiesis subsequently stimulates intestinal iron absorption. Hepatocytes eventually accumulate iron due to increased intestinal absorption and decreased hepatic export (Fleming and Sly, 2001). Fpn1 mutants in the second category localize to the cell surface, export iron, and lower intracellular iron levels. They cannot, however, be downregulated (De Domenico et al., 2005; Drakesmith et al., 2005). Their pathology, consistently, is similar to hereditary hemochromatoses caused by mutations in HFE and TfR2, which are characterized by excess absorption of dietary iron. In the absence of regulation, enterocytes and macrophages continuously export iron, thereby increasing iron levels in the body. Serum transferrin saturation increases. Parenchymal cells, particularly hepatocytes, accumulate iron, whereas macrophages and enterocytes are spared.

The export activity of Fpn1 is controlled by the small, circulating peptide hormone, hepcidin. Hepcidin regulates the localization and level of Fpn1 protein (Nemeth et al., 2004a; Knutson et al., 2005) by inducing the endocytosis and degradation of the transporter (Nemeth et al., 2004a). Consitutively active Fpn1 mutants interact with hepcidin but fail to internalize, indicating that sequences required to mediate trafficking are disrupted in these mutants.

Hepcidin Hepcidin (also LEAP-1 for liver-expressed antimicrobial peptide) is a peptide hormone found in serum and urine (Krause et al., 2000; Park et al., 2001). The *HAMP* gene encodes an 84 amino acid prepropeptide. Cleavage of a signal

sequence generates a 60 amino acid propeptide that is differentially proteolysed to generate a mature peptide of 20, 22, or 25 amino acids (Krause et al., 2000; Park et al., 2001; Pigeon et al., 2001). The three hepcidin peptides differ in their N-termini, but all include eight cysteine residues, whose disulfide bonding stabilizes an amphipathic β-sheet that curls to form a form a convex hydrophobic surface and a concave basic surface (Hunter et al., 2002).

The liver is the primary site of hepcidin synthesis and secretion (Krause et al., 2000). Hepcidin peptide localizes to the basolateral membrane of hepatocytes located in the periportal zones of the liver from where it is presumably secreted into the serum (Kulaksiz et al., 2004). Hepc25, Hepc20 and prohepcidin are present in the serum, the latter at concentrations of 5 – 15 nM in healthy individuals (Kulaksiz et al., 2004). Secreted from hepatocytes, hepcidin circulates in the serum to act in an endocrine fashion to reduce iron export from enterocytes in the intestine and macrophages in the spleen. Hepcidin expression has also been detected in splenic, peritoneal, and alveolar macrophages (Liu et al., 2005; Nguyen et al., 2006), which suggests that hepcidin may also act in a paracrine fashion to exert more immediate control over iron export from these cells. This response might be particularly important in inflammatory conditions to reduce the iron available to pathogens. Adult heart, brain, spinal cord, and kidney express lower levels of hepcidin mRNA than the liver (Park et al., 2001; Pigeon et al., 2001; Courselaud et al., 2002; Nicolas et al., 2002a; Kulaksiz et al., 2005). In the kidney hepcidin localizes to epithelial cells in the tubules of the cortex, medulla, and papilla (Kulaksiz et al., 2005). Within cells, hepcidin appears apical or intracellular, suggesting it is released into urine within the renal lumen. Hepcidin in urine from healthy individuals comprises predominantly Hepc20 and Hepc25 in concentrations from 4 – 12

nM (Park et al., 2001). Hepc25 is the bioactive form that mediates iron homeostasis (Park et al., 2001; Nemeth et al., 2006)

Hepcidin is essential for mediating changes in iron absorption, recycling, and storage in normal and pathological conditions. Mice lacking hepcidin have iron overload (Nicolas et al., 2001), whereas mice overexpressing hepcidin are severely anemic (Nicolas et al., 2002a). Aberrations of iron homeostasis in numerous diseases derives from misregulation of hepcidin. Mice and humans homozygous for mutations in HFE or TfR2 fail to upregulate hepcidin appropriately and thus develop iron overload (Ahmad et al., 2002; Kawabata et al., 2005), as do individuals with juvenile hemochromatosis who are homozygous for mutations in Hjv (Papanikolaou et al., 2004). Individuals with chronic inflammation continuously upregulate hepcidin and thus develop anemia (Nemeth et al., 2004b).

Since regulation of hepcidin is a central means by which to modulate iron, and numerous normal and pathological conditions require modulation of iron, it is not surprising that hepcidin expression responds to a variety of stimuli. Hypoxia reduces expression of hepcidin (Nicolas et al., 2002b), presumably leading to an increase in iron to support erythropoiesis and oxygen transport. Hypoxia may downregulate hepcidin directly, through the transcription factor HIF-1, or indirectly through erythropoietin (EPO), which is induced by HIF-1 during hypoxia (Wang and Semenza, 1993). Mice injected with EPO downregulate hepcidin (Nicolas et al., 2002c). Inflammation increases hepcidin expression (Nicolas et al., 2002b), reducing the iron available to pathogens. A switch from a standard diet to a high iron diet induces hepatic hepcidin expression in mice (Pigeon et al., 2001). Conversely, a switch from a high iron diet to a low iron diet reduces hepcidin expression (Frazer et al., 2002). Hepcidin expression

also decreases in mice with genetic anemia due to mutations in hephaestin (sla mouse), DMT1 (mk mouse), or transferrin (*hpx* mouse) (Weinstein et al., 2002) or experimental anemia induced by phenylhydrazine (PHZ) injection (Nicolas et al., 2002b). Similarly, in humans hepcidin increases within 24 hours after iron ingestion (Nemeth et al., 2004b). Thus, iron itself alters hepcidin expression in order to maintain iron levels that are non-toxic, but adequate to support biological functions.

When iron levels rise, hepcidin transcript levels rise. Changes in hepcidin levels probably reflect changes in transcription, though changes in transcript stability could also contribute. The mechanisms regulating hepcidin transcription are unknown. Evidence suggest that the nuclear transcription factor CCAAT/enhancer-binding protein (C/EBPα) may be involved. C/EBPα controls the expression of numerous genes whose protein products regulate metabolic processes in the liver. The hepcidin promoter region in humans and mice contains binding sites for C/EBPs, as well as for hepatocyte nuclear factor 4 (HNF4) and signal transducers and activators of transcription (STAT). C/EBPα induces strong expression from the human hepcidin promoter, while C/EBPβ induces weakly, and HNF4 attenuates. In mice with liver specific knockout of C/EBPα, expression of hepcidin is reduced. Consistent with this misregulation of hepcidin, C/EBPα knockout mice have iron overload in the liver. Developmental expression of C/EBPα correlates with that of hepcidin, appearing late in fetal development, peaking near birth, decreasing, then re-accumulating at adulthood. C/EBPα is lower in hepatoma cells than in adult hepatocytes, again correlating with the pattern of hepcidin expression. In mice fed a high iron diet C/EBPα protein increases (Courselaud et al., 2002). Thus, C/EBPα might contribute to hepcidin regulation by iron.

Hepcidin, secreted into the circulation by hepatocytes in the liver when body iron level rises, maintains iron homeostasis by inducing the internalization and degradation of Fpn1, thereby reducing iron export from enterocytes and macrophages. When body iron level lowers, hepcidin secretion decreases. This promotes Fpn1-mediated iron export. These latter processes in the homeostatic loop that maintains appropriate iron level are the best understood (Figure 4). The mechanistic details of earlier processes that monitor body iron level and regulate hepcidin accordingly have not been fully explicated, however. Individuals and mice with hemochromatosis due to mutation or knockout of Hjv, HFE, or TfR2 do not regulate hepcidin appropriately, thus indicating that these proteins are necessary for hepcidin regulation.

Regulation of hepcidin: Hjv, HFE, and TfR2

Hemojuvelin Hemojuvelin (Hjv, also HFE2, RGMc) is a member of the repulsive guidance molecule (RGM) family, whose other members have roles in the developing nervous system and muscle (Monnier et al., 2002; Niederkofler et al., 2004; Samad et al., 2004). Five alternatively spliced Hjv transcripts encode three different proteins of 426, 313, and 200 amino acids. All three proteins contain a putative C-terminal transmembrane domain. The occurrence of disease causing mutations within the N-terminal region suggests that the longest isoform is relevant to iron homeostasis. Consistent with this, northern blots detect transcript encoding the full-length isoform (Papanikolaou et al., 2004). The full-length isoform gives rise to a protein of ~50 kD, subsequently referred to as Hjv. Hjv undergoes autocatalytic cleavage to generate polypeptides of ~33 and ~14 kD, which remain associated through disulfide bonds (Lin et al., 2005; Zhang et al., 2005). The C-terminus of Hjv contains a putative GPI

attachment motif. When expressed in HEK293 cells, Hjv is processed to a GPI-linked protein (Zhang et al., 2005).

Hjv transcript is present at high levels in human fetal liver, adult liver, heart, skeletal muscle and esophagus; at lower levels in colon and pancreas (Papanikolaou et al., 2004; Rodriguez Martinez et al., 2004). Hjv transcript expression in the liver does not respond to iron or erythropoietin, but decreases after LPS injection (Krijt et al., 2004). Hjv is detectable as a 46 kD protein in human liver and as a 44 kD protein in human serum. The smaller size of the latter is consistent with cleavage of the membrane-anchored protein at the juxtamembrane region near the C-terminus . Thus, Hjv can be either cell-associated or soluble. Both forms are also detectable in cell culture systems (Lin et al., 2005).

The mechanism by which Hjv regulates hepcidin appears to involve both soluble and cell-associated forms. The finding that *Hfe2*$^{-/-}$ mice have low hepcidin levels suggests that Hjv positively regulates hepcidin expression (Huang et al., 2005). This is supported by results from cell culture experiments. Reduction of Hjv expression by siRNA decreases hepcidin expression in Hep3B cells (Lin et al., 2005), whereas transfection of Hjv into Hep3B cells increases hepcidin expression (Babitt et al., 2006). Soluble Hjv affects hepcidin expression differently, however. The addition of soluble Hjv to the medium of cultured hepatocytes results in a dose-dependent decrease in hepcidin transcript level. Treatment of HEK293 or Hep3B cells with iron reduces the release of soluble Hjv into the medium (Lin et al., 2005). These latter results indicate that soluble Hjv negatively regulates hepcidin expression in response to iron.

The role of Hjv in iron homeostasis may involve its interaction with neogenin, a cell signaling receptor that mediates the activity of other RGM family members

(Matsunaga and Chedotal, 2004; Rajagopalan et al., 2004). Neogenin is expressed in the liver (Vielmetter et al., 1994; Keeling et al., 1997; Meyerhardt et al., 1997), which also expresses Hjv, but not RGMa or RGMb (Oldekamp et al., 2004; Schmidtmer and Engelkamp, 2004). In HEK293 cells, Hjv interacts with neogenin to increase intracellular iron levels (Zhang et al., 2005). The most common disease-causing mutation in Hjv, G230V, eliminates the interaction and the effect on iron level. Regulation of the interaction between neogenin and Hjv could modulate a signaling pathway that regulates hepcidin.

Studies of knockout mice have elucidated the signaling pathway through which Hjv regulates hepcidin. Mice with liver-specific knockout of *Smad4* (*Smad4*$^{Co/Co}$*;Alb-Cre*) develop severe iron overload associated with a 100-fold reduction in hepcidin expression in the liver (Wang et al., 2005). Smad4 is the central mediator of bone morphogenic protein/transforming growth factor-β (BMP/TGF-β) signaling pathways. In complex with other Smads that have been phosphorylated by receptors activated by BMP/TGF-β binding, Smad4 translocates to the nucleus and regulates gene transcription. Whereas hepatocytes from wild-type mice induce *hepcidin* when treated with BMP4 or TGF-β1, *Smad4*$^{-/-}$ hepatocytes do not. Hepatocytes from *Smad4*$^{Co/Co}$*;Alb-Cre* increase *hepcidin* expression when transfected with Smad4. In these hepatocytes the hepcidin promoter associates with histone H3 methylated at lysine 4 (H3K4), a histone modification associated with transcriptional activation, in chromatin immunoprecipitation (ChIP) assays. Treatment of wild-type heptatocytes with BMP4 or TGF-β1 increases H3K4 methylation. The phenotype of the *Smad4*$^{Co/Co}$*;Alb-Cre* mouse, therefore, indicates that Smad4 activates hepcidin transcription in response to signaling through a BMP/TGF-β pathway. Subsequent studies showed that Hjv influences the

BMP/TGF-β/Smad4 pathway by acting as a BMP co-receptor (Babitt et al., 2006). Hjv interacts with BMP-2 and, to a lesser extent, with BMP-4. In the presence of BMP-2, Hjv also interacts with a BMP receptor. The expression of Hjv augments the induction of *hepcidin* in response to BMP-2. BMP-2 treatment increases *hepcidin* expression in hepatocytes from wild-type and *Hfe2*$^{-/-}$ mice, but the increase is significantly attenuated in the *Hfe2*$^{-/-}$ cells. Furthermore, levels of phosphorylated Smad1, Smad5, and Smad8, indicative of BMP signaling, are lower in livers from *Hfe2*$^{-/-}$ mice.

Taken together, the results suggest that signaling through a BMP pathway, independent of Hjv, maintains the hepcidin promoter in a transcriptionally active state (Wang et al., 2005) which is then responsive to signaling augmented by the interaction of Hjv with the BMP pathway (Babitt et al., 2006). This is supported by the fact that hepcidin is affected differently by inflammatory stimuli in *Smad4*$^{Co/Co}$*;Alb-Cre* and *Hfe2*$^{-/-}$ mice. *Hfe2*$^{-/-}$ mice, like wild-type mice, increase hepcidin expression in response to IL-6 (Niederkofler et al., 2005). Hjv, therefore is not needed for regulation of hepcidin in response to inflammatory stimuli. By contrast, *Smad4*$^{Co/Co}$*;Alb-Cre* mice are unable to upregulate hepcidin in response to IL-6 or iron.

Identification of the signaling pathway through which Hjv regulates hepcidin represents a major advance in the understanding of how Hjv contributes to iron homeostasis. Further explication is required, nonetheless. Links between systemic iron level, Hjv regulation, and BMP signaling have not been established. The mechanism by which the opposing effects of soluble and cell-associated Hjv integrate to regulate hepcidin remains to be demonstrated. Possibly, soluble and cell-associated Hjv compete for binding to BMPs. In response to changing iron level, an increase in Hjv shedding or expression could suppress or activate hepcidin, respectively.

Hepcidin induction in response to BMP signaling does not require either HFE or TFR2. *HFE*$^{-/-}$ and *TFR2*^{Y245X} mice increase *hepcidin* expression to a similar degree as wild-type mice when treated with BMP-2, -4, or -9 (Truksa et al., 2006). The experiments do not exclude the possibility that HFE and TfR2 may operate upstream of BMP binding, nor the possibility that they modulate the the Hjv/BMP pathway in a manner not detected. Alternatively, they may regulate hepcidin independently of Hjv. Mechanistic explanations for the contributions of HFE and TfR2 to iron homeostasis are lacking.

HFE HFE is a major histocompatability (MHC) class I-like molecule cloned and identified as the hemochromatosis protein in 1996 (Feder et al., 1996). The HFE gene encodes a protein of 343 amino acids with a signal sequence, immunoglobulin-like domain, transmembrane region, and short cytoplasmic tail. Like other MHC molecules, HFE has three external domains. The α-1 and α-2 domains form a peptide-binding pocket. The groove of the peptide-binding pocket is narrower in HFE than in other MHC molecules that function in antigen presentation, and consequently is unable to accommodate a peptide. Importantly, HFE also contains two disulfide bonds within the α-2 and α-3 domains that stabilize the α-3 domain in a conformation competent to heterodimerize with β2-microglobulin (β2m). The C282Y mutation in HFE that results in hemochromatosis eliminates a cysteine residue and a disulfide bond, consequently disrupting the structure of HFE, destabilizing its interaction with β2m, and impeding its transit to the cell surface (Feder et al., 1997).

The HFE transcript is present in most tissues, but most abundantly in the liver and intestine (Feder et al., 1996). In the intestine, crypt cells in the ileum express high levels of HFE protein on their basolateral membranes (Parkkila et al., 1997b). In the

liver, HFE mRNA and protein expression occurs predominantly in hepatocytes and to a lesser extent in Kupffer cells (Holmstrom et al., 2003; Zhang et al., 2004).

In addition to interacting with β_2m, HFE interacts with TfR1 in cells and tissues (Parkkila et al., 1997a; Feder et al., 1998). Soluble forms of the proteins bind each other with nanomolar affinity (Lebron et al., 1998). In transfected HeLa cells, HFE associates with TfR1 along the biosynthetic and endocytic pathways (Gross et al., 1998). The interaction decreases the binding of TfR1 to Fe_2Tf in vitro, consistent with the fact that the binding site for HFE on TfR1 overlaps the binding site for Fe_2Tf (Lebron et al., 1999; West et al., 2001). This data suggests that HFE might function normally to reduce iron uptake into cells by competing with Fe_2Tf for binding to TfR1. However, at physiological Fe_2Tf concentrations of ~3 μM, HFE is unlikely to affect receptor occupancy.

Numerous studies have addressed the effect of HFE and HFE/C282Y expression on intracellular iron levels and iron transport. The results vary depending on the cell system employed. Several studies suggest that HFE functions to reduce iron uptake (Roy et al., 1999; Salter-Cid et al., 1999; Drakesmith et al., 2002). Other studies suggest that HFE functions to increase intracellular iron levels (Montosi et al., 2000; Drakesmith et al., 2002; Davies and Enns, 2004). HFE affects Tf-mediated iron uptake, but also alters intracellular iron levels in a TfR1-independent manner (Zhang et al., 2003). Taken together, the studies suggest that HFE may influence iron homeostasis by more than one mechanism depending on the proteins expressed in a particular cell type. Notably, macrophages and HT-29 cells in which HFE raises iron levels express Fpn1, whereas HeLa and U937 cells in which HFE lowers iron uptake from Tf do not. Consistent with the idea that HFE may interact with TfR1 and the iron export machinery,

various mutations in HFE differentially affect its abilities to alter iron export and iron uptake from Tf (Drakesmith et al., 2002).

Though studies of HFE function have yielded ambiguous results, studies of knockout and mutant mice clearly indicate that HFE is upstream of hepcidin in a regulatory pathway that controls systemic iron level. When fed an iron rich diet, *Hfe*$^{-/-}$ and *Hfe*^{C282Y} mice differ from wild-type mice in their transcriptional regulation of hepcidin. Whereas wild-type mice upregulate hepcidin when fed an iron rich diet, *HFE*$^{-/-}$ and *Hfe*^{C282Y} mice downregulate hepcidin (Muckenthaler et al., 2003). This suggests that proper hepcidin regulation requires functional HFE. The phenotype of *Thep/Hfe*$^{-/-}$ mice strongly supports this. *Thep* mice overexpress hepcidin and, consequently, are anemic (Nicolas et al., 2002a). When bred to *Hfe*$^{-/-}$ mice, anemia persists. Despite the absence of functional HFE, iron overload does not develop because hepatocytes constitutively express hepcidin from the transgene (Nicolas et al., 2003).

Despite considerable effort devoted to the study of HFE in the years since its discovery, the mechanism by which HFE regulates hepcidin and controls systemic iron homeostasis remains elusive. One persisting question is how HFE relates to TfR2, the other protein that modulates hepcidin expression and whose mutation results in an iron overload phenotype identical to that caused by HFE mutation.

Transferrin receptor 2 The human *TFR2* gene was cloned in 1999 (Kawabata et al., 1999). The major transcript transcribed from *TFR2* gene encodes a 100 kD protein, TfR2-α or TfR2, a type II transmembrane protein that forms dimers stabilized by disulfide bonds (Kawabata et al., 1999). The second transcript encodes a truncated protein, TfR2-β, which lacks the intracellular and transmembrane domains at the N-

terminus. The mouse *Trfr2* gene on chromosome 5 gives rise to three alternative splice variants (Fleming et al., 2000; Kawabata et al., 2001a). The predominant transcript encodes a protein that is 89% identical to human TfR2 (Kawabata et al., 2001a).

TfR2 is a homolog of transferrin receptor 1 (TfR1), the ubiquitously expressed receptor that delivers iron to cells through receptor mediated-endocytosis of its ligand, Fe_2Tf. The extracellular domain of TfR2 shows 45% identity and 66% similarity in amino acid sequence to the extracellular domain of TfR1 and, consistent with this homology, binds Fe_2Tf in a pH-dependent manner (Kawabata et al., 1999). Crystal structures of TfR2 and TfR2-Fe_2Tf have not been reported to date. However, residues that mediate the interaction between TfR1 and Tf have been identified through extensive mutational analysis of the TfR1 ectodomain (West et al., 2001; Giannetti et al., 2003), and a comparison of the primary structures of TfR1 and TfR2 indicates that many of these amino acids are conserved in TfR2 (West et al., 2000). In TfR2, as in TfR1, an RGD sequence in the extracellular domain is critical for binding to Fe_2Tf (Dubljevic et al., 1999; Kawabata et al., 2004). Thus, some understanding of TfR2's interaction with Tf can be inferred, to an extent, from TfR1's interaction with Tf. The interaction of TfR1 with Fe_2Tf has been modeled by fitting the individual crystal structures of TfR1 (Lawrence et al., 1999), the N-lobe of Tf (MacGillivray et al., 1998), and the C-lobe of Tf (Hall et al., 2002) to electron density images of the Fe_2Tf-TfR1 complex acquired by cryo-electron microscropy (Cheng et al., 2004). The fitted images show that Tf binds to the lateral surface of TfR1, with one lobe interacting with a single TfR1 molecules on the side of the dimer interface and the other lobe inserting into the space between the ectodomain and the surface of the membrane (Figure 5). The images suggest that the latter lobe may interact with the stalk of TfR1.

Despite the structural homology of TfR1 and TfR2, there are differences in their interactions with Fe_2Tf that may have functional consequences. Both the full-length and a soluble form of TfR2 bind Fe_2Tf with an affinity of 27nM (Kawabata et al., 1999; West et al., 2000). The interaction is optimal at pH 7.6 – 7.2. Below pH 7.2, binding drops sharply. By contrast, both the full-length and a soluble form of TfR1 binds Fe_2Tf with an affinity of 1 nM (Tsunoo and Sussman, 1983; Enns et al., 1991; Richardson and Ponka, 1997; Lebron et al., 1999), approximately 30-fold higher than the affinity of TfR2 for Fe_2Tf, and does not release Fe_2Tf until the pH falls below 6.8 (Kawabata et al., 1999). The pH profile for the interaction of TfR1 with Tf allows apo Tf to remain bound to TfR1 within the acidic lumen of the endosome (Hopkins and Trowbridge, 1983), where iron is released, and recycle with TfR1 to the cell surface. The differences in the affinity and pH sensitivity of the interaction between TfR2 and Tf may have implications for the function of TfR2 in the cell. TfR2 may mediate internalization but not recycling of Tf. Expression of TfR2 but not TfR1 in HeLa cells increases the amount of Tf found in multi-vesicular bodies (MVB). Tf is present in MVBs in HepG2 cells that endogenously express TfR2 (Robb et al., 2004). Differences in the binding of TfR2 and TfR1 to Tf are further highlighted by the ability of TfR2, but not TfR1, to bind bovine Tf (Kawabata et al., 2004)

The cytoplasmic domain of TfR2 contains a YXXØ-type tyrosine-based motif, in which X is any amino acid and Ø is a bulky hydrophobic amino acid. TfR1 also contains such a motif, but otherwise the cytoplasmic domains of the two receptors show no similarity. In membrane receptors YXXØ motifs mediate interactions with adaptor protein (AP) complexes, which in turn stabilize membrane receptors in clathrin-coated pits for vesicular transport within the cell (Bonifacino and Traub, 2003). In

TfR1,the YXXØ motif is critical for internalization of the receptor (Collawn et al., 1990). In TfR2, the significance of the motif has not been demonstrated. The presence of a similar motif in the cytoplasmic domains of TfR1 and TfR2 suggests that the trafficking of TfR2 may share some features in common with the trafficking of TfR1, which has been extensively characterized. TfR1 undergoes constitutive clathrin-mediated endocytosis (CME) in a process that requires AP-2 and a cargo-specific adaptor protein, named TfR trafficking protein (TTP, Watts, 1985; Hinrichsen et al., 2003; Motley et al., 2003; Tosoni et al., 2005). After endocytosis, TfR1 reaches the early endosomal compartment, from which it may recycle to the cell surface directly or after first traversing the recycling endosomal compartment (Hopkins, 1983; Sheff et al., 1999; Sheff et al., 2002). On the other hand, the absence of any other homology between the cytoplasmic domains of TfR1 and TfR2 and the fact that the YXXØ-type motifs - YQRV in TfR2 and YTRF in TfR1 - are not identical hints that the trafficking of TfR2 may be differentially regulated.

Mechanisms that regulate the transcription of TfR2 or the stability of its mRNA have not been identified. Unlike TfR1, *TfR2* does not contain an iron response element (IRE) in its 3' untranslated region (UTR) and is not post-transcriptionally regulated by intracellular iron level (see Figure 3). Treatment with iron or an iron chelator does not alter TfR2 mRNA or protein levels in K562 cells (Kawabata et al., 2000) or MEL cells (Kawabata et al., 2001a). TfR2 transcript levels are the same in livers from mice fed standard, high-iron, and low-iron diets. Transcript levels are also the same in livers from wild-type and *Hfe*$^{-/-}$ mice (Fleming et al., 2000). Together, the results suggest that any iron-related regulation of TfR2 occurs at the protein level.

The expression pattern of TfR2 indicates that is it likely to function principally in hepatocytes of the liver. TfR2 mRNA is abundant in liver tissue, but is not detectable in the small intestine, kidney, brain, or heart (Kawabata et al., 1999). Expression of TfR2 transcript increases in the liver from embryonic and postnatal development to adulthood (Kawabata et al., 2001a). Within the liver, transcript level is high in hepatocytes and low in Kupffer cells and stellate cells (Fleming et al., 2000; Zhang et al., 2004). TfR2 protein has been detected in the liver (Fleming et al., 2002). In addition to the liver, TfR2 transcript has been detected in $CD34^+$ erythroid progenitor cells (Kawabata et al., 2001b; Calzolari et al., 2004). A role for TfR2 in erythroid cells is not clear, however. TfR2 is not required by erythroblasts to mediate Fe_2Tf-uptake and facilitate heme synthesis since TfR2 transcript level decreases as erythroid progenitor cells differentiate to erythroblasts. Moreover, it is unclear whether erythroid cells express TfR2 protein. One study reports reports immunohistochemical detection of TfR2 in erythroid cells from the bone marrow (Kawabata et al., 2001b), whereas a second does not detect TfR2 protein in $CD34^+$ cells or in immature and mature erythroblasts (Calzolari et al., 2004). The expression of TfR2 in cell lines is consistent with its expression in tissue. TfR2 transcript is present in HepG2 (human hepatoma), K562 (human erythroleukemia), MEL (murine erythroleukemia), and other erythroid cell lines (Kawabata et al., 1999; Kawabata et al., 2001a; Kawabata et al., 2001b). TfR2 protein is detectable in HepG2, K562, and HuH7 (human hepatoma) cells, but not in SK1-Hep and Hep3B (human hepatoma) cells (Vogt et al., 2003). The expression pattern of TfR2 contrasts the widespread distribution of TfR1. The limited tissue distribution of TfR2 perhaps accounts for its inability to compensate for TfR1 knockout in mice, which results in embryonic lethality due to severe anemia (Levy et al., 1999a).

The phenotype of *TfR1*$^{-/-}$ mice indicates that, though TfR2 is a homolog of TfR1 and binds Fe_2Tf, TfR2 does not function principally in iron delivery. Even in hepatocytes, TfR2 is not needed for iron uptake, since hepatocytes in the livers of *TfR2* knockout mice accumulate iron (Wallace et al., 2005).

The phenotype of mice with mutation of TfR2 indicates that TfR2 functions in iron homeostasis to regulate expression of hepcidin. The *Trfr2*^{Y245X} mouse is a model of hemochromatosis arising from mutation in TfR2 (Fleming et al., 2002). The Y245X nonsense mutation is orthologous to the Y250X mutation that occurs in individuals with HFE3. Mice homozygous for the mutation do not express membrane bound TfR2. Compared with wild-type mice, liver iron is four-fold higher and splenic iron is two-fold lower in mutant mice. Hematological parameters are unchanged, indicating that TfR2 is not necessary for development of the erythropoietic system. Relative to wild-type mice, *Trfr2*^{Y245X} mice express lower levels of hepcidin transcript. After iron dextran injection, *Trfr2*^{Y245X} mice do not induce hepcidin expression even though the iron levels in their livers are as high as the iron levels in the livers of wild-type mice that do upregulate hepcidin (Kawabata et al., 2005). Similarly, hepcidin levels in individuals with HFE3 are abnormally low (Nemeth et al., 2005). Thus, TfR2 contributes to hepcidin regulation.

TfR2 may modulate hepcidin expression through its interaction with other iron-related proteins. A recent study reports that HFE and TfR2 interact (Goswami and Andrews, 2006). A previous study, however, did not detect an interaction between the two proteins (West et al., 2000). The latter used surface plasmon resonance and immunoprecipitation approaches to assay for interaction between the ectodomains of TfR2 and HFE. The former study immunoprecipitated the two full-length proteins from cells stably transfected with tagged versions of HFE and TfR2. Resolution of the

discrepancy awaits further characterization. Interaction of TfR2 with other proteins has not yet been reported.

Studies of individuals and mice with mutation of TfR2 indicate clearly that TfR2 mediates iron homeostasis; precisely how, remains a mystery. TfR2 has not been shown to respond to iron, and no mechanisms for the regulation of TfR2 have been identified. TfR2 regulates hepcidin expression, but the mechanism by which it does so is unknown. TfR2 differs significantly from TfR1 in most respects, but one: the ability to bind Tf. This stands out as a starting point from which to study TfR2. Interaction with its ligand may play a significant role in the function and regulation of TfR2.

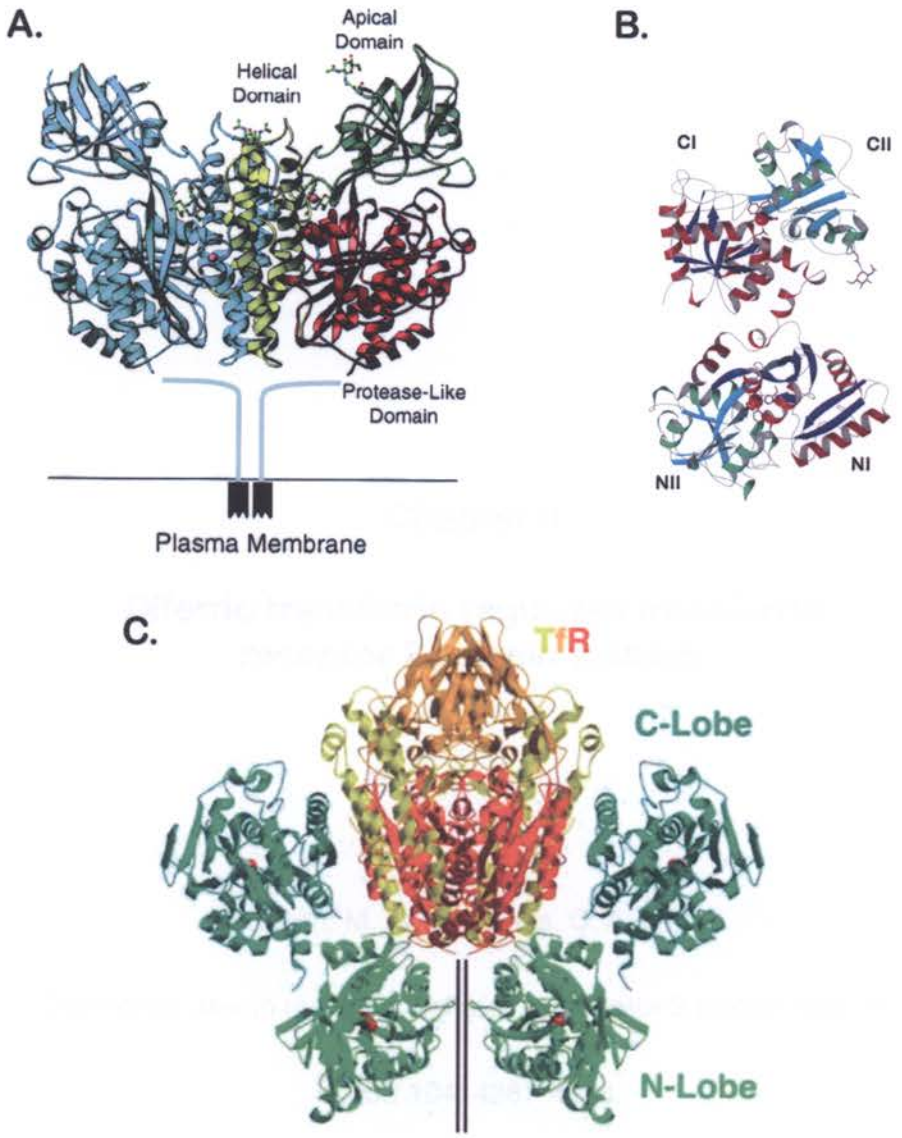

Figure 5. Structures of TfR1 and Tf. (A) Structure of the TfR1 dimer as solved by Lawrence et al. (1999). (B) Structure of porcine serum transferrin as solved by Hall et al. (2002) showing the bilobed structure and liganded iron atoms (red balls). (C) The Fe_2Tf-TfR1 complex, modeled by fitting the individual crystal structures of TfR1, the N-lobe of Tf, and the C-lobe of Tf to electron density images of the Fe_2Tf-TfR1 complex acquired by cryo-electron microscropy (Cheng et al., 2004). TfR1 is rotated 90° relative to A.

Chapter II

Diferric transferrin regulates transferrin receptor 2 protein stability

Johnson, M. B., and Enns, C. A. (2004).

Diferric transferrin regulates transferrin receptor 2 protein stability.

Blood 104: 4287-4293.

Abstract

Transferrin receptor 2 (TfR2) is a type-II transmembrane protein expressed in hepatocytes that binds iron-bound transferrin (Tf). Mutations in TfR2 cause one form of hereditary hemochromatosis, a disease in which excessive absorption of dietary iron can lead to liver cirrhosis, diabetes, arthritis, and heart failure. The function of TfR2 in iron homeostasis is unknown. We have studied the regulation of TfR2 in HepG2 cells. western blot analysis shows that TfR2 increases in a time- and dose-dependent manner after addition of diferric Tf (Fe_2Tf) to the culture medium. In cells exposed to Fe_2Tf, the amount of TfR2 returns to control levels within 8 hours after removal of Fe_2Tf from the medium. However, TfR2 does not increase when non-Tf bound iron (FeNTA) or apoTf is added to the medium. The response to Fe_2Tf appears to be hepatocyte specific. Real-time qRT-PCR analysis shows that TfR2 mRNA levels do not change in cells exposed to Fe_2Tf. Rather, the increase in TfR2 is due to an increase in the half-life of TfR2 protein in cells exposed to Fe_2Tf. Our results support a role for TfR2 in monitoring iron levels by sensing changes in the concentration of Fe_2Tf.

Introduction

The human body maintains iron homeostasis by regulating the amount of iron absorbed from the diet by the intestine. Iron must be sufficient to sustain fundamental biological processes, but should not exceed the storage capacity of cells because excess iron generates free radicals, resulting in oxidative damage. The serum protein transferrin (Tf) binds iron in the circulation and carries it to cells throughout the body. Erythrocytes use the majority of iron in the body for heme synthesis. Macrophages in

the liver and spleen phagocytose senescent erythrocytes and recycle iron to the circulation for reutilization. Hepatocytes store iron that can be released for use by erythrocytes and other cells when needed. Systemic iron homeostasis, therefore, requires the coordination of iron absorption, transport, storage, and utilization throughout the body (Fletcher and Halliday, 2002; Hentze et al., 2004).

Misregulation of iron homeostasis occurs in numerous diseases (Andrews, 2000a; Andrews, 2000b). The most common is the iron overload disorder hereditary hemochromatosis (HH). HH types I, 2A, 2B, and 3 are autosomal recessive diseases caused by mutations in HFE (Feder et al., 1996), hemojuvelin (Papanikolaou et al., 2004), hepcidin (Roetto et al., 2003), and transferrin receptor 2 (TfR2) (Camaschella et al., 2000), respectively. An autosomal dominant form of HH, type 4, is caused by mutations in the iron exporter, ferroportin 1 (Fpn1) (Donovan et al., 2002; Wallace et al., 2002). A resulting deficiency in iron export causes macrophages to retain iron that would normally recycle to the blood. This leads to accretion of iron in macrophages and reduced saturation of Tf (Pietrangelo, 2004). In HH types 1, 2, and 3, the intestine and macrophages fail to receive or interpret signals from the liver and erythrocytes communicating that body iron levels are sufficient. Consequent excess absorption of dietary iron by the intestine and release of iron from macrophages leads to an accumulation of iron in the liver and other parenchymal tissues, saturation of Tf, and elevated secretion into the serum of the cellular iron storage protein ferritin (Ft) (Bothwell et al., 1995; Fletcher and Halliday, 2002). In severe cases of HH, cirrhosis, cancer, heart abnormalities, arthritis, and diabetes ensue if the iron overload is not treated by regular phlebotomy.

The proteins implicated in HH are critical components of incompletely defined signaling pathways between the liver, erythrocytes, macrophages, and intestine that maintain iron homeostasis. An integrated understanding of the manner in which these and other proteins involved in iron transport coordinate to sense, respond to, and regulate iron remains elusive. Iron levels have been shown to modulate the synthesis and secretion by hepatocytes of the peptide hormone hepcidin, which in turn affects iron absorption by the intestine and iron export from macrophages, possibly by altering the activity of Fpn1 (Nicolas et al., 2001; Pigeon et al., 2001; Frazer et al., 2002; Nicolas et al., 2002a). The pathways connecting iron levels to hepcidin expression are not known, however. The concentration of diferric Tf (Fe_2Tf) in the blood may be an indicator of the level of iron in the body that signals to hepatocytes and regulates hepcidin (Taylor et al., 1988; Raja et al., 1999). A potential mediator of this process is the recently identified receptor for Tf, TfR2.

TfR2 is a type-II transmembrane protein and homolog of TfR1 (Kawabata et al., 1999; Fleming et al., 2000), the ubiquitously expressed receptor for Tf that delivers iron to cells (Richardson and Ponka, 1997). The two proteins are 45% identical and 66% similar in their extracellular domains. Like TfR1, TfR2 binds Fe_2Tf at neutral pH and apo Tf at acidic pH (Kawabata et al., 2000). Heterologous expression of TfR2 in Chinese hamster ovary (CHO) cells lacking transferrin receptors (TRVb cells) increases uptake of Tf-bound iron (Kawabata et al., 2000) and promotes cell growth under low iron conditions (Kawabata et al., 2000), indicating that TfR2 can function as a receptor for Tf. However, differences in the activity, regulation, and expression of TfR1 and TfR2, and in the pathophysiology of disorders caused by their deficiency, indicate that they have different roles in iron homeostasis. The affinity at pH 7.5 of TfR2 for Fe_2Tf, $K_d \sim 27$

nM, is approximately 25-fold lower than that of TfR1, K_d ~ 1 nM (Tsunoo and Sussman, 1983; Kawabata et al., 2000; West et al., 2000). Unlike TfR1, TfR2 does not appear to interact with HFE (West et al., 2000). TfR1 mRNA expression inversely correlates with intracellular iron levels (Mattia et al., 1984; Ward et al., 1984; Rao et al., 1985; Sciot et al., 1987; Lu et al., 1989) due to post-transcriptional regulation by iron-response elements (IRE) located in the 3' untranslated regions (UTR) of TfR1 transcripts (Owen and Kuhn, 1987; Casey et al., 1988; Mullner and Kuhn, 1988; Mullner et al., 1989). In contrast, TfR2 mRNA expression does not change in K562 erythroleukemia or murine erythroleukemia (MEL) cells treated with $Fe_2(NO_3)$ or the iron chelator desferrioxamine (DFO) (Kawabata et al., 2000; Kawabata et al., 2001a), nor in iron-deficient or iron-overloaded mice (Fleming et al., 2000), consistent with the absence of IREs in the 3' UTR of the TfR2 transcript (Kawabata et al., 1999; Fleming et al., 2000). Unlike TfR1, TfR2 has a limited tissue distribution, with prominent expression of protein in the liver (Kawabata et al., 1999; Fleming et al., 2000; Fleming et al., 2002; Vogt et al., 2003; Calzolari et al., 2004). Finally, TfR2 cannot compensate for loss of TfR1. Knock-out of TfR1 in mice results in embryonic lethality at day 12.5 (Levy et al., 1999a). Mutations in TfR2, on the other hand, result in HH type 3 (HH3) in both humans and mice (Camaschella et al., 2000; Fleming et al., 2002). In humans homozygous for the Y250X TfR2 mutation and mice transgenic for the orthologous Y245X mutation, the liver accumulates iron, despite an absence of membrane-bound TfR2 and a reduction in TfR1 (Fleming et al., 2002), suggesting that the uptake of Tf-bound iron for use by the hepatocytes is not the principal role of TfR2.

The fact that mutations in TfR2 cause HH indicates that TfR2 has an important but as yet unknown role in iron homeostasis. TfR2 may sense body iron levels by

sensing the level of Fe_2Tf in the serum. One prediction of this hypothesis is that TfR2 should respond to changes in the extracellular concentration of Fe_2Tf. To test this, we characterized the response of TfR2 to Tf in HepG2 cells, a human hepatocarcinoma cell line that endogenously expresses TfR2 and other iron-related proteins. We demonstrate an increase in TfR2 protein in response to elevated exogenous Fe_2Tf and show that this increase is a result of an increase in the half-life of TfR2.

Results

Response of TfR2 to diferric Tf in HepG2 cells

To determine if Tf alters TfR2 protein levels, we cultured HepG2 cells in medium with 25 μM (2 mg/mL) Fe_2Tf for 4 – 72 hours and examined levels of TfR2 and Tf by western blot. An increase in TfR2 was evident within 4 hours, maximal at 48 hours, and sustained for at least 72 hours (Figure 6A, upper panel). The increase in TfR2 paralleled an increase in Tf associated with the cells (Figure 6A, lower panel). Treatment with Tf did not increase the levels of Tf transcript (measured by real-time qRT-PCR) or the rate of Tf protein synthesis (measured by metabolic labeling with [S-35]-cysteine/ methionine, Appendix A), suggesting that this Tf was exogenous rather than endogenous. When Fe_2Tf was withdrawn after 24 hours, TfR2 returned to basal levels within 8 hours, subsequent to the return of Tf to basal levels within 2 hours (Figure 6B).

The dose response of TfR2 to Fe_2Tf was examined by adding 0 – 25 μM (0 – 2 mg/mL) Fe_2Tf to the medium for 24 hours. Western blot showed that TfR2 increased as the concentration of Fe_2Tf increased from approximately 0 – 12.5 μM (Figure 6C). In contrast, TfR1 decreased at the lowest concentration of Fe_2Tf assayed and remained at

this level as the concentration of Fe_2Tf increased (results not shown). We quantified the effect of Fe_2Tf on TfR2 by western blot detection with fluorescently-labeled secondary antibodies. The increase in TfR2 was half-maximal when the concentration of Fe_2Tf was ~2.5 μM (Figure 6C).

Since Fe_2Tf supplies cells with iron, we considered that the increase in TfR2 might be a response to elevated cellular iron levels. To address this, we added 100 μM FeNTA, a non-Tf bound iron source, to the medium of cells for 24 hours and examined protein levels by western blot. The levels of TfR1 and Ft, which are regulated by the IRE system in response to changes in intracellular iron, served as positive controls. As expected, Ft increased and TfR1 decreased in cells treated with FeNTA (Figure 6D). TfR2 levels, however, remained the same, indicating that TfR2 responds specifically to Fe_2Tf rather than to iron loading of cells. When cells were cultured in medium with 25 μM apoTf for 24 hours, TfR2 remained the same (Figure 6E). Since the interaction of apoTf with its receptors is weak at neutral pH, the results suggest that the response of TfR2 to Fe_2Tf requires interaction of Tf with TfR1 or TfR2 or the delivery of iron specifically by Fe_2Tf.

Response of TfR2 to Tf in other cell lines

The effect of Fe_2Tf on TfR2 in other cells lines was investigated (Figure 7). In TRVb2 cells (CHO cells lacking detectable expression of endogenous TfR1(McGraw et al., 1987) and stably transfected with TfR2) addition of Fe_2Tf to the medium had no effect on TfR2 protein level. Similarly, in K562 cells, an erythroleukemia cell line endogenously expressing TfR2, Fe_2Tf had no effect. However, in HuH7 cells, a human hepatoma cell line endogenously expressing TfR2, the addition of 25 μM Fe_2Tf to the

medium for 24 hours produced an increase in TfR2. These results suggest that regulation of TfR2 by Tf involves a hepatocyte-specific mechanism.

Effect of diferric Tf on TfR2 mRNA and protein stability

To determine if the increase in TfR2 was a consequence of an increase in TfR2 transcript, we measured TfR2 mRNA in control cells and in cells cultured in medium with 25 μM Fe_2Tf for 24 hours using real-time qRT-PCR. As a positive control for the effect of Fe_2Tf, TfR1 mRNA was also measured. Levels of TfR1 and TfR2 transcripts were quantified relative to GAPDH levels. Three independent experiments were conducted, and for each experiment samples were analyzed twice in triplicate. As expected, TfR1 mRNA decreased when cells were cultured with Fe_2Tf (Figure 8A). By contrast, TfR2 mRNA did not change, indicating that the increase in protein does not derive from an increase in TfR2 transcript.

The elevation in TfR2 could be a consequence of an increase in protein stability. To investigate this possibility, we measured the half-life of TfR2 protein in untreated and Fe_2Tf-treated cells. After culturing cells for 24 hours in 25 μM Fe_2Tf, 100 μg/mL cycloheximide was added to the medium for 0 – 4 hours to inhibit protein synthesis. Levels of TfR2 and TfR1 protein were quantitated by western blot (Figure 8B). TfR1 did not change detectably over the period assayed. As measured from three independent experiments, in untreated cells the half-life of TfR2 was 4 hours, and in Tf-treated cells the half-life of TfR2 increased to 14 hours.

Requirement for TfR1 in mediating the effect of diferric Tf on TfR2

HepG2 cells express both TfR1 and TfR2, thus regulation of TfR2 stability may involve the binding of Fe_2Tf to either or both of its receptors. To investigate whether interaction of TfR1 is required to mediate the effect of Fe_2Tf on TfR2, we utilized the 42/6 monoclonal antibody to TfR1, which has been previously shown to block binding of Fe_2Tf to TfR1 and to reduce TfR1 levels in a variety of cell lines (Trowbridge and Lopez, 1982; Taetle et al., 1986). The 42/6 antibody is isotype IgA. Dimerization between IgA molecules induces clustering of TfR1, which is consequently targeted to the lysosome for degradation. We first verified the specificity and activity of this antibody in HepG2 cells. Immunoprecipitation of lysates from HepG2 cells demonstrated interaction of 42/6 antibody with TfR1 but not with TfR2 (Figure 9A), indicating the 42/6 antibody interacts specifically with TfR1. Cells cultured in medium with 25 µg/mL 42/6 antibody for 28 hours show a marked reduction in TfR1 protein when compared to cells cultured in normal medium (Figure 9B, bottom panel, lanes 1-2) or medium containing 25 µg/mL non-specific IgA (data not shown). Treatment with 42/6 antibody for 4 hours was sufficient to produce this reduction in TfR1 (data not shown). Since Tf competes with 42/6 for binding to TfR1, 25 µM Fe_2Tf was added to the medium 4 hours after the addition of 42/6 antibody. TfR1 remained downregulated in the presence of Tf and 42/6 antibody (Figure 9B, bottom panel, lanes 3-4).

Having verified that the 42/6 antibody interacts specifically with TfR1 to downregulate TfR1 expression in HepG2 cells, we assessed the effect of this antibody on TfR2 regulation by Fe_2Tf. HepG2 cells were cultured with and without 25 µg/mL 42/6 antibody for 4 hours, then with and without 25 µM Fe_2Tf for 24 hours. In a parallel set of experiments, 100 µM FeNTA was added at the same time as antibody to control

for any possible effects of iron deprivation brought about by downregulation of TfR1. TfR1 and TfR2 protein levels were assessed simultaneously using two-color western blot detection with fluorescently-labeled secondary antibodies that specifically detect rabbit (anti-TfR2) and mouse (anti-TfR1) IgG (Figure 9B). The 42/6 antibody reduced TfR1 by 80 - 90% in all conditions tested, but had no effect on TfR2 in control cells. An increase in TfR2 induced by Fe_2Tf is evident in cells cultured with or without 42/6. However, in the absence of 42/6 antibody, Fe_2Tf caused a ~2.5-fold increase inTfR2, whereas in the presence of 42/6 antibody this increase abated to ~1.6-fold (Figure 9C). The difference was statistically significant, with $P = 0.02$ when evaluated by Student's one-tailed paired t-test. Supplementation of cells with iron did not alter either the ability of the 42/6 antibody to downregulate TfR1 or the response of the cells to Fe_2Tf. These results indicate that downregulation of TfR1 partially inhibits the increase in TfR2 by Tf.

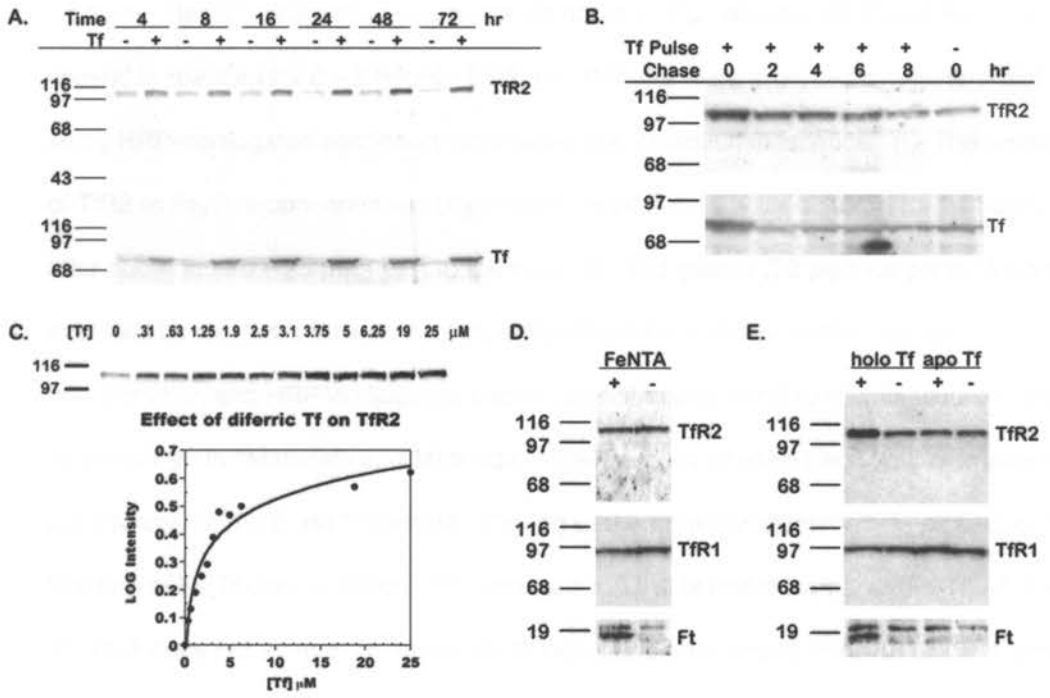

Figure 6. TfR2 increases after addition of diferric Tf to the medium of HepG2 cells.

Figure 6. TfR2 increases after addition of diferric Tf to the medium of HepG2 cells. (A) TfR2 increases in a time dependent manner. HepG2 cells were cultured for 4 – 72 hours after addition of 25 μM Fe_2Tf or HBS to the medium. Lysates (20 μg total protein) were transferred to nitrocellulose, probed for TfR2 and Tf, and visualized by chemiluminescence. The increase in TfR2 was paralleled by an increase in Tf associated with the cells. (B) TfR2 returns to basal levels after withdrawal of Tf from the medium. HepG2 cells were cultured for 24 hours in the presence of 25 μM Fe_2Tf then chased in medium for 0 – 8 hours. TfR2 and Tf levels were analyzed by western blot using HRP-conjugated secondary antibodies and chemiluminescence. (C) The response of TfR2 to Fe_2Tf is concentration dependent. HepG2 cells were cultured for 24 hours after addition of 0 – 25 μM Fe_2Tf to the medium, and lysates (20 μg total protein) were analyzed by western blot with fluorescently-labeled secondary antibodies for quantification and HRP-conjugated secondary antibodies for chemiluminescent imaging as described in "Materials and Methods." The intensity of each band was normalized to the intensity of the 0 μM Tf sample. The log of the normalized intensity is plotted as a function of Fe_2Tf concentration. The increase in TfR2 is half-maximal at [Fe_2Tf] ~2.5 μM. (D) TfR2 does not increase in response to non-transferrin bound iron. TfR2, TfR1, and Ft protein levels were assessed by western blots of lysates (20 μg total protein) from HepG2 cells cultured for 24 hours in the presence of 100 μM FeNTA (lane 1, +) or 4mM NTA (lane 2, -). Bands were detected by chemiluminescence. Ft heavy and light chains are visible as a doublet in the lower panel. (E) TfR2 does not increase in response to apoTf. HepG2 cells were incubated in medium containing 25 μM Fe_2Tf (lane 1, labeled holo Tf) or apoTf (lane 3) for 24 hours. Lysates (20 μg total protein) were analyzed by western blot for TfR2, TfR1, and Ft protein. Bands were detected by chemiluminescence.

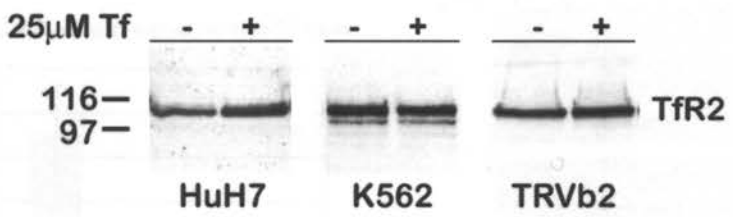

Figure 7. TfR2 increases in HuH7 cells, but not in K562 or TRVb2 cells. Cells were cultured for 24 hours after the addition of 25 μM Fe_2Tf to the medium. The level of TfR2 in lysates from HuH7 (50 μg), K562 (20 μg), and TRVb2 (10 μg) cells was determined by western blot with chemiluminescent detection. In cells endogenously expressing TfR2, treatment with Fe_2Tf increased TfR2 in HuH7 human hepatoma cells but not in K562 erythroleukemia cells. TRVb cells stably transfected with TfR2 (TRVb2) did not respond to Fe_2Tf.

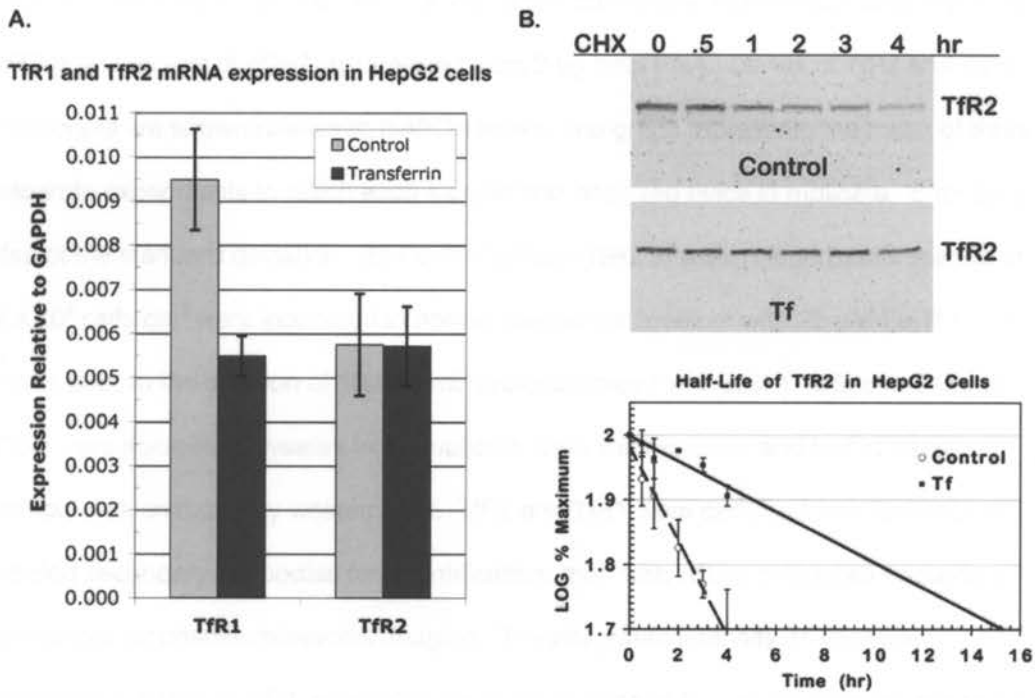

Figure 8. Regulation of TfR2 occurs at the protein level.

Figure 8. Regulation of TfR2 occurs at the protein level. (A) TfR2 transcript in HepG2 cells does not increase in response to Fe_2Tf. Total RNA was isolated from ~1 x 10^7 HepG2 cells 24 hours after addition of 25 µM Fe_2Tf or equal volume HBS to the medium. Expression of TfR2, TfR1, and GAPDH transcripts was measured by real-time qRT-PCR analysis of cDNA synthesized from 2 µg total RNA. Levels of TfR2 and TfR1 transcripts are shown relative to GAPDH levels. The graph represents the mean of three separate experiments in which each sample was analyzed twice in triplicate. Error bars depict the standard deviation. (B) Fe_2Tf stabilizes TfR2 protein. HepG2 cells seeded at 2 x 10^4 cells/cm^2 were incubated in normal medium or medium with 25 µM Fe_2Tf for 24 hours prior to the addition of 100 µg/mL cycloheximide for 4, 3, 2, 1, 0.5, and 0 hours. Cells were solubilized, lysates from duplicate wells were pooled, and half of each sample was analyzed by western blot. TfR2 and TfR1 were detected with fluorescently-labeled secondary antibodies for quantification, then with HRP-conjugated secondary antibodies for chemiluminescent imaging. The integrated intensity of TfR2 was normalized to that of TfR1, which did not change detectably over the time-course of the experiment. The normalized intensity was expressed as percentage of the normalized intensity at time 0, and the log of this value was plotted. Half-life was determined by linear regression analysis. The graph shows the mean of three experiments. Error bars indicate average deviation from the mean.

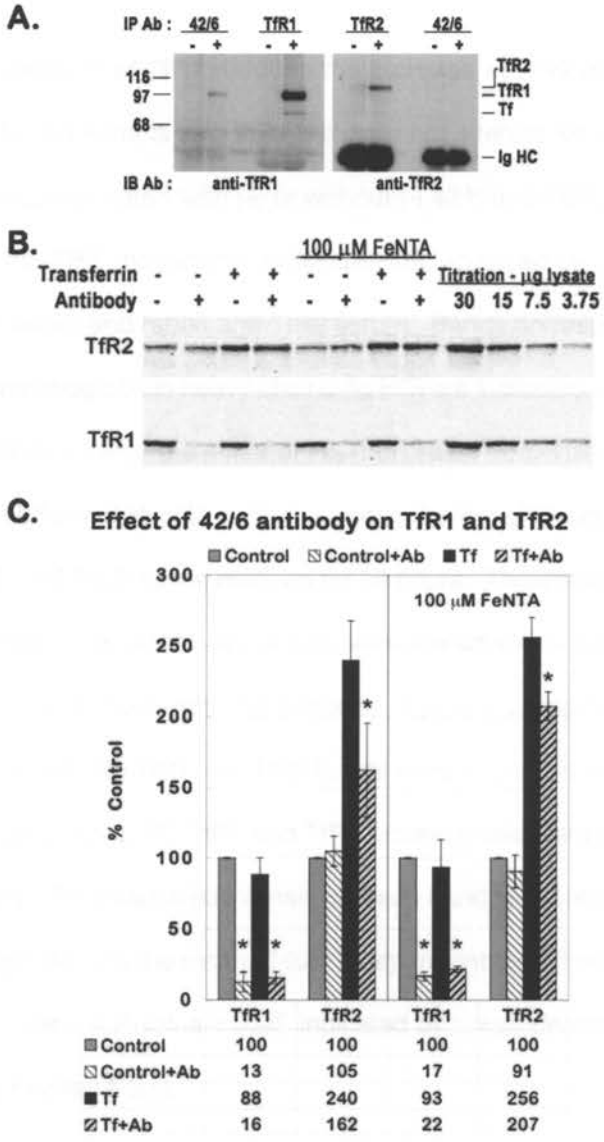

Figure 9. Downregulation of TfR1 reduces the increase in TfR2 protein.

Figure 9. Downregulation of TfR1 reduces the increase in TfR2 protein. (A) The 42/6 anti-TfR1 antibody interacts with TfR1 but does not interact with TfR2. HepG2 cell lysates were immunoprecipitated with (+) or without (-) 42/6 anti-TfR1, 3B82A1 anti-TfR1, or 9F81C11 anti-TfR2 monoclonal antibodies and analyzed by western blot with sheep anti-TfR1/Tf serum and rabbit anti-TfR2 serum. Bands corresponding to TfR2, TfR1, Tf, and the immunoglobulin heavy chains (Ig HC) are indicated. (B and C) Treatment with 42/6 diminishes the effect of Fe_2Tf on TfR2. Anti-TfR1 antibody 42/6 was added to the medium of HepG2 cells at a concentration of 25 µg/mL 4 hours prior to the addition of 25 µM Fe_2Tf to the medium for 24 hours. To control for possible effects of iron deprivation, a second set of cells was treated identically, but 100 µM FeNTA was added concomitant with 42/6 antibody. Lysates (20 µg total protein) were analyzed by western blot. (B) TfR1 and TfR2 bands were visualized with fluorescently-labeled secondary antibodies. (C) TfR1 and TfR2 protein levels were quantitated by fluorescent scanning. The integrated intensity of each band is expressed as percentage of control. The graph depicts the mean of four independent experiments average deviation from the mean. A P-value < 0.05, indicated by *, was determined by a Student's one-tailed paired t-test.

Discussion

Following its identification in 1999 (Kawabata et al., 1999), TfR2 was shown to bind Tf and mediate Fe uptake (Kawabata et al., 2000), functions that are consistent with its homology to the classical transferrin receptor, TfR1. Unlike TfR1, however, TfR2 expression did not respond to iron and, in a mouse model of HFE1 (*Hfe*$^{-/-}$), persisted when TfR1 expression was minimal despite iron overload (Fleming et al., 2000). The presence of TfR2 in hepatocytes offered a plausible explanation for the accumulation of iron that occurs in the livers of mice and people with HH1. The finding that mutation of TfR2 caused hemochromatosis with the same phenotype of iron overload in the liver was a surprise, therefore, and suggested that TfR2 might have a role in maintaining iron homeostasis (Camaschella et al., 2000; Fleming et al., 2002). We hypothesized that TfR2 might sense iron levels through its interaction with Tf. To test this, we examined the response of TfR2 to human Fe_2Tf in HepG2 human hepatoma cells. We found that TfR2 increased when the concentration of Fe_2Tf in the medium increased. We detected no change in TfR2 transcript, but measured a 3.5-fold elongation of TfR2 protein half-life when Fe_2Tf was added to the medium of cells. This does not preclude the possibility that Fe_2Tf might also affect the rate of TfR2 translation. Because the low level of TfR2 expression in HepG2 cells prohibits detection by metabolic labeling, future experiments will assay the effect of Tf on TfR2 translation using hepatoma cells stably transfected with the full-length TfR2 transcript.

TfR2 is sensitive to changes in Fe_2Tf concentration that would occur physiologically in response to normal fluctuations in iron. Human serum contains 30 – 60 μM Tf comprising apo (Tf), monoferric (FeTf), and diferric (Fe_2Tf) forms. Saturation of Tf is approximately 30% in nonpathological states, but may reach 100% during severe

iron overload. At 30% saturation, 10% of the total Tf is diferric (Huebers et al., 1984). Thus, concentrations of Fe_2Tf in healthy individuals range from approximately 3 – 6 μM. In our studies, TfR2 increased as Fe_2Tf increased from 0.3 – 13 μM, with half-maximal response at around 2.5 μM. By sensing changes in the concentration of Fe_2Tf, the body could monitor iron levels and modulate intestinal iron uptake to maintain Fe_2Tf within this range. This would likely involve regulation of hepcidin expression and secretion. Given that hepcidin expression occurs in the liver (Krause et al., 2000; Park et al., 2001; Pigeon et al., 2001), sensing of iron levels is likely to occur there. TfR2 binds Tf, is expressed at high levels in hepatocytes (Fleming et al., 2000), and thus, is a good candidate to signal serum Tf saturation to the hepatocyte.

Fe_2Tf regulates TfR2 stability through an undefined mechanism. This mechanism could involve the interaction of Tf with TfR2, with TfR1, or with both receptors. We knocked down TfR1 expression to investigate whether the regulation of TfR2 by Tf requires TfR1. The results were inconclusive. In cells expressing reduced levels of TfR1, TfR2 still increased in response to Tf, but not to the same extent as in cells expressing normal levels of TfR1. Downregulation of TfR1 by 80 – 90% reduced TfR2 by 36% in Tf-treated cells. Multiple mechanisms could account for this result. First, the interaction of Tf with TfR1 alone could regulate TfR2 through a signal transduction cascade. This would account for the disproportionate reductions in TfR2 and TfR1. Alternatively, total uptake of Tf may be the mediating factor. Upon addition of Fe_2Tf to the medium, an increase in the uptake of Tf would still occur when TfR1 is downregulated, leading to higher TfR2 levels that could partially offset the reduction in uptake by TfR1. Finally, Tf could regulate TfR2 directly. A small proportion of TfR2 immunoprecipitates with TfR1 in extracts from liver (Vogt et al., 2003), K562 cells (Vogt

et al., 2003), and HepG2 cells (our unpublished results). The 36% reduction of TfR2 in cells treated with 42/6 antibody and Fe_2Tf may be a consequence of this interaction and not due to an effect on regulation of TfR2 by Tf. Downregulation of TfR2 by the 42/6 antibody as a side effect of heterodimerization with TfR1 is undetectable in untreated cells but might become pronounced as TfR2 levels increase in cells treated with Tf. Additional future experiments are required to distinguish between these possibilities and to define the mechanism by which Tf regulates TfR2 stability. Our finding that Tf increases TfR2 in HepG2 and HuH7 hepatoma cell lines, but not in other non-hepatoma cell lines tested, suggests that the mechanism may involve proteins or compartments specific to hepatocytes.

Our finding that Fe_2Tf regulates the half-life of TfR2 predicts that TfR2 levels will be altered in diseases that affect the concentration of Fe_2Tf in the blood. In diseases in which saturation of serum Tf increases, such as HH and -thalassemia, TfR2 would be elevated. Conversely, TfR2 would be reduced in diseases in which serum Tf decreases, such as hypotransferrinemia. In a companion paper, Robb and Wessling-Resnick examine TfR2 levels in mouse models of HFE1 (*Hfe*$^{-/-}$, (Levy et al., 1999b)), β-thalassemia (*Hbb*$^{th-1}$, (Skow et al., 1983)), and hypotransferrinemia (*hpx*, (Bernstein, 1987)) and show that this does indeed occur. Relative to congenic controls, TfR2 levels are increased in *Hfe*$^{-/-}$ and *Hbb*$^{th-1}$ mice, but decreased in *hpx* mice.

The phenotypes of mice deficient in either TfR2 or Tf are consistent with a role for TfR2 in regulating iron homeostasis in the body by sensing Fe_2Tf. *Hpx* mice are deficient in serum Tf due to a mutation within the Tf gene that disrupts splicing. As a consequence there is a lack of Tf-bound iron, causing severe iron deficiency in erythrocytes, and an elevation in non-Tf bound iron, producing iron overload in other

cell types. *Hpx* mice express low levels of hepcidin despite iron loading in parenchymal tissues (Ahmad et al., 2002; Weinstein et al., 2002). Consistent with the low level of hepcidin, intestinal iron absorption is high in these mice. Interestingly, infusion of erythrocytes into *hpx* mice to remedy anemia does not reduce iron uptake, but transfusion of Tf does (Raja et al., 1999). This suggests that Tf contributes to the regulation of iron absorption (Ponka, 2002) and that the absence of Tf produces a discontinuity between iron levels and intestinal absorption. It is plausible that TfR2 senses the lack of Fe_2Tf in the serum and in turn regulates hepcidin. The decreased TfR2 and hepcidin, accurately reflecting levels of Fe_2Tf, but not of iron, may aberrantly signal that iron levels are low. This would account for the occurrence of iron overload in *hpx* mice and the effects of Tf transfusion. We would predict an increase in TfR2 and hepcidin following transfusion of *hpx* mice with Tf.

As with *hpx* mice, the phenotype of $Trfr2^{Y245X}$ mice is consistent with disruption of a signaling pathway that senses iron through Tf saturation and alters intestinal iron uptake. $Trfr2^{Y245X}$ mice have a mutation in TfR2 that is orthologous to one causing HH in humans. They develop hemochromatosis similar to $Hfe^{-/-}$ mice, with parenchymal iron loading, increased Tf saturation, and elevated serum ferritin (Fleming et al., 2002). Unlike in *hpx* mice, Tf is present, and the erythrocytes in $Trfr2^{Y245X}$ mice acquire sufficient iron. However, according to our hypothesis, in the absence of TfR2 hepatocytes would not be able to sense Tf or regulate hepcidin secretion appropriately.

Based on published studies of TfR2 and current understanding of the consequences of mutations in TfR2, Tf, and hepcidin we speculate that these proteins may be part of an iron sensing system whose disruption causes the body to respond as if iron levels are low. Under normal conditions, serum Tf saturation indicates iron levels

in the body. TfR2 mediates a signal in proportion to Tf saturation that regulates hepcidin expression and consequently iron uptake by the intestine. Low iron levels would reduce Tf saturation, attenuate this signal, lower hepcidin secretion, and increase intestinal iron uptake. Deficiency in TfR2 or Tf would disrupt this system. In people and mice with mutations in TfR2, the absence of functional TfR2 is akin to the attenuation of TfR2 signaling that occurs when iron levels are low.

If hepatocytes sense iron through this system, then treatment with Fe_2Tf should result in an increase in hepcidin expression in HepG2 cells. Contrary to this expectation, no significant increase in hepcidin mRNA was observed when HepG2 cells were incubated with 63 μM Fe_2Tf for 24 hours (Gehrke et al., 2003). In HepG2 cells, proteins intermediate between TfR2 and hepcidin might not be expressed at appropriate levels. HFE, for example, is expressed at high levels in hepatocytes of the rat liver, but at low levels in HepG2 cells (our unpublished results). Hemojuvelin, the newly identified gene that causes juvenile hemochromatosis, is expressed in the liver but is not detectable in HepG2 cells (our unpublished results and (Papanikolaou et al., 2004; Zhang et al., 2004)). Alternatively, the iron sensing system that regulates hepcidin expression may require factors provided by other cell types in the liver or by the serum.

The in vitro K_d measurements of the affinity of Tf for TfR2 (Kawabata et al., 2000; West et al., 2000) complicate the hypothesis that TfR2 senses Fe_2Tf. These measurements predict that TfR2 would be saturated by the concentrations of Tf found in the blood. We have shown, though, that TfR2 protein responds to changes in Fe_2Tf at physiologic concentrations. Understanding how the stability of TfR2 is regulated by concentrations of Fe_2Tf that are 100-fold higher than the K_d of TfR2 and determining

whether the response of TfR2 to Fe_2Tf affects other iron-related proteins will contribute significant details to our understanding of iron homeostasis.

Materials & Methods

Cell lines

HepG2 and K562 cells were obtained from American Type Culture Collection (ATCC, Manassas, VA). HuH7 cells were provided by Dr. Philip Aisen (Einstein University, Bronx, NY). The TRVb2 cell line was generated by transfecting TRVb cells with a pcDNA 3 vector encoding TfR2 as described previously (Vogt et al., 2003).

Antibodies

Generation of monoclonal antibodies 3B82A1 and 9F81C11 against the ectodomains of human TfR1 and TfR2, respectively, was described previously (Vogt et al., 2003). Rabbit anti-hTfR2 serum was produced at Pocono Rabbit Farm and Laboratory, Inc. (Canadensis, PA) by immunizing rabbits with purified human TfR2 ectodomain. The specificity of the rabbit anti-TfR2 serum was verified in the manner described for the 9F81C11 mouse anti-TfR2 antibody (Vogt et al., 2003). Mouse anti-TfR1 42/6 antibody was obtained from Dr. Ian Trowbridge (Salk Institute, La Jolla, CA). Goat anti-Tf serum was described previously (Enns and Sussman, 1981). Sheep anti-ferritin antibody was purchased from The Binding Site (Birmingham, UK). Secondary antibodies against rabbit, mouse, and sheep immunoglobulin G (IgG) conjugated to horseradish peroxidase (HRP) were purchased from Chemicon (Temecula, CA). The fluorescently-labeled Alexa 688 goat anti-rabbit IgG and IRDye 800 donkey anti-mouse IgG secondary antibodies were from Molecular Probes (Eugene, OR) and Rockland

Immunochemicals (Gilbertsville, PA), respectively. Rabbit anti-mouse IgG was from Jackson ImmunoResearch Laboratories (Jackson, ME). Rabbit anti-mouse IgA was from Zymed Laboratories Inc. (San Francisco, CA). Purified mouse IgA was from Bethyl Laboratories, Inc. (Montgomery, TX).

Reagent preparation

Stock solutions of Tf were prepared by dissolving Fe_2Tf (Intergen Co., Purchase, NY) or apo Tf (Serologicals, Norcross, GA) in HEPES- (N-2-hydroxyethylpiperazine-N'-2-ethanesulfonic acid) buffered saline (HBS, pH 7.4). Protein concentration was determined by measuring the A280. Saturation of Fe_2Tf was verified by an A465/A280 ratio of 0.045 (Welch, 1992). For FeNTA, stock solutions of 400 mM nitrilotriacetic acid (NTA, Sigma, St. Louis, MO) in phosphate buffered saline (PBS, pH 7.4) and 400 mM FeCl3 in 0.1 N HCl were prepared. Prior to each experiment $FeCl_3$ and NTA were combined in a 1:40 molar ratio to give a final Fe concentration of 10 mM. For control, NTA was combined with the appropriate volume of 0.1 N HCl. Stock solutions of 10 mg/mL cycloheximide (Sigma, St. Louis, MO) were prepared in water.

Cell culture

HepG2 and HuH7 cells were maintained in Minimal Essential Medium (MEM; Life Technologies, Inc.) supplemented with 1.0 mM sodium pyruvate, 0.1 mM MEM non-essential amino acids (Life Technologies, Inc), and 10% fetal bovine serum (FBS). In all experiments, HepG2 cells were seeded at 2×10^4 cell/cm^2 4 days prior to harvesting. K562 cells were cultured in RPMI-1640 (Life Technologies, Inc.) supplemented with 10% FBS. TRVb2 cells were maintained in F12-nutrient mixture (Life Technologies, Inc.) supplemented with 5% FBS and 800 µg/mL G418 (Calbiochem, La Jolla, CA).

Fe_2Tf, apo Tf, FeNTA, cycloheximide, and antibodies were added to the culture medium of cells as described in the figure legends.

Western blot

Cells were lysed on ice in NET-Triton buffer (150 mM NaCl, 5 mM EDTA (ethylenediaminetetraacetic acid), 10 mM Tris (tris(hydroxymethyl)aminomethane), pH 7.4, 1% Triton X-100) containing 1x Complete Mini Protease Inhibitor Cocktail (Roche Diagnostic Corp., Indianapolis, IN) and 1 mM phenylmethylsulfonyl fluoride (PMSF). Lysates were cleared by centrifugation at 16,000 x g for 5 minutes. Protein concentration was measured by BCA Protein Assay (Pierce, Rockford, IL). Aliquots of lysates containing 10-50 µg total protein were incubated in 3.6x Laemmli buffer (Laemmli, 1970) for 5 minutes at 95°C and subjected to reducing SDS-PAGE on 10% gels for analysis of TfR1, TfR2, and Tf or 12% gels for analysis of Ft. Protein was transferred to nitrocellulose and detected using rabbit anti-hTfR2 (1:10,000), mouse anti-hTfR1 (1:10,000), goat anti-hTf (1:10,000) or sheep anti-hFt (1:100) primary antibodies followed by HRP-conjugated (1:10,000) or fluorescently-labeled (1:5,000) secondary antibodies. Bands were visualized by chemiluminescence (SuperSignal WestPico, Pierce, Rockford, IL) or visualized and quantified by fluorescent scanning (Odyssey Infrared Imaging System, Li-Cor, Lincoln, NB). The species specificity of the Alexa 680 goat anti-rabbit and the IRDye 800 donkey anti-mouse fluorescent secondary antibodies enabled blots to be probed simultaneously with rabbit anti-hTfR2 and mouse anti-hTfR1 antibodies. For quantification, serial dilutions of lysate were loaded onto the same gel to ensure that samples were within the linear range of detection.

Real-Time qRT-PCR

RNA was isolated from ~1 x 10^7 HepG2 cells using the RNeasy RNA Isolation Kit (Qiagen, Valencia, CA). After treating RNA with 10 units DNase (Roche Diagnostics Corp., Indianapolis, IN) to remove contaminating genomic DNA, cDNA was synthesized from 2 µg RNA using Oligo dT primers and Superscript II Reverse Transcriptase (RT) (Invitrogen, Carlsbad, CA). cDNA was diluted 1:10 and analyzed by PCR using GAPDH primers spanning an intron/exon junction to verify yield and to confirm the absence of product from contaminating genomic DNA. Samples were analyzed by real-time qRT-PCR using the SYBR green detection system on an ABI PRISM 7900 machine (Applied Biosystems, Foster City, CA). Primer pairs were designed with Primer Express software (Applied Biosystems) and synthesized by IDT Technologies (Coralville, IA). Primer pairs used were: GAPDH 868F/968R (5'-ACCCACTCCTCCACCTTTGA-3' and 5'-CTGTTGCTGTAGCCAAATTCGT-3'); TfR1 305F/435R (5'-CAGGAACCGAGTCTCCAGTGA-3' and 5'-CTTGATGGTGCCGGTGAA GT-3'); and TfR2 1461F/1563R (5'-GGAGTGGCTAGAAGGCTACCTCA-3' and 5'-GGTCTTGGCATGAAACTTGTC A-3'). Primers were verified and data was analyzed by the ΔCT method as described previously (Davies and Enns, 2004; Zhang et al., 2004).

Immunoprecipitation

Pansorbin (Calbiochem, La Jolla, CA) was coated with rabbit-anti mouse IgG for immunoprecipitation with anti-TfR1 and anti-TfR2 mouse monoclonal antibodies and with rabbit-anti mouse IgA for immunoprecipitation with 42/6 anti-TfR1 mouse monoclonal antibody. Cells (~2 x 10^6) were washed twice with ice-cold PBS then lysed in 100 µL NET-Triton buffer containing 1x Complete Mini Protease Inhibitor Cocktail

(Roche Diagnostic Corp., Indianapolis, IN) and 1 mM PMSF. Lysates were preadsorbed by incubation for 1 hour at 4°C with 50 µL Pansorbin/IgA or Pansorbin/IgG to reduce non-specific interactions. Preadsorbed lysates were incubated for 1 hour at 4°C with 25 µL Pansorbin/IgG and 1.5 µL mouse anti-TfR1 or mouse anti-TfR2 antibodies or with 25 µL Pansorbin/IgA and 5 µg 42/6 anti-TfR1 antibody. Pansorbin was pelleted by centrifugation at 16,000 x g for 2 minutes, resuspended in 100 µL NET-Triton buffer, and washed through 1 mL NET-Triton buffer with 15% sucrose. Samples were eluted into 20 µL 2x Laemmli buffer (Laemmli, 1970) heated at 95°C for 5 minutes, then analyzed by western blot. Proteins were detected with rabbit anti-hTfR2 (1:10,000) or sheep anti-hTfR1/Tf serum (1:10,000).

Chapter III

Transferrin receptor 2: evidence for ligand-induced stabilization and redirection to a recycling pathway

Johnson, M.B., Chen, J., Murchison, N., Green, F.A., and Enns, C.A. (2006)

Transferrin receptor 2: evidence for ligand-induced

stabilization and redirection to a trafficking pathway.

Molecular Biology of the Cell in press.

Abstract

Transferrin receptor 2 (TfR2) is a homolog of transferrin receptor 1 (TfR1), the protein that delivers iron to cells through receptor-mediated endocytosis of diferric transferrin (Fe_2Tf). TfR2 also binds Fe_2Tf, but appears to function primarily in the regulation of systemic iron homeostasis. In contrast to TfR1, the trafficking of TfR2 within the cell has not been extensively characterized. Previously, we showed that Fe_2Tf increases TfR2 stability, suggesting that trafficking of TfR2 may be regulated by interaction with its ligand. In the present study, therefore, we sought to identify the mode of TfR2 degradation, characterize TfR2 trafficking, and determine how Fe_2Tf stabilizes TfR2. Stabilization of TfR2 by bafilomycin implies that TfR2 traffics to the lysosome for degradation. Confocal microscopy reveals that treatment of cells with Fe_2Tf increases the fraction of TfR2 localizing to recycling endosomes and decreases the fraction of TfR2 localizing to late endosomes. Mutational analysis of TfR2 shows that the mutation G679A, which blocks TfR2 binding to Fe_2Tf, increases the rate of receptor turnover and prevents stabilization by Fe_2Tf, indicating a direct role of Fe_2Tf in TfR2 stabilization. The mutation Y23A in the cytoplasmic domain of TfR2 inhibits its internalization and degradation, implicating YQRV as an endocytic motif.

Introduction

A truncation mutant of transferrin receptor 2 (TfR2), TfR2/Y250X, causes a rare form of hereditary hemochromatosis (type 3, HFE3), an iron overload disorder characterized by excess absorption of dietary iron and consequent deposition of iron in liver and other parenchymal tissues (Camaschella et al., 1999; Camaschella et al.,

2000). The analogous mutation or knock-out of *Trfr2* in mice reproduces the disease phenotype (Fleming et al., 2002; Wallace et al., 2005). Thus, TfR2 is required for normal iron homeostasis.

TfR2, cloned in 1999, is a homolog of transferrin receptor 1 (TfR1, Kawabata et al., 1999). The extracellular domains of the two receptors are 45% identical and 67% similar. TfR1 functions to deliver iron to cells through receptor-mediated endocytosis of its ligand, transferrin (Tf), a serum protein that transports iron (Dautry-Varsat et al., 1983; Klausner et al., 1983). On the cell surface, TfR1 binds iron-saturated transferrin (Fe_2Tf) at slightly basic pH. Fe_2Tf-TfR1 then internalizes in clathrin-coated vesicles to early endosomes. In the acidic pH of early endosomes, iron releases from Tf while Tf remains bound to TfR1. The complex then recycles, from either early or recycling endosomes, to the cell surface. At the slightly basic pH of the cell surface, TfR1 releases unsaturated Tf (apoTf) and again binds Fe_2Tf. TfR1 expression is ubiquitous, consistent with its role in cellular iron delivery. The stability of TfR1 mRNA is negatively regulated by intracellular iron levels (Lu et al., 1989; Mattia et al., 1984; Rao et al., 1985; Sciot et al., 1987; Ward et al., 1984) through iron-responsive elements (IRE) in the 3' untranslated region (Casey et al., 1988; Mullner and Kuhn, 1988; Mullner et al., 1989; Owen and Kuhn, 1987).

TfR2 differs from TfR1 in notable ways. TfR2 binds Tf in a pH-dependent manner, but its affinity for Fe_2Tf (K_D ~ 30 nM, Kawabata et al., 2000; West et al., 2000) is significantly lower than that of TfR1 (K_D ~ 1 nM, Tsunoo and Sussman, 1983; Enns et al., 1991; Richardson and Ponka, 1997). Unlike TfR1, TfR2 expression is limited predominantly to hepatocytes (Calzolari et al., 2004; Fleming et al., 2002; Fleming et al., 2000; Kawabata et al., 1999; Vogt et al., 2003; Zhang et al., 2004) in the liver and is not

regulated by intracellular iron (Fleming et al., 2000; Kawabata et al., 2001; Kawabata et al., 2000). TfR2 cannot compensate for TfR1, whose knockout in mice results in embryonic lethality due to severe anemia (Levy et al., 1999). Because *Trfr2* mutation or knockout results in iron overload, TfR2 seems to function, not principally in cellular iron uptake and delivery, but rather in systemic iron homeostasis. The exact function of TfR2, however, is not known.

To investigate the function of TfR2, we previously characterized the response of TfR2 to Fe_2Tf in a human hepatoma cell line, HepG2, that endogenously expresses TfR2. Whereas ligand-receptor interactions frequently result in receptor down-regulation, addition of Fe_2Tf to the medium of HepG2 cells increases TfR2 by extending the half-life of TfR2 from 4 to 14 hr (Johnson and Enns, 2004). Interestingly, regulation of TfR2 by its ligand has only been observed in hepatoma cell lines (Johnson and Enns, 2004; Robb and Wessling-Resnick, 2004), suggesting the mechanism involves proteins, compartments, or pathways specific to the hepatocyte. Moreover, TfR2 regulation observed in HepG2 cells seems to recapitulate physiological regulation. Robb and Wessling-Resnick (2004) showed that TfR2 levels are elevated in mice with high serum transferrin saturation and reduced in mice with low serum transferrin saturation. In HepG2 cells, the response to Fe_2Tf was half-maximal at ~1-3 μM Fe_2Tf , a physiologically relevant concentration range (Johnson and Enns, 2004; Robb and Wessling-Resnick, 2004).

The stabilization of TfR2 by Fe_2Tf suggests that the trafficking of this receptor may be regulated by its ligand. To test this hypothesis, we characterized the effect of Fe_2Tf and mutations on TfR2 localization and stabilization in two human hepatoma cell lines, HepG2 and Hep3B. We demonstrate that Fe_2Tf directs TfR2 from a degradative

pathway to a recycling pathway, establish that direct interaction of TfR2 with Fe_2Tf stabilizes TfR2, and identify an endocytic motif in the intracellular domain of TfR2 necessary for TfR2 internalization and regulation.

Results

TfR2 undergoes lysosomal degradation

Fe_2Tf increases the half-life of TfR2 from 4 to 14 hrs in HepG2 cells (Johnson and Enns, 2004), indicating that TfR2 degradation is a regulated process. To further understand this process, we set out to determine whether TfR2 degradation occurs in the lysosome. Lysosomal degradation of TfR2 was assessed by treating HepG2 cells with bafilomycin, an inhibitor of the vacuolar H^+-ATPase (Bowman et al., 1988), to dissipate the endosomal pH gradient and thereby block transport to lysosomes (van Weert et al., 1995). Cells were treated in the absence and presence of cycloheximide, an inhibitor of protein synthesis, to prevent further TfR2 synthesis. The presence of bafilomycin resulted in a significant increase in TfR2 protein (Figure 10). Consistent with previous results, TfR2 decreased significantly over a 4 hr time course in cells treated with cycloheximide. In these cells, the addition of bafilomycin attenuated this effect, restoring the TfR2 level to that in control cells, a result in keeping with lysosomal degradation of TfR2. The role of the proteasome in TfR2 degradation was assessed by treating HepG2 cells with ALLN and MG-132 to inhibit proteasome activity. To control for the inhibition of calpains and cathepsins by ALLN, cells were also treated with ALLM, which inhibits calpains and cathepsins, but not the proteasome. Inhibition of proteasome activity did not significantly alter TfR2 level (Figure 10C).

Subcellular localization of TfR2

Based on our results, we hypothesized that Fe_2Tf prevents lysosomal degradation of TfR2 by diverting TfR2 from a degradative pathway and predicted that Fe_2Tf would alter the subcellular localization of TfR2. Because the subcellular localization of TfR2 has not been fully described, we first characterized its intracellular trafficking by examining its colocalization with various established markers of subcellular compartments. Antibodies against early endosome antigen 1 (EEA1), TfR1, and Rab7 were used to label early (Mu et al., 1995), early/recycling, and late endosomal (Chavrier et al., 1990) populations (Figures 11A, 11D, and 11G), respectively. Confocal microscopy analysis showed that TfR2 was present in punctate structures in the perinuclear region and throughout the cell periphery (Figure 11). TfR2 partially colocalized with all three endosomal markers (Figures 11C, 11F, and 11I), indicating that TfR2 traffics through endocytic, recycling, and degradative pathways.

Although results show that TfR2 degradation occurs in the lysosome (Figure 10), we observed very little colocalization of TfR2 with the lysosomal marker, lysosome-associated membrane protein 1 (LAMP-1) by immunofluorescence (Figure 11, M-O). The lack of colocalization between TfR2 and LAMP-1 is likely due to rapid degradation of TfR2 within the lysosome. These results are consistent with the lack of degradation intermediates seen in western blots and immunoprecipitations of TfR2 from HepG2 cells (Johnson and Enns, 2004).

We also examined the colocalization of TfR2 with markers of the trans-Golgi network (TGN). Membrane proteins reach the TGN during biosynthesis and, in some cases, after internalization from the plasma membrane (Snider and Rogers, 1985; Stoorvogel et al., 1988). TfR2 was observed to colocalize with TGN marker Golgin97 in

the perinuclear region of cells (Figure 11R). Colocalization of TfR2 with adaptor protein 1 (AP-1, Figure 11U), which facilitates vesicle transport between endosomes and the TGN and localizes to both compartments, was also observed. TfR2 and AP-1 colocalization was predominantly in the perinuclear region (Figure 11U) and only occasionally detectable in peripheral vesicles (data not shown).

Diferric Tf regulates the subcellular localization of TfR2

The subcellular localization of TfR2 is consistent with that of a membrane protein trafficking through biosynthetic, recycling, and degradative pathways (Figure 11). Because Fe_2Tf stabilizes TfR2, we predicted that the fraction of TfR2 localizing to recycling endosomes might increase in cells treated with Fe_2Tf. Quantitative colocalization analysis was used to measure the colocalization of TfR2 with EEA1, TfR1, Rab7, Golgin97, or AP-1 in HepG2 cells untreated or treated with Fe_2Tf (Figure 12A). No difference in the fraction of TfR2 colocalizing with EEA1, Golgin97, or AP-1 was detected. The colocalization of TfR2 with TfR1 increased from 0.42 ± 0.028 in untreated cells to 0.51 ± 0.022 in Fe_2Tf-treated cells. Because no increase in the colocalization of TfR2 with the early endosome marker EEA1 was detected, we interpret the increase in colocalization of TfR2 with the early/recycling endosome marker TfR1 as an increase in TfR2 localization to recycling endosomes. The increase in TfR2 colocalization to recycling endosomes was accompanied by a decrease in TfR2 colocalization with Rab7 in late endosomes, from 0.21 ± 0.015 in untreated cells to 0.17 ± 0.009 in Fe_2Tf-treated cells. Taken together, these results suggest that Fe_2Tf redirects TfR2 from a degradative pathway to a recycling pathway through recycling endosomes.

In addition to assessing the effect of Fe_2Tf on the steady state localization of TfR2 to subcellular compartments, we also examined the effect of Fe_2Tf on the steady state distribution of TfR2 to the cell surface. DIfferential immunoprecipitation was used to isolate sequentially surface and internal TfR2 from HepG2 cells. In untreated cells, 31 ± 5% of TfR2 was at the cell surface and 67 ± 1% of TfR2 was intracellular (Figure 12C, open bars). In Fe_2Tf treated cells, the amount of TfR2 in surface and intracellular fractions increased relative to untreated cells (Figure 12B). However, the partitioning of TfR2 between these fractions remained the same (31 ± 3% surface vs. 71 ± 2% intracellular; Figure 12C, closed bars). Thus, Fe_2Tf does not alter the proportion of surface and intracellular TfR2.

Characterization of wild-type TfR2 in transfected Hep3B cells

Hep3B cells, in which TfR2 protein is not detectable (Figure 13A), were used to express TfR2 mutants in order to study the mechanism of TfR2 regulation. Because TfR2 forms dimers (Kawabata et al., 1999), a null background was particularly important. We first established that regulation of transfected wild-type TfR2 was similar to that of endogenous TfR2 in HepG2 cells. Hep3B cells stably transfected to express TfR2/WT (Hep3B/TfR2WT cells) regulated TfR2 in response to Fe_2Tf (Figure 13A). In cells treated with Fe_2Tf, an increased level of TfR2 protein correlated with an increased half-life of the protein (Figure 13B). The magnitude of stabilization in Hep3B/TfR2WT cells, from 10 to 28 hr, matched that in HepG2 cells, from 4 to 14 hr (Johnson and Enns, 2004). Due to the low level of endogenous TfR2 expression in HepG2 cells, assessment of the effect of Fe_2Tf on TfR2 biosynthetic rate was not feasible. In Hep3B/ TfR2WT cells, TfR2 was synthesized at the same rate in untreated and Fe_2Tf-treated

cells (Figure 13C), indicating that Fe_2Tf affects the rate of TfR2 degradation and not its rate of biosynthesis.

We determined the distribution of TfR2 in Hep3B/TfR2WT cells by using differential immunoprecipitation to isolate plasma membrane and intracellular fractions of TfR2. At steady state, ~ 50% (48 ± 3) of TfR2 localized to the cell surface and ~50% (48 ± 4) to intracellular compartments (Figure 13D). This distribution was different from that determined for HepG2 cells, in which TfR2 localized ~30% (31± 5) to the cell surface and ~70% (67 ± 1) to intracellular compartments. This difference is likely a consequence of the high levels of TfR2 expression in the Hep3B/TfR2WT cells. Results from uptake experiments using iodinated anti-TfR2 antibody indicated that the TfR2 endocytic pathway is saturated in Hep3B/TfR2WT cells (data not shown), resulting in an accumulation of receptors on the cell surface, as previously seen with overexpression of other receptors (Marks et al., 1996; Warren et al., 1997; Warren et al., 1998).

Confocal microscopy was used to determine whether TfR2 showed a similar pattern of localization in Hep3B/TfR2WT cells as in HepG2 cells. Immunofluorescent labeling of TfR2 at 4°C before fixation and permeabilization detected TfR2 at the cell surface (Figures 14Ab and 14Ae). Under these conditions, TfR1 at the cell surface can be detected with an antibody recognizing the extracellular domain (3B82A1, Figure 14Aa) but not with an antibody recognizing the intracellular domain (H68.4, Figure 14Ad), indicating that the plasma membrane is intact. immunofluorescent detection of TfR2 at room temperature in fixed and permeabilized cells detected intracellular protein, visible as punctate staining in the perinuclear and peripheral regions of the cell (Figure 14B). TfR2 colocalized with EEA1 in early endosomes (Figure 14Bc), TfR1 in early/ recycling endosomes (Figure 14Bf), and Golgin97 in the TGN (Figure 14Bi). Together,

these experiments established Hep3B cells as a suitable cell line in which to express and characterize TfR2 mutants. In addition, they corroborate previous results indicating that the mechanism of TfR2 regulation by Fe_2Tf is conserved in hepatocyte-derived cells (Johnson and Enns, 2004).

Binding of TfR2 to diferric Tf is prerequisite for TfR2 stabilization

Our results indicate that Fe_2Tf redirects TfR2 from a degradative pathway through late endosomes and lysosomes into a pathway through recycling endosomes and thereby stabilizes TfR2. Because HepG2 cells express both TfR1 and TfR2, TfR2 stabilization might be consequent on binding of Fe_2Tf to either receptor. Previous efforts to determine which transferrin receptor mediates TfR2 stabilization, using an antibody that blocks and downregulates TfR1, yielded ambiguous results (Johnson and Enns, 2004). To answer this question directly, site-directed mutagenesis was used to generate a TfR2 construct with mutation G679A. This mutation, in the extracellular domain of TfR2, eliminated detectable binding of TfR2 to Fe_2Tf (Kawabata et al., 2004). If TfR2 stabilization results from interaction of Fe_2Tf with TfR2, rather than from interaction of Fe_2Tf with TfR1, the G679A mutation in TfR2 should eliminate Fe_2Tf-induced stabilization of TfR2. The failure of TfR2/G679A to increase in Hep3B cells transiently transfected with TfR2/G679A and treated with Fe_2Tf (Figures 16B and 16C) provided preliminary evidence that interaction of Fe_2Tf with TfR2 stabilizes TfR2.

We therefore went on to characterize the effect of mutation G679A on TfR2 localization and regulation in Hep3B cells stably transfected with plasmid encoding TfR2/G679A (Hep3B/TfR2G679A cells). Confocal microscropy analysis of cells labeled with anti-TfR2 antibody at 4°C showed TfR2/G679A at the cell surface (Figure 15Ab),

indicating that this mutation does not prevent transit of TfR2 through the biosynthetic pathway. Immunofluorescent detection of TfR2/G679A showed that it colocalized with EEA1 (Figure 15Bc), TfR1 (Figure 15Bf), and Golgin97 (Figure 15Bi). When TfR2/G679A was isolated by differential immunoprecipitation, ~30% (33 ± 7) was found in the plasma membrane fraction and ~60% (58 ±6) was found in the intracellular fraction, a distribution similar to that of endogenous TfR2 in HepG2 cells (Figure 15C), indicating that this mutation does not affect surface and intracellular steady state levels of TfR2.

Given that TfR2/G679A neither binds nor responds to Fe_2Tf, we predicted that the half-life of TfR2/G679A would be short and unaffected by Fe_2Tf treatment. In metabolic labeling experiments, TfR2/G679A had a very short half-life of 2.6 hr (Figure 15D), which is significantly shorter than that of endogenous TfR2 in HepG2 cells and TfR2/WT transfected into Hep3B cells. Fe_2Tf did not significantly increase this half-life (Figure 15D). From these results, we propose that stabilization of TfR2 by Fe_2Tf requires direct ligand-receptor interaction.

Preliminary characterization of mutations in the cytoplasmic domain of TfR2

Stabilization of TfR2 by Fe_2Tf involves a change in the trafficking of TfR2. Because the cytoplasmic domain of membrane proteins often contain signals that direct the protein's trafficking, we used site-directed mutagenesis to alter residues in the cytoplasmic domain of TfR2 (Figure 16A). V22I is a naturally occurring mutation that was speculated to perturb iron homeostasis (Biasiotto et al., 2003). It is adjacent to a putative endocytic motif, YQRV. The YQRV motif is similar to the established endocytic motif in TfR1, YTRF, in which mutation of the tyrosine decreases the rate of TfR1 endocytosis (Jing et al., 1990; McGraw and Maxfield, 1990; Alvarez et al., 1990). We

generated the corresponding mutation, Y23A, in TfR2 to assess the role of the YQRV motif in TfR2 trafficking. K31 is the only lysine residue within the cytoplasmic domain of TfR2 and is a potential site for ubiquitination, a post-translational modification that regulates the trafficking and degradation of membrane proteins. We introduced the mutation K31A to assess whether ubiquitination plays a role in the regulation of TfR2 stability by Fe_2Tf.

To assess whether these mutations affected the ability of Fe_2Tf to regulate TfR2, Hep3B cells were transiently transfected with constructs encoding the wild-type and mutant proteins. To control for variations in transfection efficiency, a single transfection was split and reseeded prior to treatment of cells in triplicate without or with Fe_2Tf for 24 hr. Western blot analysis using fluorescence-labeled secondary antibodies showed that TfR2/WT, TfR2/V22I, and TfR2/K31A increased significantly in cells treated with Fe_2Tf (Figure 16B and C). By contrast, TfR2/Y23A did not respond to Fe_2Tf. This mutant was selected for further characterization in a stable cell line.

A tyrosine in the cytoplasmic domain of TfR2 is critical for internalization

The Y23A mutation alters a putative tyrosine-based endocytic motif, YQRV, in the cytoplasmic domain of TfR2. If YQRV acts as an endocytic motif, this mutation should inhibit internalization of TfR2. Such an effect might impede normal trafficking of TfR2 through its degradative pathway and render TfR2 insensitive to Fe_2Tf. Thus, TfR2/Y23A should have a long half-life in the absence and presence of Fe_2Tf. Metabolic labeling experiments in Hep3B cells stably expressing TfR2/Y23A (Hep3B/TfR2Y23A cells) confirmed this. In marked contrast to both TfR2/WT and TfR2/G679A, TfR2/Y23A

was extremely stable, changing little over a 24-hr time-course, in both the absence and presence of Fe_2Tf (Figure 17A).

To test whether endocytosis of TfR2/Y23A is impaired, we measured the distribution of TfR2/Y23A in plasma membrane and intracellular fractions isolated by differential immunoprecipitation. In Hep3B/TfR2Y23A cells, only ~20% (19 ± 2) of TfR2 was intracellular (Figure 17B), compared with ~50% in Hep3B/TfR2WT cells (Figure 13D). Consistent with this observation, no measurable internalization of TfR2/Y23A was detected compared with TfR2/WT and TfR2/G679A, which does not bind Tf (Figure 17C). The altered localization of TfR2/Y23A was demonstrated by confocal microscopy images of Hep3B/TfR2Y23A cells that were fixed, permeabilized, and labeled for total protein. TfR2/Y23A seems blanketed across the cell surface (Figure 17Db) rather than punctate in the cytoplasm (TfR1 in Figure 17Da and TfR2/WT in Figure 14Be). Whereas immunofluorescent labeling of TfR2 at 4°C detected cell surface TfR2 similarly in both Hep3B/TfR2WT and Hep3B/TfR2Y23A cells (Figures 14Ae and 17Eb), immunofluorescent labeling of total TfR2 showed a cell surface pattern of staining for TfR2 only in the Hep3B/TfR2Y23A cells (Figure 17Db). The results of these experiments are consistent with YQRV as an endocytic motif that mediates TfR2 internalization from the plasma membrane.

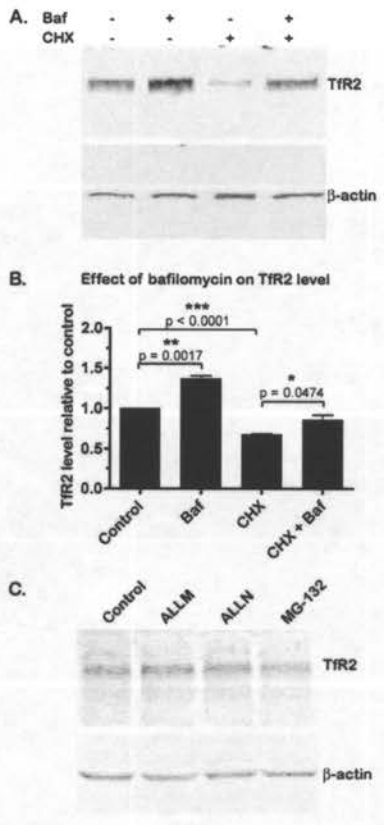

Figure 10. Bafilomycin blocks lysosomal degradation of TfR2. HepG2 cells were seeded at 2.5 x 10^4 cells/cm^2 in 12-well plates 4 days prior to treatment with 50 μM bafilomycin (BAF) in the presence or absence of 100 μg/mL cycloheximide (CHX) for 4 hr. (A) Lysates (20 μg total protein) were separated by SDS-PAGE and immunoblotted with anti-TfR2 serum and anti-β actin antibody followed by fluorescence-labeled secondary antibodies (all 1:10,000). (B) The intensities of TfR2 bands were normalized to the intensities of β-actin bands and expressed relative to untreated cells (control). Graph represents data averaged from four independent experiments. P-values of 0.01 - 0.05, 0.01 - 0.001, and < 0.001 indicate changes that are significant (*), very significant (**), and extremely significant (***), respectively, when evaluated by Student's t-test. (C) Cells were treated with 100 μM ALLM, 100 μM ALLN, or 25 μM MG-132 as indicated for 4 hr. Lysates were analyzed as described for A. ALLM, ALLN, and MG-132 did not significantly alter TfR2 levels in three independent experiments.

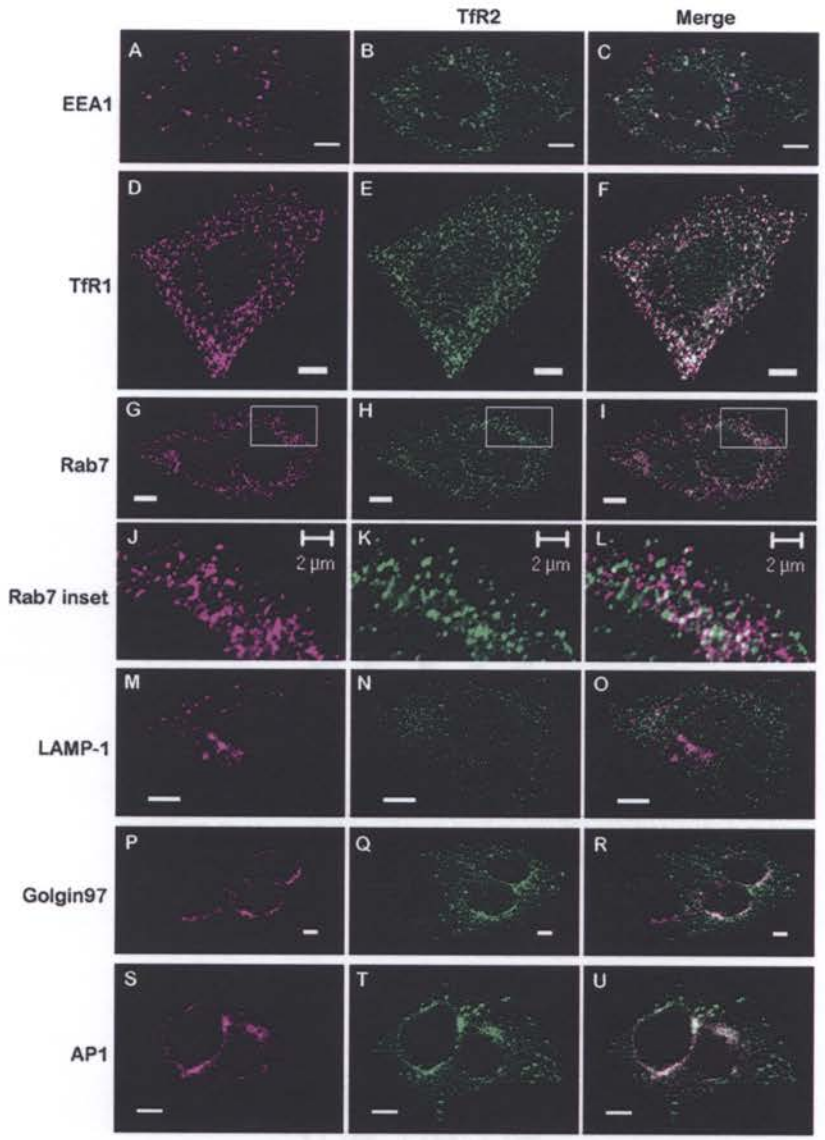

Figure 11. Subcellular localization of TfR2 in HepG2 cells. (A-U) TfR2 localizes to endosomes and the trans-Golgi network. HepG2 cells were seeded at 6.25 x 10^3 cells/ cm^2 on poly-L-lysine treated glass coverslips and cultured for 2 days prior to fixation, permeabilization, and labeling as described in Materials & Methods. Indicated markers are shown in magenta (A, D, G, J, M, P, S), TfR2 is shown in green (B, E, H, K, N, Q, T), and colocalization is shown in white (C, F, I, L, O, R, U). Unless otherwise indicated, scale bar is 5 µm.

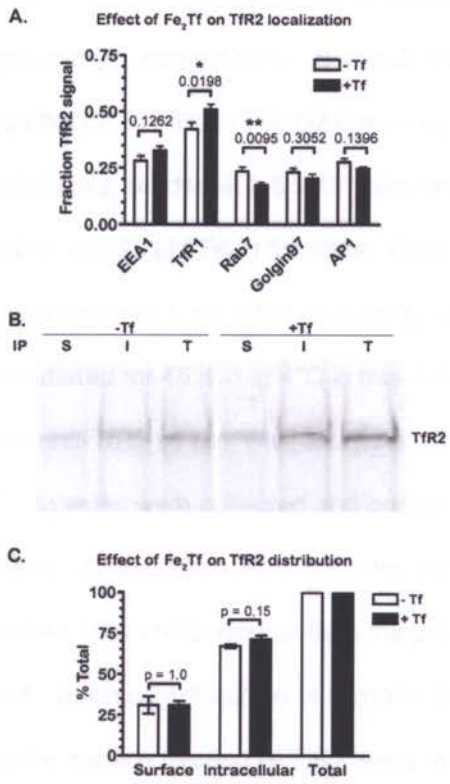

Figure 12. Diferric Tf regulates the subcellular localization of TfR2.

Figure 12. Diferric Tf regulates the subcellular localization of TfR2. (A) Fe_2Tf alters the trafficking of TfR2. Prior to the experiment, HepG2 cells were incubated for 48 hr without or with 25μM Fe_2Tf. As in Figure 11, cells were double-labeled and visualized by scanning confocal microscopy. The effect of Fe_2Tf on the subcellular localization of TfR2 was assessed by quantitative colocalization analysis. The fraction of TfR2 signal colocalizing with EEA1, TfR1, Rab7, Golgin97, or AP-1 signal was analyzed in 20-40 images per condition acquired in 2-3 independent experiments. Data was evaluated by Student's t-test. P-values of 0.01 - 0.05 and 0.01 - 0.001 indicate changes that are significant (*) and very significant (**), respectively. (B and C) Fe_2Tf does not retain TfR2 at the cell surface. The distribution of TfR2 in HepG2 cells was assessed by differential immunoprecipitation. HepG2 cells, seeded at 2.5 x 10^4 cells/cm^2 in 35 mm wells, were cultured in medium without or with 25 μM Fe_2Tf for 48 hr. Cells were then placed on ice and culture medium was replaced with 1 mL MEM containing 10% FBS and 25 mM HEPES. Cells were then incubated for 45 min at 4°C in this medium with (M+Ab) or without (M-Ab) 16637 rabbit anti-TfR2 serum, washed twice with PBS, and lysed for 15 min at 4°C in 250 μL NETT. Lysates were collected and pooled with a second 250 μL NETT wash. After the addition of 50 μL Pansorbin, samples were rotated for 45 min at 4°C to pre-clear M-Ab samples or to immunoprecipitate the plasma membrane fraction of TfR2 from M+Ab samples. Upon centrifugation of samples at 13,000 x g, pellets from M+Ab samples, containing the surface fraction of TfR2, were resuspended in 50 μL 2x Laemmli sample buffer. To immunoprecipitate intracellular and total fractions of TfR2, supernatants from M+Ab and M-Ab samples, respectively, were incubated with rabbit anti-TfR2 serum for 45 min and with 50 μL Pansorbin for an additional 45 min at 4°C, centrifuged, and resuspended in 2x Laemmli sample buffer. Samples were heated at 95°C for 5 min, centrifuged, separated by SDS-PAGE and analyzed by western blot. (B) TfR2 was detected with mouse anti-TfR2 antibody followed by a fluorescence-labeled secondary antibody. (C) Results from three experiments were quantified.

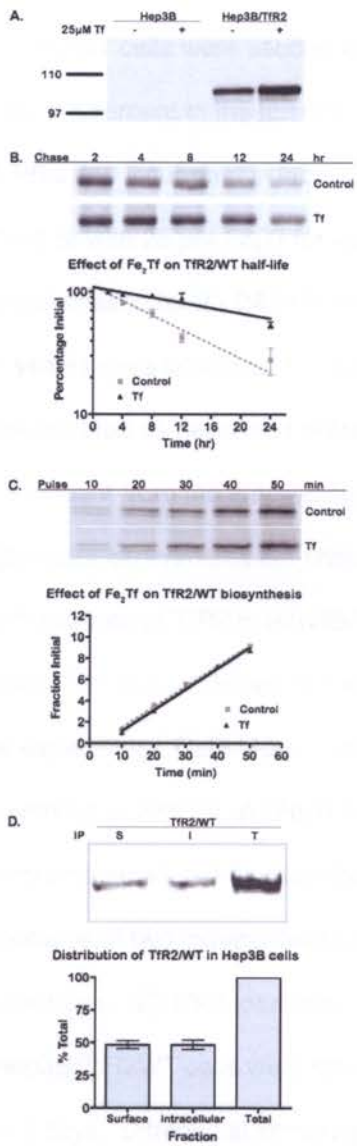

Figure 13. Diferric Tf stabilizes TfR2/WT in Hep3B cells. (A) Fe_2Tf increases TfR2 protein level in Hep3B/TfR2WT cells. Hep3B cells and Hep3B cells stably expressing wild-type TfR2 (Hep3B/TfR2WT) were seeded at 8.3 x 10^3 cells/cm^2 in 12-well plates and cultured for 24 hr without or with Fe_2Tf. Lysates were analyzed by SDS-PAGE and western blot. Blots were probed with rabbit anti-TfR2 serum (1:10,000) and HRP-conjugated goat anti-rabbit secondary (1:10,000). Protein was visualized by chemiluminescence. TfR2 protein is not detectable in Hep3B cells. In Hep3B/TfR2WT

cells, TfR2 increases in cells exposed to Fe_2Tf. (B) Fe_2Tf stabilizes TfR2 protein in Hep3B/TfR2WT cells. Hep3B/TfR2WT cells were seeded at 1.25 x 10^5 cells/cm^2 in 35 mm dishes two days prior to the experiment in the absence or presence of 25 μM Fe_2Tf. Cells were washed twice with PBS and incubated in labeling medium containing 100 μM [^{35}S]-cysteine/methionine without or with 25 μM Fe_2Tf for 45 min at 37°C. Cells were washed three times with PBS and chased for 2 - 24 hr in normal media in the absence or presence of 25 μM Fe_2Tf. Lysates were collected, stored at -80°C until all time points were collected, and immunoprecipitated as described in Materials & Methods. The stabilization of TfR2 by Fe_2Tf is evident from the autoradiogram (top). Means of measurements from two independent experiments are shown in the graph (bottom). (C) Fe_2Tf does not alter the biosynthetic rate of TfR2 in Hep3B/TfR2 cells. Hep3B/TfR2 cells were seeded at 1.25 x 10^5 cells/cm^2 in 35 mm dishes in the absence or presence of 25 μM Fe_2Tf two days prior to the experiment. Cells were washed twice with PBS and incubated in labeling medium without or with 25 μM Fe_2Tf for 10 - 50 min at 37°C. Lysates were collected and immunoprecipitated as described in Materials & Methods. Autoradiogram (top) is representative of two independent experiments, the means of which are shown in the graph (bottom). (D) TfR2 localizes to the plasma membrane and intracellular compartments. Hep3B/TfR2WT cells were seeded at 2.5 x 10^4 cells/cm^2 in 24-well plates and cultured for 2 days. Differential immunoprecipitation to isolate surface and intracellular fractions of TfR2 was performed as described in Figure 12B. A representative western blot probed with mouse anti-TfR2 antibody and a fluorescence-labeled secondary antibody (both 1:10,000) is shown (top). The averaged results of duplicates from three independent experiments are shown in the graph (bottom). In Hep3B/TfR2WT cells, TfR2 distributes evenly between the cell surface and intracellular compartments, with 48 ± 3.0% at the surface and 48 ± 3.5% in intracellular compartments.

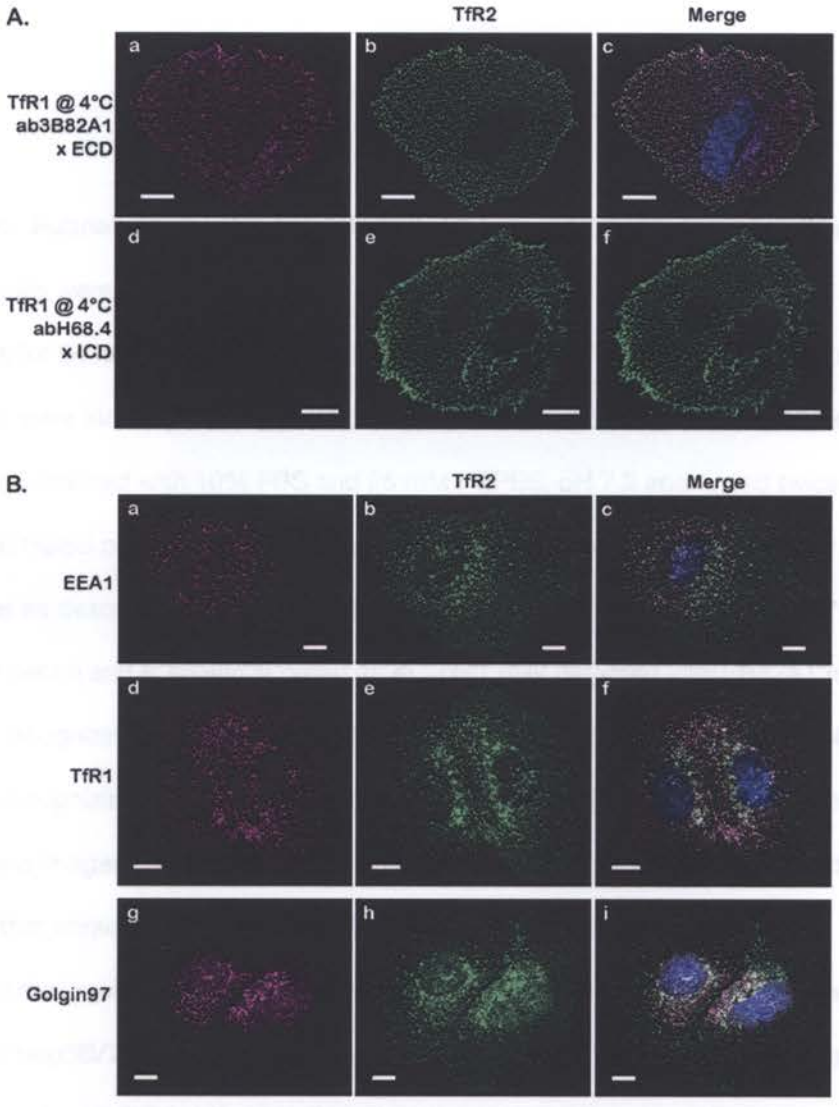

Figure 14. Subcellular localization of TfR2/WT in Hep3B cells.

Figure 14. Subcellular localization of TfR2/WT in Hep3B cells. (A and B) Hep3B/TfR2WT cells were seeded at 2.5 x 10^3 cells/cm^2 on poly-L-lysine coated glass coverslips for 24 hr prior labeling. (A) To detect TfR1 and TfR2 at the cell surface, coverslips were incubated at 4°C for 45 min in primary antibodies diluted into ice-cold MEM supplemented with 10% FBS and 25 mM HEPES, pH 7.2 and rinsed twice on ice in ice-cold HBSS prior to fixation, permeabilization, and labeling with secondary antibodies as described in Materials & Methods. TfR2 was detected with 16637 rabbit anti-TfR2 serum and is shown in green (b, e). TfR1 was detected with 3B82A1 mouse antibody recognizing the extracellular domain (ECD) of TfR1 (a) or with the H68.4 mouse antibody recognizing the intracellular domain (ICD) of TfR1 (d) and is shown in magenta. The merged images (c, f) show nuclei in blue. The absence of TfR1 staining in (d) confirms that intracellular protein was inaccessible to primary antibody. Under conditions that prohibit labeling of intracellular protein, TfR1 and TfR2 are visible at the surface of Hep3B/TfR2WT cells (a-c). (B) TfR2 colocalizes with EEA1, TfR1, and Golgin97 in Hep3B/TfR2 WT cells. To detect total protein by immunofluorescence, cells were fixed, permeabilized, and labeled as described in Materials & Methods. Indicated markers are shown in magenta (a, d, g), TfR2 is shown in green (b, e, h), and *colocalization is shown in white (c, f, i). Nuclei are shown in blue in the merged images.* Scale bar is 10 μm.

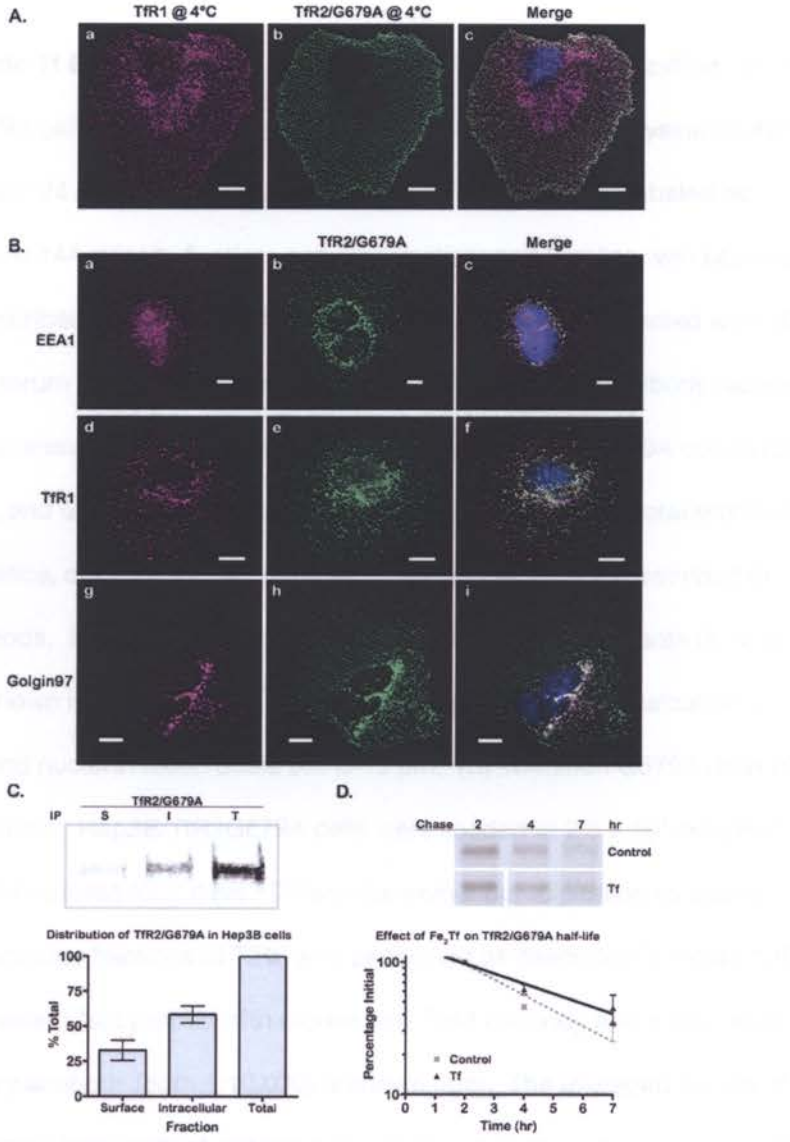

Figure 15. Diferric Tf Binding to TfR2 is prerequisite for TfR2 stabilization.

Figure 15. Diferric Tf Binding to TfR2 is prerequisite for TfR2 stabilization. (A and B) Hep3B/TfR2G679A cells were seeded at 2.5 x 10^3 cells/cm^2 on poly-L-lysine coated glass coverslips for 24 hr prior labeling. (A) Surface TfR2/G679A was labeled as described in Figure 14A prior to fixation, permeabilization, and labeling with secondary antibodies as described in Materials & Methods. TfR2/G679A was detected with 16637 rabbit anti-TfR2 serum (b). TfR1 was detected with 3B82A1 mouse antibody recognizing the extracellular domain of TfR1 (a). Scale bar is 10 μm. (B) TfR2/G679A colocalizes with EEA1, TfR1, and Golgin97 in Hep3B/TfR2G679A cells. To detect total protein by immunofluorescence, cells were fixed, permeabilized, and labeled as described in Materials & Methods. Indicated endosomal markers are shown in magenta (a, d, g), TfR2/G679A is shown in green (b, e, h). In merged images (c, f, l) colocalization is shown in white and nuclei in blue. Scale bar is 10 μm. (C) Mutation G679A does not alter TfR2 distribution. Hep3B/TfR2G679A cells were seeded at 2.5 x 10^4 cells/cm^2 in 12-well plates and cultured for 2 days. Differential immunoprecipitation to isolate surface and intracellular fractions of TfR2 was performed as described in Figure 12B. A representative western blot probed with mouse anti-TfR2 antibody and a fluorescence-labeled secondary antibody (both 1:10,000) is shown (top). The averaged results of duplicates from three independent experiments are shown in the graph (bottom). (D) Fe_2Tf does not stabilize TfR2/G679A protein. Hep3B/TfR2G679A cells were seeded and labeled as described in Figure 13B. Labeled TfR2/G679A was immunoprecipitated and detected as described in Materials & Methods. Representative autoradiogram shows the rapid loss of TfR2/G679A in untreated and Fe_2Tf-treated cells over the course of 7 hr (top). The mean of measurements from two independent experiments are shown in the graph (bottom). The rate of TfR2/G679A decay does not differ significantly in untreated and Fe_2Tf-treated cells (p-value = 0.2108).

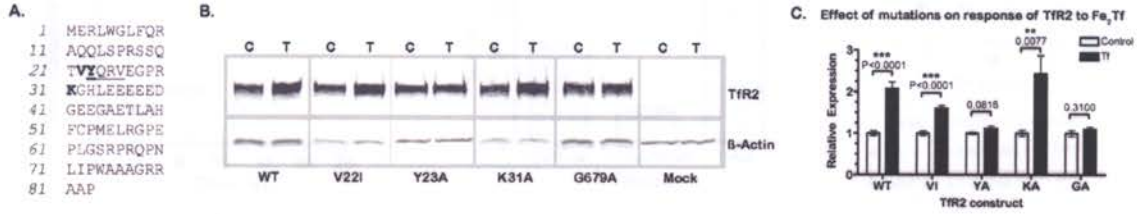

Figure 16. Response of TfR2 mutants to diferric Tf in Hep3B cells. (A) Sequence of TfR2's intracellular domain. Residues mutated by site-directed mutagenesis are in bold. The putative endocytic motif is underlined. The position of an additional mutation at G679 in the extracellular domain of TfR2 is not shown. (B and C) To test the effect of mutations on TfR2's response to Fe_2Tf, Hep3B cells were transiently transfected with constructs encoding wild-type and mutant TfR2 proteins, re-plated, and treated in triplicate without (C) or with (T) 25 μM Fe_2Tf. Lysates were subjected to SDS-PAGE and western blot analysis. Blots were probed with rabbit anti-TfR2 serum and mouse anti-β-actin antibody followed by fluorescence-labeled secondary antibodies (all 1:10,000). (B) Representative blots show that TfR2/WT, TfR2/V22I, and TfR2/K31A increase in Fe_2Tf-treated cells whereas TfR2/Y23A and TfR2/G679A do not. (C) Graph shows the averaged results of triplicate treatments from two independent experiments. Significance was assessed with two-tailed Student's t-test. P-values of 0.01 - 0.001 and < 0.001 indicate changes that are very significant (**) and extremely significant (***), respectively.

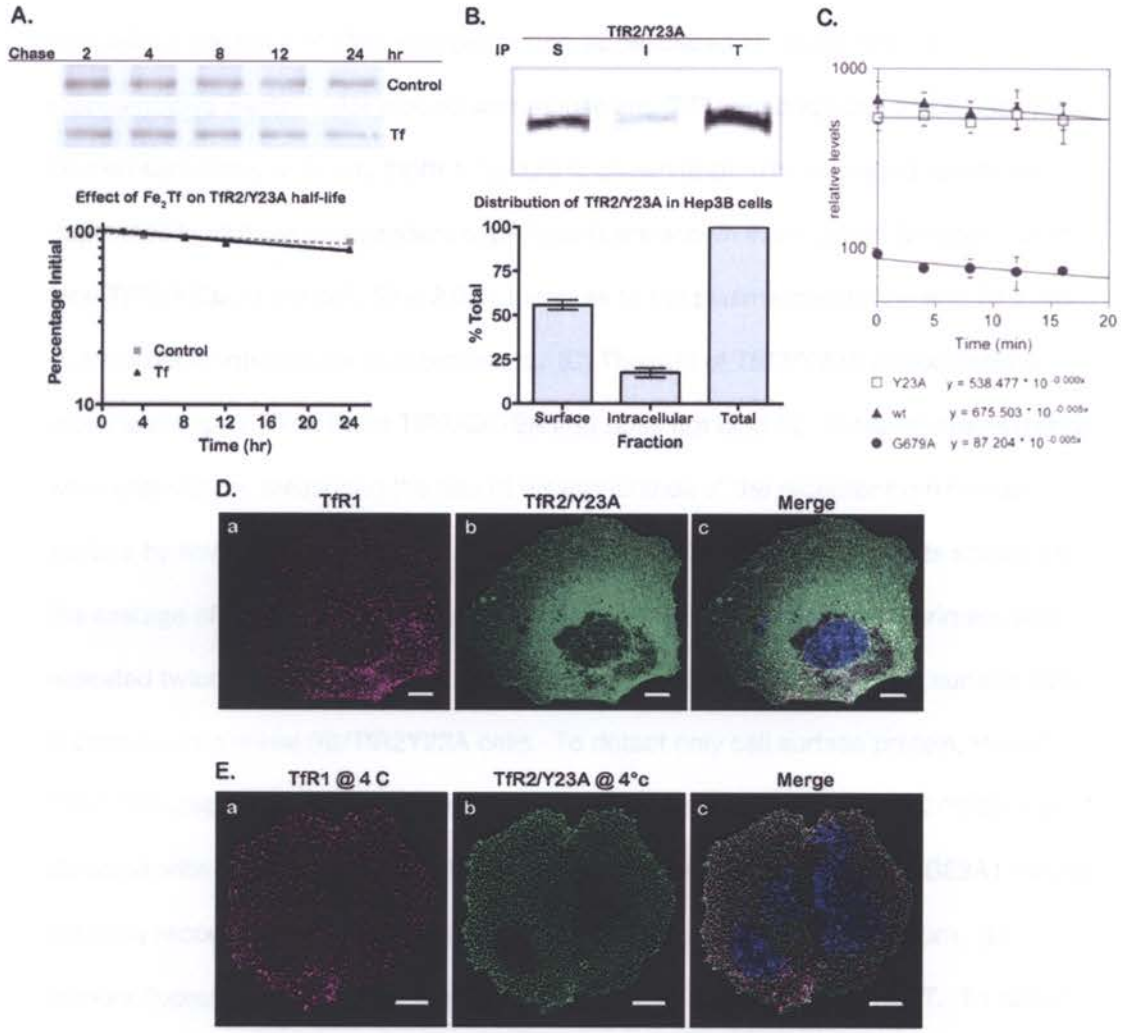

Figure 17. A tyrosine in the cytoplasmic domain of TfR2 is critical for internalization. (A) TfR2/Y23A is stable in the presence and absence of Fe_2Tf. Hep3B/TfR2Y23A cells were seeded and labeled as described in Figure 13B. Labeled TfR2/Y23A was immunoprecipitated and detected as described in Materials & Methods. Representative autoradiogram shows only a slight decrease in TfR2/Y23A level over the course of a 24 hr pulse in both untreated and Fe_2Tf-treated cells. The mean of measurements from two independent experiments are shown in the graph (bottom). The half-life of TfR2/Y23A in both conditions is > 60 hr. (B) Mutation Y23A alters TfR2 distribution. Hep3B/TfR2Y23A cells were seeded at 2.5 x 10^4 cells/cm^2 in 24-well plates

and cultured for 2 days. Differential immunoprecipitation to isolate surface and intracellular fractions of TfR2 was performed as described in Figure 12B. A representative western blot probed with mouse anti-TfR2 antibody and a fluorescence-labeled secondary antibody (both 1:10,000) is shown (top). The averaged results of duplicates from three independent experiments are shown in the graph (bottom). Of the total TfR2/Y23A in the cell, 58 ± 2.0 % localizes to the plasma membrane and 19 ± 3.0 % localizes to intracellular compartments. (C) The rate of TfR2/Y23A endocytosis is much less than TfR2/WT and TfR2/G679A that does not bind Tf. Rates of internalization were analyzed by measuring the rate of disappearance of the receptor from the cell surface by flow cytometry as described in Materials & Methods. The results shown are the average of three separate transfections with each construct. The experiment was repeated twice with similar results. (D) Immunofluorescent labeling of cell surface TfR2 is conspicuous in Hep3B/TfR2Y23A cells. To detect only cell surface protein, Hep3B/ TfR2Y23A cells were seeded and labeled as described in Figure 14A. TfR2/Y23A was detected with 16637 rabbit anti-TfR2 serum (b). TfR1 was detected with 3B82A1 mouse antibody recognizing the extracellular domain of TfR1 (a). Scale bar is 10 μm. (E) Immunofluorescent labeling of total TfR2/Y23A is similar to that of TfR2/WT. To detect total protein by immunofluorescence, cells were fixed, permeabilized, and labeled as described in Materials & Methods. TfR1 is shown in magenta (a), TfR2 is shown in green (b), and colocalization is shown in white (c). Nuclei are visible in blue in the merged image. Scale bar is 10 μm.

Discussion

In this study, we show that the regulation of TfR2 by its ligand is different from that of other membrane receptors. Ligand binding to growth factor receptors and G-protein coupled receptors triggers receptor endocytosis and degradation, thereby reducing the amount of surface and intracellular receptor (reviewed in Sorkin and Von Zastrow, 2002). The binding of Fe_2Tf to TfR2, by contrast, increases the amounts of surface and intracellular TfR2 by inhibiting receptor degradation. The amounts of surface and intracellular TfR2 increase proportionately. This indicates that the steady state distribution of TfR2 is unchanged and suggests that ligand binding neither stimulates nor inhibits endocytosis. An analysis of the kinetics of TfR2 trafficking is required to confirm this.

Fe_2Tf appears to play a direct role in the stabilization of TfR2. In transfected Hep3B cells, Fe_2Tf stabilizes TfR2/WT but does not stabilize TfR2/G679A, a mutated TfR2 that does not bind Fe_2Tf (Kawabata et al., 2004). Notably, the half-life of TfR2/G679A is shorter than that of TfR2 endogenously expressed in HepG2 cells (Johnson and Enns, 2004) and of TfR2/WT stably overexpressed in Hep3B/TfR2WT cells. This is consistent with the finding that TfR2, unlike TfR1, binds appreciably to bovine Fe_2Tf, which is present in tissue culture serum (Kawabata et al., 2004). Medium supplemented with 10% fetal bovine serum (FBS) contains approximately 2.5 μM (0.2 mg/mL) bovine Tf (Kakuta et al., 1997), a variable fraction of which is fully saturated with iron and capable of binding to TfR2. Thus, under standard cell culture conditions, TfR2 levels reflect a basal stabilization by bovine Fe_2Tf.

Monoubiquitination of membrane proteins at cytoplasmic lysine residues targets them to lysosomes for degradation. We had hypothesized that monoubiquitination of

TfR2 at lysine 31, the only lysine in the intracellular domain of TfR2, might target TfR2 for degradation. Thus, mutating the lysine to alanine would stabilize TfR2, and TfR2 would no longer be regulated by Fe_2Tf. However, the mutation K31A did not affect regulation of TfR2 by Fe_2Tf. Our preliminary characterization of the K31A mutation does not exclude the possibility that ubiquitination of lysine 31 might regulate TfR2 in other ways.

We have identified a residue within the cytoplasmic domain of TfR2 that is critical for TfR2 trafficking. Mutation of tyrosine 23 to alanine resulted in a redistribution of the receptor to the cell surface in Hep3B/TfR2Y23A cells. Tyrosine 23 is part of a tyrosine-based, putative endocytic motif, YQRV, at residues 23-26. Tyrosine-based motifs patterned as YXXØ, where Ø represents a hydrophobic amino acid, function as sorting signals in the intracellular domains of membrane proteins (reviewed in Mellman and Simons, 1992; Marks et al., 1997; Bonifacino and Traub, 2003). The tyrosine residue is required to mediate interaction with the medium (μ) subunit of adaptor protein (AP) complexes. APs interact with clathrin and thereby concentrate YXXØ-containing proteins in clathrin-coated pits. Our results indicate that tyrosine 23 mediates internalization of TfR2. This is likely to involve the interaction of TfR2 with AP-2, which functions at the plasma membrane. In the case of TfR1, a cargo-specific adaptor protein, called TfR trafficking protein (TTP), is also critical for endocytosis (Tosoni et al., 2005). TTP binds to TfR1 and the endocytic machinery. Whether such an adaptor protein might also specifically mediate TfR2 endocytosis is not known. AP-1 and AP-3 interact with a subset of YXXØ motifs to mediate vesicle transport between endosomes and the TGN and to lysosomes and lysosomal-like compartments, respectively.

Whether the YQRV motif has additional roles in directing TfR2 trafficking remains to be determined.

Even though the endocytic motifs of TfR1 and TfR2 are similar, the trafficking of these receptors differs. We found that the two receptors only partially colocalized. In addition, Tf traffics to late endosomal compartments in HeLa cells transfected with TfR2 but not in untransfected cells expressing only endogenous TfR1 (Robb et al., 2004). This implies a possible role for TfR2 in Tf sequestration distinct from TfR1. Finally, whereas Fe_2Tf does not affect the trafficking of TfR1, which internalizes constitutively and recycles (Watts, 1985), it does alter the trafficking of TfR2, redirecting it from a degradative pathway to a recycling pathway.

The mechanism by which Fe_2Tf binding to the extracellular domain of TfR2 regulates receptor stability and trafficking is unclear. Ligand binding to the extracellular domain might reposition TfR2 medially in the membrane. This could bury or expose sites for protein interaction or post-transcriptional modification. Alternatively, such repositioning could alter the proximity of residues to the membrane which can in some cases affect their ability to function as targeting signals (Rohrer et al., 1996). Ligand binding might also disrupt or facilitate interaction between the extracellular domain of TfR2 and a second membrane protein whose intracellular domain is positioned to interact or mediate an interaction with the intracellular domain of TfR2. In such a way, an extracellular event could trigger an intracellular response.

The consequence of ligand-induced stabilization, by increasing receptor number, could be the augmentation of a constitutive receptor function, be it signaling, delivering ligand, or interacting with other proteins. Regulated in such a manner, modulation of receptor number could relay changes in ligand concentration. In the

present case, this would enable changes in transferrin saturation to modulate processes that maintain iron homeostasis. In healthy individuals, the degree to which Tf in the circulation is saturated with iron generally reflects the supply of iron in the body. Because TfR2 is expressed in hepatocytes, it is positioned to regulate the expression of hepcidin, a small peptide hormone synthesized and secreted by hepatocytes that controls systemic iron levels by modulating cellular iron efflux (Nicolas et al., 2001; Nicolas et al., 2002; Pigeon et al., 2001; Roetto et al., 2003; Nemeth et al., 2004). Consistent with this hypothesis, individuals and mice with disease-causing mutations in TfR2 fail to regulate hepcidin appropriately (Kawabata et al., 2005; Nemeth et al., 2005). TfR2 might, therefore, sense systemic iron levels through interaction with its ligand.

Materials & Methods

Reagents and antibodies

Bovine serum albumin was obtained from Intergen (Burlington, MA). Bafilomycin, cycloheximide, poly-L-lysine, ovalbumin, and saponin were obtained from Sigma-Aldrich (St. Louis, MO). Paraformaldehyde was from Electron Microscopy Sciences (Hatfield, PA). EasyTag Express Protein Labeling Mix containing [35S]-cysteine/ methionine was obtained from PerkinElmer Life and Analytical Sciences (Boston, MA). Generation of anti-TfR1 monoclonal antibody 3B82A1, anti-TfR2 monoclonal antibody 9F81C11, and anti-TfR2 rabbit serum was described previously (Vogt et al., 2003; Johnson and Enns, 2004). H4A3 anti-LAMP1 ascites, developed by J.T. August and J. E. K. Hildreth, was obtained from the Developmental Studies Hybridoma Bank (University of Iowa, Iowa City, Iowa) under the auspices of the National Institute of Child

Health and Human Development. Other primary antibodies were obtained from the following companies: mouse anti-β-actin, mouse anti-γ adaptin, and rabbit anti-Rab7 from Sigma-Aldrich (St. Louis, MO); mouse anti-EEA1 from Abcam (Cambridge, UK); mouse anti-Golgin97 from Invitrogen (Carlsbad, CA); and H68.4 mouse anti-TfR1 from Zymed Laboratories (San Francisco, CA). HRP-conjugated secondary antibodies were purchased from Chemicon (Temecula, CA). Fluorescently-labeled Alexa 488, Alexa 543, and Alexa 680 secondary antibodies were from Invitrogen. Fluorescently-labeled IRDye 800 secondary antibody was from Rockland Immunochemicals (Gilbertsville, PA).

Constructs

Full-length *TfR2* transcript was amplified by PCR from HepG2 cDNA using the forward primer 5'-gaattcgcaggcttcaggaggggacacaagcatg-3' and the reverse primer 5'-gcggccgcggcttattgatatcaggtgg-3', designed to introduce flanking EcoR1 and Not1 restriction sites, respectively. The PCR product was cloned into a pGemT (Promega, Madison, WI) vector and subcloned into a pcDNA3.1+/Neo vector (Invitrogen, Carlsbad, CA). Mutations were introduced by site-directed mutagenesis using the QuikChange XL Kit (Stratagene, La Jolla, CA).

Cell culture

HepG2 and Hep3B human hepatoma cells obtained from American Type Culture Collection (ATCC, Manassas, VA) were cultured in Minimal Essential Medium (MEM, Life Technologies, Inc.) supplemented with 10% fetal bovine serum (FBS), 1.0 mM sodium pyruvate, and 0.1 mM non-essential amino acids (Life Technologies, Inc.). For metabolic labeling, cells were washed twice with PBS and incubated in labeling medium (MEM without l-methionine or l-glutamine (PromoCell, Heidelberg, Germany)

supplemented with 10% FBS, 1.0 mM sodium pyruvate, 0,1 mM non-essential amino acids, and 100 μM [^{35}S]-cysteine/methionine) without or with 25 μM Fe_2Tf for the indicated times at 37°C.

Transfection

Hep3B cells, seeded at 3.1 x 10^4 cells/cm^2 16 hr earlier, were transfected in Opti-MEM (Invitrogen) using Lipofectamine (Invitrogen) according to the manufacturer's instructions, 0.2 μg/cm^2 plasmid, and a Lipofectamine:DNA ratio of 2.5 (μL/μg). Normal medium was replaced 4 hr later. For stable transfections in 6-well plates, cells were split to 4 (100 mm) dishes 3 days later and selected with 400 μg/mL G418 (Calbiochem, SanDiego, CA). Colonies were picked after two weeks. For transient transfections in 60 mm dishes, cells were split to 6 (4 mm) wells 30 hr later, cultured for 16 hr, and then cultured for an additional 24 hr in the absence or presence of 25 μM Fe_2Tf. This approach was found to minimize fluctuations in expression level that result from variations in transient transfection efficiency.

Sodium dodecycl sulfide-polyacrylamide gel electrophoresis and western blot

Cells were lysed in NETT (150 mM NaCL, 5 mM EDTA (ethylenediaminetetraacetic acid), 10 mM Tris base (tris(hydroxymethyl)aminomethane), pH 7.4 with 1.0% (v/v) Triton X-100) with 1x Complete Mini Protease Inhibitor cocktail (Roche Diagnostic Corp., Indianapolis, IN) on ice for 15 min. Lysates were collected and cleared by centrifugation at 5000 x g for 15 min. Total protein concentration was measured by bicinchoninic acid assay (Pierce, Rockford, IL). Samples containing 10-20 μg total protein were diluted into 4x Laemmli buffer, heated to 95°C for 5 min, loaded on 10% denaturing gels, and analyzed by SDS-PAGE, followed by western blot with HRP-

conjugated or fluorescence-conjugated secondary antibodies as described previously (Johnson and Enns, 2004).

Immunofluorescence

The subcellular localization of TfR2 was assessed by double-labeling immunofluorescent detection. For colocalization with Rab7, TfR2 was detected using the purified IgG fraction of the 9F81C11 mouse anti-TfR2 supernatant (4.8 µg/mL), and Rab7 was detected with a rabbit polycolonal antibody (1:1000). For colocalization with all other markers, TfR2 was detected using the purified IgG fraction of the 16637 rabbit anti-TfR2 polyclonal anti-serum (8 µg/mL). Established markers of other intracellular compartments were detected with various mouse monoclonal antibodies as follows: TfR1 (3B82A1 at 1.5 µg/mL, H68.4 at 1:500), EEA1 (1:100), AP-1 (1:100), Golgin97 (1:125). Rabbit polyclonal antibodies were detected with goat anti-rabbit AlexaFluor 488 (1:500). Mouse monoclonal antibodies were detected with goat anti-mouse AlexaFluor 543 (1:500).

For colocalization with Rab7, cells were rinsed twice with wash buffer (1.8 mM calcium chloride, 2.5 mM magnesium acetate, 75 mM potassium acetate, 25 mM HEPES, pH 7.2), permeabilized and extracted with permeabilization buffer (0.1% saponin (w/v) and 0.1% bovine serum albumin (w/v) in wash buffer) for 30 min at RT, rinsed twice with wash buffer, fixed in 2% (v/v) paraformaldehyde in PBS for 30 min at RT, rinsed twice with wash buffer, and quenched with 10 mM glycine in wash buffer for 10 min at RT. All subsequent dilutions and washes were done with permeabilization buffer to maintain cell permeabilization. Cells were incubated in primary antibodies for 30 min, washed three times for 5 min, incubated with secondary antibodies for 30 min,

and washed five times for 5 min. Coverslips were rinsed an additional three times in wash buffer and two times in distilled deionized water prior to mounting.

For colocalization of TfR2 with all other markers, cells were washed twice in Hank's Balanced Salt Solution (HBSS, Sigma-Aldrich), fixed for 15 min with 4% (v/v) paraformaldehyde in HBSS, quenched for 10 min in 10 mM glycine in HBSS, permeabilized for 10 min with 0.2% Triton-X 100 in HBSS, and blocked with 3% BSA in HBSS for 30 min at room temperature. Cells were incubated in primary antibodies, diluted into 3% BSA in HBSS, for 30 min, washed three times for 5 min with HBSS, incubated with secondary antibodies diluted in 3% BSA in HBSS for 30 min, washed five times for 5 min with HBSS, and rinsed twice with distilled deionized water. Where indicated, nuclei were stained by addition of ToPro3 (1:1000, Molecular Probes/ Invitrogen) to the secondary antibody incubation. Coverslips were mounted in ProLong Gold anti-fade reagent (Molecular Probes/Invitrogen, Eugene OR).

Confocal microscopy

Images were acquired by laser-scanning confocal microscopy using the Zeiss X100/1.45 NA oil immersion objective lens (α Plan-Fluar) on a Zeiss LSM 5 Pascal confocal inverted microscope. AlexaFluor 543 and AlexaFluor 488 signals were sequentially excited with helium neon (543 nm) and argon (488 nm) lasers, respectively, and obtained using the multi-tracking function. Colocalization was quantified using the colocalization module in Pascal. After correcting for background in each image, colocalization was assessed as the fraction of TfR2 pixels colocalizing with TfR1, EEA1, Golgin97, AP-1, or Rab7 pixels.

Immunoprecipitation of [35]S-labeled TfR2

At the indicated times, cells were placed on ice, washed two times with ice-cold PBS, and lysed in NETT with 1 mg/mL ovalbumin. Lysates were pre-cleared with 50 µL Pansorbin for 1 hr at 4°C. Pansorbin was pelleted by centrifugation for 2 min at 13,000 x g. The cleared lysate was then transferred to a tube containing 2.5 µL of 16637 rabbit anti-TfR2 antiserum pre-bound to 50 µL Pansorbin and immunoprecipitated for 1 hr at 4°C. The sample was pelleted, resuspended in 100 µL NETT/ovalbumin, and washed through NETT/ovalbumin containing 15% sucrose (w/v). Sample was resuspended in 50 µL 2x Laemmli buffer (Laemmli, 1970), heated at 95°C for 5 min, centrifuged at 13,000 x g for 2 min to pellet Pansorbin, and electrophoresed through a reducing 10% SDS-PAGE gel. The gel was then dried and exposed to a Phosphorimager screen (Molecular Dynamics) for quantification and film for image acquisition.

Rates of endocytosis of WT, Y23A, and G679A TfR2

Hep3B cells, seeded at 2.8 x 104 cells/cm2 16 hr earlier in 10 cm plates, were transfected in Opti-MEM (Invitrogen) using 12 µg WT, Y23A, or G679A TfR2 plasmid and 36 µL Lipofectamine (Invitrogen) according to the manufacturer's instructions. MEM containing 20% FBS was added to the plates 6 hr later and replaced 24 hr later by growth medium. Forty-eight hours after transfection both the plasmid-transfected and mock-transfected Hep3B cells were washed twice with ice-cold PBS and then detached from 10 cm dishes using cell dissociation buffer (Gibco) for 10 minutes at 37° C. Cells were collected, divided into five tubes, and pelleted by centrifugation at 1500 rpm for 5 minutes. To label cell-surface TfR2, cells were incubated in 25 µg/ml rabbit anti-TfR2 serum diluted in ice-cold FACS staining buffer (FSB: Hank's balanced salt solution without Ca, Mg or phenol red, 10mM HEPES, pH 7.4, 1% FBS) on ice for 30

minutes, after which they were washed by under-layering with FBS and centrifugation. Cells were transferred to 37° C assay medium for 0, 4, 8, 12, 16 minutes in 5% CO2 to allow for internalization of TfR2/anti-TfR2 complexes. Cells were then fixed in 4% paraformaldehyde-PBS for 20 minutes on ice. The fixed cells were washed once with cold FSB. Uninternalized antibody was detected by incubating cells with an Alexa Fluor-488 goat anti-rabbit secondary antibody (1:600 dilution in FSB) for 30 min on ice followed by washing with cold FBS. Surface antibody was quantified by fluorescence flow cytometry using a Becton Dickinson FACSCalibur flow cytometer. Profiles were gated on intact cells based on morphology. Arithmetic mean fluorescent intensity, at each time t, was subtracted from the Hep3B mock-transfected control.

Chapter IV

Conclusion

Fe_2Tf stabilizes TfR2 in hepatoma cells. This regulation is specific to the interaction of Fe_2Tf with TfR2: TfR2 is not stabilized by iron or by the binding of Fe_2Tf to TfR1. Significantly, TfR2 is half-maximally stabilized by concentrations of Fe_2Tf in the range of 1 - 3 μM, which approximates the concentration of Fe_2Tf in the serum of a healthy individual. The finding that TfR2 protein level is elevated in mice with high serum Tf concentrations and reduced in mice with low serum concentrations (Robb and Wessling-Resnick, 2004) substantiates the physiological relevance of this finding.

Mutation of a glycine in the extracellular domain of TfR2 that is critical for Fe_2Tf-binding precludes receptor stabilization. Thus, Fe_2Tf must interact directly with TfR2 to inhibit the receptor's degradation. This mode of regulation is unusual. Ligand-binding often causes membrane receptors to be ubiquitinated and targeted to the lysosome for degradation, as with EGFR and β-adrenergic receptor, for example. By contrast, TfR2 undergoes lysosomal degradation, but at a slower rate upon binding Fe_2Tf. Mutation of the only lysine in the cytoplasmic domain of TfR2 does not affect its response to Fe_2Tf. Either ubiquitination does not mediate TfR2 degradation, or Fe_2Tf further enhances the stability conferred by the lysine mutation.

The mechanism by which Fe_2Tf stabilizes TfR2 involves a change in the trafficking of the receptor. TfR2 localizes to early, recycling, and late endosomes, as well as to the plasma membrane and the trans-Golgi network. This pattern of localization is consistent with the trafficking of TfR2 along biosynthetic, recycling, and degradative pathways. Ligand binding directs TfR2 into a recycling pathway, thereby reducing degradation and increasing receptor number.

Proper trafficking of TfR2 through endosomal compartments depends upon a tyrosine in the cytoplasmic domain of TfR2. This tyrosine, at residue 23, is part of

YXXØ motif. Such motifs in the cytoplasmic domain of membrane proteins typically mediate recruitment into clathrin-coated vesicles. The failure of TfR2 to internalize when tyrosine 23 is mutated to alanine implicates the YQRV sequence as an endocytic motif. By inhibiting endocytosis, the Y23A mutation prevents degradation of TfR2 and supersedes stabilization by Fe_2Tf.

Redirection of TfR2 to a recycling pathway may do more than increase receptor number by delaying degradation. Endocytosis delivers membrane receptors to intracellular compartments where they encounter molecules that differentially modify their activity (reviewed in Sorkin and Von Zastrow, 2002; Miaczynska et al., 2004; Polo and Di Fiore, 2006). EGFR signaling continues after internalization in a manner that is dependent on molecules associated with particular endosomes and therefore distinct from signaling at the plasma membrane (Teis et al., 2002). Transforming growth factor-β (TGF-β) signaling and degradation are regulated by its delivery to particular endosomes (Di Guglielmo et al., 2003). Clathrin-independent endocytosis (CIE) delivers TGF-β receptors to caveolin-positive endosomes where a ubiquitin ligase complex promotes their degradation. By contrast, clathrin-mediated endocytosis (CME) delivers TGF-β receptors to EEA1-positive endosomes where an anchor protein facilitates their interaction with downstream effectors and thereby promotes their signaling . Thus, the trafficking of TGF-β affects not only its stability, but also its activity. Recycling of TfR2 may be important because it alters TfR2 localization, and thus possibly its interaction with other proteins that mediate its regulation of hepcidin. If TfR2 interacts with HFE, as recently reported (Goswami and Andrews, 2006), the co-trafficking of HFE with TfR2 to a particular compartment in response to Fe_2Tf binding might also be significant. HFE has a short cytoplasmic domain with limited capacity to mediate interactions that

regulate the protein's localization. Co-trafficking with TfR2, though, could direct HFE to subcellular compartments from which HFE relays a signal to regulate hepcidin.

We hypothesized that TfR2 senses body iron levels by sensing the concentration of Fe_2Tf in the circulation. This hypothesis predicts that changes in the concentration of Fe_2Tf will induce a response from TfR2 and that this response will modulate the expression of hepcidin. Our results validate the first prediction and suggest ways by which to test the second in the absence of a cell culture system in which iron regulates hepcidin. If binding of Fe_2Tf to TfR2 relays a signal that modulates hepcidin expression, transgenic expression in mice of a TfR2 mutant unable to bind Fe_2Tf (TfR2/G679A) should disrupt iron homeostasis and cause hemochromatosis. Further insight into the mechanism by which TfR2 mediates iron homeostasis could be gained from transgenic expression of a TfR2 mutant that does not traffic properly (TFR2/Y23A, for example). Such a mutant might reveal whether TfR2 trafficking to or signaling from a particular location is important for its function.

References

Abboud, S., and Haile, D. J. (2000). A novel mammalian iron-regulated protein involved in intracellular iron metabolism. J. Biol. Chem. *275*, 19906-19912.

Adrian, G. S. *et al.* (1990). Human transferrin. Expression and iron modulation of chimeric genes in transgenic mice. J. Biol. Chem. *265*, 13344-13350.

Ahmad, K. A., Ahmann, J. R., Migas, M. C., Waheed, A., Britton, R. S., Bacon, B. R., Sly, W. S., and Fleming, R. E. (2002). Decreased liver hepcidin expression in the hfe knockout mouse. Blood Cells Mol. Dis. *29*, 361-366.

Alvarez, E., Girones, N., and Davis, R. J. (1990). A point mutation in the cytoplasmic domain of the transferrin receptor inhibits endocytosis. Biochem. J. *267*, 31-35.

Andrews, N. C. (1999). Disorders of iron metabolism. N. Engl. J. Med. *341*, 1986-1995.

Andrews, N. C. (2000b). Inherited iron overload disorders. Curr. Opin. Pediatr. *12*, 596-602.

Andrews, N. C. (2000a). Iron homeostasis: insights from genetics and animal models. Nat. Rev. Genet. *1*, 208-217.

Babitt, J. L. *et al.* (2006). Bone morphogenetic protein signaling by hemojuvelin regulates hepcidin expression. Nat. Genet. *38*, 531-539.

Barnum-Huckins, K., and Adrian, G. S. (2000). Iron regulation of transferrin synthesis in the human hepatoma cell line HepG2. Cell Biol Int *24*, 71-77.

Biasiotto, G., Belloli, S., Ruggeri, G., Zanella, I., Gerardi, G., Corrado, M., Gobbi, E., Albertini, A., and Arosio, P. (2003). Identification of new mutations of the HFE, hepcidin, and transferrin receptor 2 genes by denaturing HPLC analysis of individuals with biochemical indications of iron overload. Clin. Chem. *49*, 1981-1988.

Bernstein, S. E. (1987). Hereditary hypotransferrinemia with hemosiderosis, a murine disorder resembling human atransferrinemia. J. Lab. Clin. Med. *110*, 690-705.

Bonifacino, J. S., and Traub, L. M. (2003). Signals for sorting of transmembrane proteins to endosomes and lysosomes. Annu. Rev. Biochem. *72*, 395-447.

Bothwell, T. H., Charlton, R. W., and Motulsky, A. G. (1995). The Metabolic and Molecular Basis of Inherited Disease. Chapter 69, Hemochromatosis *II*, 2237-2269.

Bowman, E. J., Siebers, A., and Altendorf, K. (1988). Bafilomycins: a class of inhibitors of membrane ATPases from microorganisms, animal cells, and plant cells. Proc. Natl. Acad. Sci. USA *85*, 7972-7976.

Calzolari, A., Deaglio, S., Sposi, N. M., Petrucci, E., Morsilli, O., Gabbianelli, M., Malavasi, F., Peschle, C., and Testa, U. (2004). Transferrin receptor 2 protein is not expressed in normal erythroid cells. Biochem.. J. *381*, 629-634.

Camaschella, C., Fargion, S., Sampietro, M., Roetto, A., Bosio, S., Garozzo, G., Arosio, C., and Piperno, A. (1999). Inherited HFE-unrelated hemochromatosis in Italian families. Hepatology *29*, 1563-1564.

Camaschella, C., Roetto, A., Cali, A., De Gobbi, M., Garozzo, G., Carella, M., Majorano, N., Totaro, A., and Gasparini, P. (2000). The gene TFR2 is mutated in a new type of haemochromatosis mapping to 7q22. Nat. Genet. *25*, 14-15.

Casey, J. L., Hentze, M. W., Koeller, D. M., Caughman, S. W., Rouault, T. A., Klausner, R. D., and Harford, J. B. (1988). Iron-responsive elements: regulatory RNA sequences that control mRNA levels and translation. Science *240*, 924-928.

Chavrier, P., Parton, R. G., Hauri, H. P., Simons, K., and Zerial, M. (1990). Localization of low molecular weight GTP binding proteins to exocytic and endocytic compartments. Cell *62*, 317-329.

Cheng, Y., Zak, O., Aisen, P., Harrison, S. C., and Walz, T. (2004). Structure of the human transferrin receptor-transferrin complex. Cell *116*, 565-576.

Collawn, J. F., Stangel, M., Kuhn, L. A., Esekogwu, V., Jing, S. Q., Trowbridge, I. S., and Tainer, J. A. (1990). Transferrin receptor internalization sequence YXRF implicates a tight turn as the structural recognition motif for endocytosis. Cell *63*, 1061-1072.

Courselaud, B. *et al.* (2002). C/EBPalpha regulates hepatic transcription of hepcidin, an antimicrobial peptide and regulator of iron metabolism. Cross-talk between C/EBP pathway and iron metabolism. J. Biol. Chem. *277*, 41163-41170.

Cox, L. A., and Adrian, G. S. (1993). Posttranscriptional regulation of chimeric human transferrin genes by iron. Biochemistry *32*, 4738-4745.

Cox, L. A., Kennedy, M. C., and Adrian, G. S. (1995). The 5'-untranslated region of human transferrin mRNA, which contains a putative iron-regulatory element, is bound by purified iron-regulatory protein in a sequence-specific manner. Biochem. Biophys. Res. Commun. *212*, 925-932.

Dautry-Varsat, A., Ciechanover, A., and Lodish, H. F. (1983). pH and the recycling of transferrin during receptor-mediated endocytosis. Proc. Natl. Acad. Sci. USA *80*, 2258-2262.

Davies, P. S., and Enns, C. A. (2004). Expression of the Hereditary Hemochromatosis Protein HFE Increases Ferritin Levels by Inhibiting Iron Export in HT29 Cells. J. Biol. Chem. *279*, 25085-25092.

De Domenico, I., Ward, D. M., Nemeth, E., Vaughn, M. B., Musci, G., Ganz, T., and Kaplan, J. (2005). The molecular basis of ferroportin-linked hemochromatosis. Proc. Natl. Acad. Sci. USA *102*, 8955-8960.

Devalia, V., Carter, K., Walker, A. P., Perkins, S. J., Worwood, M., May, A., and Dooley, J. S. (2002). Autosomal dominant reticuloendothelial iron overload associated with a 3-base pair deletion in the ferroportin 1 gene (SLC11A3). Blood *100*, 695-697.

Di Guglielmo, G. M., Le Roy, C., Goodfellow, A. F., and Wrana, J. L. (2003). Distinct endocytic pathways regulate TGF-beta receptor signalling and turnover. Nat. Cell Biol. *5*, 410-421.

Donovan, A., Brownlie, A., Dorschner, M. O., Zhou, Y., Pratt, S. J., Paw, B. H., Phillips, R. B., Thisse, C., Thisse, B., and Zon, L. I. (2002). The zebrafish mutant gene chardonnay (cdy) encodes divalent metal transporter 1 (DMT1). Blood *100*, 4655-4659.

Donovan, A. *et al.* (2000). Positional cloning of zebrafish ferroportin1 identifies a conserved vertebrate iron exporter. Nature *403*, 776-781.

Drakesmith, H. *et al.* (2005). Resistance to hepcidin is conferred by hemochromatosis-associated mutations of ferroportin. Blood *106*, 1092-1097.

Drakesmith, H., Sweetland, E., Schimanski, L., Edwards, J., Cowley, D., Ashraf, M., Bastin, J., and Townsend, A. R. (2002). The hemochromatosis protein HFE inhibits iron export from macrophages. Proc. Natl. Acad. Sci. USA *99*, 15602-15607.

Dubljevic, V., Sali, A., and Goding, J. W. (1999). A conserved RGD (Arg-Gly-Asp) motif in the transferrin receptor is required for binding to transferrin. Biochem. J. *341*, 11-14.

Enns, C. A. (2001). Pumping iron: the strange partnership of the hemochromatosis protein, a class I MHC homolog, with the transferrin receptor. Traffic *2*, 167-174.

Enns, C. A., Clinton, E. M., Reckhow, C. L., Root, B. J., Do, S. I., and Cook, C. (1991). Acquisition of the functional properties of the transferrin receptor during its biosynthesis. J. Biol. Chem. *266*, 13272-13277.

Enns, C. A., and Sussman, H. H. (1981). Similarities between the transferrin receptor proteins on human reticulocytes and human placentae. J. Biol. Chem. *256*, 12620-12623.

Feder, J. N. *et al.* (1997). The hemochromatosis founder mutation in HLA-H disrupts b2-microglobulin interaction and cell surface expression. J. Biol. Chem. *272*, 14025-14028.

Feder, J. N. *et al.* (1996). A novel MHC class I-like gene is mutated in patients with hereditary haemochromatosis. Nat. Genet. *13*, 399-408.

Feder, J. N., Penny, D. M., Irrinki, A., Lee, V. K., Lebron, J. A., Watson, N., Tsuchihashi, Z., Sigal, E., Bjorkman, P. J., and Schatzman, R. C. (1998). The hemochromatosis gene product complexes with the transferrin receptor and lowers its affinity for ligand binding. Proc. Natl. Acad. Sci. USA *95*, 1472-1477.

Fleming, M. D., Romano, M. A., Su, M. A., Garrick, L. M., Garrick, M. D., and Andrews, N. C. (1998). Nramp2 is mutated in the anemic Belgrade (b) rat: evidence of a role for Nramp2 in endosomal iron transport. Proc. Natl. Acad. Sci. USA *95*, 1148-1153.

Fleming, M. D., Trenor, C. C., 3rd, Su, M. A., Foernzler, D., Beier, D. R., Dietrich, W. F., and Andrews, N. C. (1997). Microcytic anaemia mice have a mutation in Nramp2, a candidate iron transporter gene. Nat. Genet. *16*, 383-386.

Fleming, R. E., Ahmann, J. R., Migas, M. C., Waheed, A., Koeffler, H. P., Kawabata, H., Britton, R. S., Bacon, B. R., and Sly, W. S. (2002). Targeted mutagenesis of the murine transferrin receptor-2 gene produces hemochromatosis.Proc. Natl. Acad. Sci. USA *99*, 10653-10658.

Fleming, R. E., Migas, M. C., Holden, C. C., Waheed, A., Britton, R. S., Tomatsu, S., Bacon, B. R., and Sly, W. S. (2000). Transferrin receptor 2: continued expression in mouse liver in the face of iron overload and in hereditary hemochromatosis. Proc. Natl. Acad. Sci. USA *97*, 2214-2219.

Fleming, R. E., and Sly, W. S. (2001). Ferroportin mutation in autosomal dominant hemochromatosis: loss of function, gain in understanding. J. Clin. Invest. *108*, 521-522.

Fletcher, L. M., and Halliday, J. W. (2002). Haemochromatosis: Understanding the mechanism of disease and implications for diagnosis and patient management following the recent cloning of novel genes involved in iron metabolism. J. Intern. Med. *251*, 181-192.

Frazer, D. M., Wilkins, S. J., Becker, E. M., Vulpe, C. D., McKie, A. T., Trinder, D., and Anderson, G. J. (2002). Hepcidin expression inversely correlates with the expression of duodenal iron transporters and iron absorption in rats. Gastroenterology *123*, 835-844.

Frazer, D. M., Wilkins, S. J., Millard, K. N., McKie, A. T., Vulpe, C. D., and Anderson, G. J. (2004). Increased hepcidin expression and hypoferraemia associated with an acute phase response are not affected by inactivation of HFE. Br. J. Haematol. *126*, 434-436.

Gehrke, S. G., Kulaksiz, H., Herrmann, T., Riedel, H. D., Bents, K., Veltkamp, C., and Stremmel, W. (2003). Expression of hepcidin in hereditary hemochromatosis: evidence for a regulation in response to the serum transferrin saturation and to non-transferrin-bound iron. Blood *102*, 371-376.

Giannetti, A. M., Snow, P. M., Zak, O., and Bjorkman, P. J. (2003). Mechanism for Multiple Ligand Recognition by the Human Transferrin Receptor. PLoS Biol *1*, 341-350.

Goswami, T., and Andrews, N. C. (2006). Hereditary hemochromatosis protein, HFE, interaction with transferrin receptor 2 suggests a molecular mechanism for mammalian iron sensing. J. Biol. Chem. in press.

Gross, C. N., Irrinki, A., Feder, J. N., and Enns, C. A. (1998). Co-trafficking of HFE, a nonclassical major histocompatibility complex class I protein, with the transferrin receptor implies a role in intracellular iron regulation. J. Biol. Chem. *273*, 22068-22074.

Gunshin, H., Mackenzie, B., Berger, U. V., Gunshin, Y., Romero, M. F., Boron, W. F., Nussberger, S., Gollan, J. L., and Hediger, M. A. (1997). Cloning and characterization of a mammalian proton-coupled metal-ion transporter. Nature *388*, 482-488.

Hall, D.R., Hadden, J.M., Leonard, G.A., Bailey, S., Neu, M., Winn, M., and Lindley, P.F. (2002). The crystal and molecular structures of diferric porcine and rabbit serum transferrins at resolutions of 2.15 and 2.60 Å, respectively. Acta. Cryst. *D58*, 70-80.

Harris, Z. L., Durley, A. P., Man, T. K., and Gitlin, J. D. (1999). Targeted gene disruption reveals an essential role for ceruloplasmin in cellular iron efflux. Proc. Natl. Acad. Sci. USA *96*, 10812-10817.

Hentze, M. W., Caughman, S. W., Rouault, T. A., Barriocanal, J. G., Dancis, A., Harford, J. B., and Klausner, R. D. (1987). Identification of the iron-responsive element for the translational regulation of human ferritin mRNA. Science *238*, 1570-1573.

Hentze, M. W., Muckenthaler, M. U., and Andrews, N. C. (2004). Balancing acts: molecular control of mammalian iron metabolism. Cell *117*, 285-297.

Hinrichsen, L., Harborth, J., Andrees, L., Weber, K., and Ungewickell, E. J. (2003). Effect of clathrin heavy chain- and alpha-adaptin-specific small inhibitory RNAs on endocytic accessory proteins and receptor trafficking in HeLa cells. J. Biol. Chem. *278*, 45160-45170.

Holmstrom, P., Dzikaite, V., Hultcrantz, R., Melefors, O., Eckes, K., Stal, P., Kinnman, N., Smedsrod, B., Gafvels, M., and Eggertsen, G. (2003). Structure and liver cell expression pattern of the HFE gene in the rat. J. Hepatol. *39*, 308-314.

Hopkins, C., and Trowbridge, I. S. (1983). Internalization and processing of transferrin and the transferrin receptor in human carcinoma A431 cells. J. Cell Biol. *97*, 508-521.

Hopkins, C. R. (1983). Intracellular routing of transferrin and transferrin receptors in epidermoid carcinoma A431 cells. Cell *35*, 321-330.

Huang, F. W., Pinkus, J. L., Pinkus, G. S., Fleming, M. D., and Andrews, N. C. (2005). A mouse model of juvenile hemochromatosis. J. Clin. Invest. *115*, 2187-2191.

Huebers, H. A., Josephson, B., Huebers, E., Csiba, E., and Finch, C. A. (1984). Occupancy of the iron binding sites of human transferrin. Proc. Natl. Acad. Sci. USA *81*, 4326-4330.

Hunter, H. N., Fulton, D. B., Ganz, T., and Vogel, H. J. (2002). The solution structure of human hepcidin, a peptide hormone with antimicrobial activity that is involved in iron uptake and hereditary hemochromatosis. J. Biol. Chem. *277*, 37597-37603.

Jing, S. Q., Spencer, T., Miller, K., Hopkins, C., and Trowbridge, I. S. (1990). Role of the human transferrin receptor cytoplasmic domain in endocytosis: Localization of a specific signal sequence for internalization. J. Cell Biol. *110*, 283-294.

Johnson, M. B., and Enns, C. A. (2004). Diferric transferrin regulates transferrin receptor 2 protein stability. Blood *104*, 4287-4293.

Johnson, M. B., Murchison, N., Green, F. A., and Enns, C. A. (2006). Transferrin receptor 2: evidence for ligand-induced stabilization and redirection to a recycling pathway. submitted

Kakuta, K., Orino, K., Yamamoto, S., and Watanabe, K. (1997). High levels of ferritin and its iron in fetal bovine serum. Comp. Biochem. Physiol. A. Physiol. *118*, 165-169.

Kaplan, J. (2002). Mechanisms of Cellular Iron Acquisition: Another Iron in the Fire. Cell *111*, 603-606.

Kawabata, H., Fleming, R. E., Gui, D., Moon, S. Y., Saitoh, T., O'Kelly, J., Umehara, Y., Wano, Y., Said, J. W., and Koeffler, H. P. (2005). Expression of hepcidin is down-regulated in TfR2 mutant mice manifesting a phenotype of hereditary hemochromatosis. Blood *105*, 376-381.

Kawabata, H., Tong, X., Kawanami, T., Wano, Y., Hirose, Y., Sugai, S., and Koeffler, H. P. (2004). Analyses for binding of the transferrin family of proteins to the transferrin receptor 2. Br. J. Haematol. *127*, 464-473.

Kawabata, H., Germain, R. S., Ikezoe, T., Tong, X., Green, E. M., Gombart, A. F., and Koeffler, H. P. (2001a). Regulation of expression of murine transferrin receptor 2. Blood *98*, 1949-1954.

Kawabata, H., Germain, R. S., Vuong, P. T., Nakamaki, T., Said, J. W., and Koeffler, H. P. (2000). Transferrin receptor 2-alpha supports cell growth both in iron-chelated cultured cells and in vivo. J. Biol. Chem. *275*, 16618-16625.

Kawabata, H., Nakamaki, T., Ikonomi, P., Smith, R. D., Germain, R. S., and Koeffler, H. P. (2001b). Expression of transferrin receptor 2 in normal and neoplastic hematopoietic cells. Blood *98*, 2714-2719.

Kawabata, H., Yang, R., Hirama, T., Vuong, P. T., Kawano, S., Gombart, A. F., and Koeffler, H. P. (1999). Molecular cloning of transferrin receptor 2. A new member of the transferrin receptor-like family. J. Biol. Chem. *274*, 20826-20832.

Keeling, S. L., Gad, J. M., and Cooper, H. M. (1997). Mouse Neogenin, a DCC-like molecule, has four splice variants and is expressed widely in the adult mouse and during embryogenesis. Oncogene *15*, 691-700.

Klausner, R. D., Ashwell, G., van Renswoude, J., Harford, J. B., and Bridges, K. R. (1983). Binding of apotransferrin to K562 cells: Explanation of the transferrin cycle. Proc. Natl. Acad. Sci. USA *80*, 2263-2266.

Knutson, M. D., Oukka, M., Koss, L. M., Aydemir, F., and Wessling-Resnick, M. (2005). Iron release from macrophages after erythrophagocytosis is up-regulated by ferroportin 1 overexpression and down-regulated by hepcidin. Proc. Natl. Acad. Sci. USA *102*, 1324-1328.

Krause, A., Neitz, S., Magert, H. J., Schulz, A., Forssmann, W. G., Schulz-Knappe, P., and Adermann, K. (2000). LEAP-1, a novel highly disulfide-bonded human peptide, exhibits antimicrobial activity. FEBS Lett. *480*, 147-150.

Krijt, J., Vokurka, M., Chang, K. T., and Necas, E. (2004). Expression of Rgmc, the murine ortholog of hemojuvelin gene, is modulated by development and inflammation, but not by iron status or erythropoietin. Blood *104*, 4308-4310.

Kulaksiz, H., Gehrke, S. G., Janetzko, A., Rost, D., Bruckner, T., Kallinowski, B., and Stremmel, W. (2004). Pro-hepcidin: expression and cell specific localisation in the liver and its regulation in hereditary haemochromatosis, chronic renal insufficiency, and renal anaemia. Gut *53*, 735-743.

Kulaksiz, H., Theilig, F., Bachmann, S., Gehrke, S. G., Rost, D., Janetzko, A., Cetin, Y., and Stremmel, W. (2005). The iron-regulatory peptide hormone hepcidin: expression and cellular localization in the mammalian kidney. J Endocrinol *184*, 361-370.

Laemmli, U. K. (1970). Cleavage of structural proteins during the assembly of the head of bacteriophage T4. Nature *227*, 680-685.

Lawrence, C. M., Ray, S., Babyonyshev, M., Galluser, R., Borhani, D. W., and Harrison, S. C. (1999). Crystal structure of the ectodomain of human transferrin receptor. Science *286*, 779-782.

Lebron, J. A., Bennett, M. J., Vaughn, D. E., Chirino, A. J., Snow, P. M., Mintier, G. A., Feder, J. N., and Bjorkman, P. J. (1998). Crystal structure of the hemochromatosis protein HFE and characterization of its interaction with transferrin receptor. Cell *93*, 111-123.

Lebron, J. A., West, A. P. J., and Bjorkman, P. J. (1999). The hemochromatosis protein HFE competes with transferrin for binding to the transferrin receptor. J. Mol. Biol. *294*, 239-245.

Lee, P., Peng, H., Gelbart, T., and Beutler, E. (2004). The IL-6- and lipopolysaccharide-induced transcription of hepcidin in HFE-, transferrin receptor 2-, and beta 2-microglobulin-deficient hepatocytes. Proc. Natl. Acad. Sci. USA *101*, 9263-9265.

Lee, P., Peng, H., Gelbart, T., Wang, L., Beutler, E. (2005). Regulation of hepcidin transcription by interleukin-1 and interleukin-6. Proc. Natl. Acad. Sci. USA *102*, 1906-1910.

Levy, J. E., Jin, O., Fujiwara, Y., Kuo, F., and Andrews, N. C. (1999a). Transferrin receptor is necessary for development of erythrocytes and the nervous system. Nat. Genet. *21*, 396-399.

Levy, J. E., Montross, L. K., Cohen, D. E., Fleming, M. D., and Andrews, N. C. (1999b). The C282Y mutation causing hereditary hemochromatosis does not produce a null allele. Blood *94*, 9-11.

Lin, L., Goldberg, Y. P., and Ganz, T. (2005). Competitive regulation of hepcidin mRNA by soluble and cell-associated hemojuvelin. Blood *106*, 2884-2889.

Liu, X. B., Nguyen, N. B., Marquess, K. D., Yang, F., and Haile, D. J. (2005). Regulation of hepcidin and ferroportin expression by lipopolysaccharide in splenic macrophages. Blood Cells Mol. Dis. *35*, 47-56.

Lu, J. P., Hayashi, K., and Awai, M. (1989). Transferrin receptor expression in normal, iron-deficient and iron- overloaded rats. Acta. Pathol. Jpn *39*, 759-764.

MacGillivray, R. T. *et al.* (1998). Two high-resolution crystal structures of the recombinant N-lobe of human transferrin reveal a structural change implicated in iron release. Biochemistry *37*, 7919-7928.

Marks, M. S., Ohno, H., Kirchhausen, T., and Bonifacino, J. S. (1997). Protein sorting by tyrosine-based signals: adapting to the Ys and wherefores. Trends in Cell Biology *7*, 124-128.

Marks, M. S., Woodruff, L., Ohno, H., and Bonifacino, J. S. (1996). Protein targeting by tyrosine- and di-leucine-based signals: evidence for distinct saturable components. J. Cell Biol. *135*, 341-354.

Matsunaga, E., and Chedotal, A. (2004). Repulsive guidance molecule/neogenin: a novel ligand-receptor system playing multiple roles in neural development. Dev. Growth Differ. *46*, 481-486.

Mattia, E., Rao, D., Shapiro, D. S., Sussman, H. H., and Klausner, R. D. (1984). Biosynthetic regulation of the human transferrin receptor by desferrioxamine in K562 cells. J. Biol. Chem. *259*, 2689-2692.

McGraw, T., Greenfield, L., and Maxfield, F. R. (1987). Functional expression of the human transferrin receptor cDNA in Chinese hamster ovary cells deficient in endogenous transferrin receptor. J. Cell Biol. *105*, 207-214.

McGraw, T. E., and Maxfield, F. R. (1990). Human transferrin receptor internalization is partially dependent upon an aromatic amino acid on the cytoplasmic domain. Cell Regulation *1*, 369-377.

McKie, A. T. *et al.* (2001). An iron-regulated ferric reductase associated with the absorption of dietary iron. Science *291*, 1755-1759.

McKie, A. T. *et al.* (2000). A Novel Duodenal Iron-Regulated Transporter, IREG1, Implicated in the Basolateral Transfer of Iron to the Circulation. Molecular Cell *5*, 299-309.

Mellman, I., and Simons, K. (1992). The Golgi complex: in vitro veritas?. [Review] [126 refs]. Cell *68*, 829-840.

Meyerhardt, J. A., Look, A. T., Bigner, S. H., and Fearon, E. R. (1997). Identification and characterization of neogenin, a DCC-related gene. Oncogene *14*, 1129-1136.

Miaczynska, M., Pelkmans, L., and Zerial, M. (2004). Not just a sink: endosomes in control of signal transduction. Curr. Opin. Cell Biol. *16*, 400-406.

Monnier, P. P. *et al.* (2002). RGM is a repulsive guidance molecule for retinal axons. Nature *419*, 392-395.

Montosi, G., Donovan, A., Totaro, A., Garuti, C., Pignatti, E., Cassanelli, S., Trenor, C. C., Gasparini, P., Andrews, N. C., and Pietrangelo, A. (2001). Autosomal-dominant hemochromatosis is associated with a mutation in the ferroportin (SLC11A3) gene. J. Clin. Invest. *108*, 619-623.

Montosi, G., Paglia, P., Garuti, C., Guzman, C. A., Bastin, J. M., Colombo, M. P., and Pietrangelo, A. (2000). Wild-type HFE protein normalizes transferrin iron accumulation in macrophages from subjects with hereditary hemochromatosis. Blood *96*, 1125-1129.

Morgan, E. H. (1983). Synthesis and secretion of transferrin. In Plasma protein secretion by the liver, Glauman, H., T. J. Peters, and C. Redman, eds. (London ; New York: Academic Press), pp. 331-355.

Motley, A., Bright, N. A., Seaman, M. N., and Robinson, M. S. (2003). Clathrin-mediated endocytosis in AP-2-depleted cells. J. Cell Biol. *162*, 909-918.

Mu, F. T., Callaghan, J. M., Steele-Mortimer, O., Stenmark, H., Parton, R. G., Campbell, P. L., McCluskey, J., Yeo, J. P., Tock, E. P., and Toh, B. H. (1995). EEA1, an early endosome-associated protein. EEA1 is a conserved alpha-helical peripheral membrane protein flanked by cysteine "fingers" and contains a calmodulin-binding IQ motif. J. Biol. Chem. *270*, 13503-13511.

Muckenthaler, M., Roy, C. N., Custodio, A. O., Minana, B., DeGraaf, J., Montross, L. K., Andrews, N. C., and Hentze, M. W. (2003). Regulatory defects in liver and intestine implicate abnormal hepcidin and Cybrd1 expression in mouse hemochromatosis. Nat. Genet. *34*, 102-107.

Mukhopadhyay, C. K., Attieh, Z. K., and Fox, P. L. (1998). Role of ceruloplasmin in cellular iron uptake. Science *279*, 714-717.

Mullner, E. W., and Kuhn, L. C. (1988). A stem-loop in the 3' untranslated region mediates iron dependent regulation of transferrin receptor mRNA stability in the cytoplasm. Cell *53*, 815-825.

Mullner, E. W., Neupert, B., and Kuhn, L. C. (1989). A specific mRNA binding factor regulates the iron-dependent stability of cytoplasmic transferrin receptor mRNA. Cell *58*, 373-382.

Nemeth, E., Preza, G. C., Jung, C. L., Kaplan, J., Waring, A. J., and Ganz, T. (2006). The N-terminus of hepcidin is essential for its interaction with ferroportin: structure-function study. Blood *107*, 328-333.

Nemeth, E., Roetto, A., Garozzo, G., Ganz, T., and Camaschella, C. (2005). Hepcidin is decreased in TFR2 hemochromatosis. Blood *105*, 1803-1806.

Nemeth, E., Rivera, S., Gabayan, V., Keller, C., Taudorf, S., Pedersen, B. K., and Ganz, T. (2004b). IL-6 mediates hypoferremia of inflammation by inducing the synthesis of the iron regulatory hormone hepcidin. J. Clin. Invest. *113*, 1271-1276.

Nemeth, E., Tuttle, M. S., Powelson, J., Vaughn, M. B., Donovan, A., Ward, D. M., Ganz, T., and Kaplan, J. (2004a). Hepcidin regulates cellular iron efflux by binding to ferroportin and inducing its internalization. Science *306*, 2090-2093.

Nemeth, E., Valore, E. V., Territo, M., Schiller, G., Lichtenstein, A., and Ganz, T. (2003). Hepcidin, a putative mediator of anemia of inflammation, is a type II acute-phase protein. Blood *101*, 2461-2463.

Nguyen, N. B., Callaghan, K. D., Ghio, A. J., Haile, D. J., and Yang, F. (2006). Hepcidin expression and iron transport in alveolar macrophages. Am. J. Physiol. Lung Cell Mol. Physiol. *291*, L417-25.

Nicolas, G., Viatte, L., Bennoun, M., Beaumont, C., Kahn, A., and Vaulont, S. (2002c). Hepcidin, a new iron regulatory peptide. Blood Cells Mol Dis *29*, 327-335.

Nicolas, G., Bennoun, M., Devaux, I., Beaumont, C., Grandchamp, B., Kahn, A., and Vaulont, S. (2001). Lack of hepcidin gene expression and severe tissue iron overload in upstream stimulatory factor 2 (USF2) knockout mice. Proc. Natl. Acad. Sci. USA *98*, 8780-8785.

Nicolas, G., Bennoun, M., Porteu, A., Mativet, S., Beaumont, C., Grandchamp, B., Sirito, M., Sawadogo, M., Kahn, A., and Vaulont, S. (2002a). Severe iron deficiency anemia in transgenic mice expressing liver hepcidin. Proc. Natl. Acad. Sci. USA *99*, 4596-4601.

Nicolas, G., Chauvet, C., Viatte, L., Danan, J. L., Bigard, X., Devaux, I., Beaumont, C., Kahn, A., and Vaulont, S. (2002b). The gene encoding the iron regulatory peptide hepcidin is regulated by anemia, hypoxia, and inflammation. J. Clin. Invest. *110*, 1037-1044.

Nicolas, G., Viatte, L., Lou, D. Q., Bennoun, M., Beaumont, C., Kahn, A., Andrews, N. C., and Vaulont, S. (2003). Constitutive hepcidin expression prevents iron overload in a mouse model of hemochromatosis. Nat. Genet. *34*, 97-101.

Niederkofler, V., Salie, R., and Arber, S. (2005). Hemojuvelin is essential for dietary iron sensing, and its mutation leads to severe iron overload. J. Clin. Invest. *115*, 2180-2186.

Niederkofler, V., Salie, R., Sigrist, M., and Arber, S. (2004). Repulsive guidance molecule (RGM) gene function is required for neural tube closure but not retinal topography in the mouse visual system. J. Neurosci. *24*, 808-818.

Njajou, O. T. *et al.* (2001). A mutation in SLC11A3 is associated with autosomal dominant hemochromatosis. Nat. Genet. *28*, 213-214.

Oldekamp, J., Kramer, N., Alvarez-Bolado, G., and Skutella, T. (2004). Expression pattern of the repulsive guidance molecules RGM A, B and C during mouse development. Gene Expr. Patterns *4*, 283-288.

Owen, D., and Kuhn, L. C. (1987). Noncoding 3' sequences of the transferrin receptor gene are required for mRNA regulation by iron. EMBO J. *6*, 1287-1293.

Papanikolaou, G. *et al.* (2004). Mutations in HFE2 cause iron overload in chromosome 1q-linked juvenile hemochromatosis. Nat. Genet. *36*, 77-82.

Park, C. H., Valore, E. V., Waring, A. J., and Ganz, T. (2001). Hepcidin, a urinary antimicrobial peptide synthesized in the liver. J. Biol. Chem. *276*, 7806-7810.

Parkkila, S., Waheed, A., Britton, R. S., Bacon, B. R., Zhou, X. Y., Tomatsu, S., Fleming, R. E., and Sly, W. S. (1997a). Association of the transferrin receptor in human placenta with HFE, the protein defective in hereditary hemochromatosis. Proc. Natl. Acad. Sci. USA *94*, 13198-13202.

Parkkila, S., Waheed, A., Britton, R. S., Feder, J. N., Tsuchihashi, Z., Schatzman, R. C., Bacon, B. R., and Sly, W. S. (1997b). Immunohistochemistry of HLA-H, the protein defective in patients with hereditary hemochromatosis, reveals unique pattern of expression in gastrointestinal tract. Proc. Natl. Acad. Sci. USA *94*, 2534-2539.

Philpott, C. C. (2002). Molecular aspects of iron absorption: Insights into the role of HFE in hemochromatosis. Hepatology *35*, 993-1001.

Pietrangelo, A. (2002). Physiology of iron transport and the hemochromatosis gene. Am J. Physiol. Gastrointest. Liver Physiol. *282*, G403-14.

Pietrangelo, A. (2004). Hereditary hemochromatosis--a new look at an old disease. N. Engl. J. Med. *350*, 2383-2397.

Pietrangelo, A., Caleffi, A., Henrion, J., Ferrara, F., Corradini, E., Kulaksiz, H., Stremmel, W., Andreone, P., and Garuti, C. (2005). Juvenile hemochromatosis associated with pathogenic mutations of adult hemochromatosis genes. Gastroenterology *128*, 470-479.

Pigeon, C., Ilyin, G., Courselaud, B., Leroyer, P., Turlin, B., Brissot, P., and Loreal, O. (2001). A new mouse liver-specific gene, encoding a protein homologous to human antimicrobial peptide hepcidin, is overexpressed during iron overload. J. Biol. Chem. *276*, 7811-7819.

Polo, S., and Di Fiore, P. P. (2006). Endocytosis conducts the cell signaling orchestra. Cell *124*, 897-900.

Ponka, P. (2002). Rare causes of hereditary iron overload. Semin. Hematol. *39*, 249-262.

Raja, K. B., Pountney, D. J., Simpson, R. J., and Peters, T. J. (1999). Importance of anemia and transferrin levels in the regulation of intestinal iron absorption in hypotransferrinemic mice. Blood *94*, 3185-3192.

Rajagopalan, S., Deitinghoff, L., Davis, D., Conrad, S., Skutella, T., Chedotal, A., Mueller, B. K., and Strittmatter, S. M. (2004). Neogenin mediates the action of repulsive guidance molecule. Nat. Cell Biol. *6*, 756-762.

Rao, K. K., Shapiro, D., Mattia, E., Bridges, K., and Klausner, R. (1985). Effects of alterations in cellular iron on biosynthesis of the transferrin receptor in K562 cells. Mol. Cell. Biol. *5*, 595-600.

Richardson, D. R., and Ponka, P. (1997). The molecular mechanisms of the metabolism and transport of iron in normal and neoplastic cells. Biochim. Biophys. Acta. *1331*, 1-40.

Robb, A., and Wessling-Resnick, M. (2004). Regulation of transferrin receptor 2 protein levels by transferrin. Blood *104*, 4294-4299.

Robb, A. D., Ericsson, M., and Wessling-Resnick, M. (2004). Transferrin receptor 2 mediates a biphasic pattern of transferrin uptake associated with ligand delivery to multivesicular bodies. Am. J. Physiol. Cell Physiol. *287*, C1769-75.

Rodriguez Martinez, A., Niemela, O., and Parkkila, S. (2004). Hepatic and extrahepatic expression of the new iron regulatory protein hemojuvelin. Haematologica *89*, 1441-1445.

Roetto, A., Papanikolaou, G., Politou, M., Alberti, F., Girelli, D., Christakis, J., Loukopoulos, D., and Camaschella, C. (2003). Mutant antimicrobial peptide hepcidin is associated with severe juvenile hemochromatosis. Nat. Genet. *33*, 21-22.

Rohrer, J., Schweizer, A., Russell, D., and Kornfeld, S. (1996). The Targeting of Lamp1 to Lysosomes Is Dependent on the Spacing of its Cytoplasmic Tail Tyrosine Sorting Motif relative to the Membrane. J. Cell Biol. *132*, 565-576.

Rouault, T. A., Hentze, M. W., Caughman, S. W., Harford, J. B., and Klausner, R. D. (1988). Binding of a cytosolic protein to the iron-responsive element of human ferritin messenger RNA. Science *241*, 1207-1210.

Roy, C. N. *et al.* (2004). An Hfe-dependent pathway mediates hyposideremia in response to lipopolysaccharide-induced inflammation in mice. Nat. Genet. *36*, 481-485.

Roy, C. N., Penny, D. M., Feder, J. N., and Enns, C. A. (1999). The hereditary hemochromatosis protein, HFE, specifically regulates transferrin-mediated iron uptake in HeLa cells. J. Biol. Chem. *274*, 9022-9028.

Salter-Cid, L., Brunmark, A., Li, Y., Leturcq, D., Peterson, P. A., Jackson, M. R., and Yang, Y. (1999). Transferrin receptor is negatively modulated by the hemochromatosis protein HFE: implications for cellular iron homeostasis. Proc. Natl. Acad. Sci. USA *96*, 5434-5439.

Samad, T. A. *et al.* (2004). DRAGON: a member of the repulsive guidance molecule-related family of neuronal- and muscle-expressed membrane proteins is regulated by DRG11 and has neuronal adhesive properties. J. Neurosci. *24*, 2027-2036.

Schimanski, L. M. *et al.* (2005). In vitro functional analysis of human ferroportin (FPN) and hemochromatosis-associated FPN mutations. Blood *105*, 4096-4102.

Schmidtmer, J., and Engelkamp, D. (2004). Isolation and expression pattern of three mouse homologues of chick Rgm. Gene Expr Patterns *4*, 105-110.

Sciot, R., Paterson, A. C., Van den Oord, J. J., and Desmet, V. J. (1987). Lack of hepatic transferrin receptor expression in hemochromatosis. Hepatology *7*, 831-837.

Sheff, D., Pelletier, L., O'Connell, C. B., Warren, G., and Mellman, I. (2002). Transferrin receptor recycling in the absence of perinuclear recycling endosomes. J. Cell Biol. *156*, 797-804.

Sheff, D. R., Daro, E. A., Hull, M., and Mellman, I. (1999). The receptor recycling pathway contains two distinct populations of early endosomes with different sorting functions. J. Cell Biol. *145*, 123-139.

Skow, L. C., Burkhart, B. A., Johnson, F. M., Popp, R. A., Popp, D. M., Goldberg, S. Z., Anderson, W. F., Barnett, L. B., and Lewis, S. E. (1983). A mouse model for beta-thalassemia. Cell *34*, 1043-1052.

Snider, M. D., and Rogers, O. C. (1985). Intracellular movement of cell surface receptors after endocytosis: Resialylation of asialo-transferrin receptor in human erythroleukemia cells. J. Cell Biol. *100*, 826-834.

Sorkin, A., and Von Zastrow, M. (2002). Signal transduction and endocytosis: close encounters of many kinds. Nat. Rev. Mol. Cell Biol. *3*, 600-614.

Stoorvogel, W., Geuze, H. J., Griffith, J. M., and Strous, G. J. (1988). The pathways of endocytosed transferrin and secretory protein are connected in the trans-Golgi reticulum. J. Cell Biol. *106*, 1821-1829.

Taetle, R., Castagnola, J., and Mendelsohn, J. (1986). Mechanisms of growth inhibition by anti-transferrin receptor monoclonal antibodies. Cancer Res. *46*, 1759-1763.

Taylor, P., Martinez-Torres, C., Leets, I., Ramirez, J., Garcia-Casal, M. N., and Layrisse, M. (1988). Relationships among iron absorption, percent saturation of plasma transferrin and serum ferritin concentration in humans. J. Nutr. *118*, 1110-1115.

Teis, D., Wunderlich, W., and Huber, L. A. (2002). Localization of the MP1-MAPK scaffold complex to endosomes is mediated by p14 and required for signal transduction. Dev. Cell *3*, 803-814.

Tosoni, D., Puri, C., Confalonieri, S., Salcini, A. E., De Camilli, P., Tacchetti, C., and Di Fiore, P. P. (2005). TTP specifically regulates the internalization of the transferrin receptor. Cell *123*, 875-888.

Townsend, A., and Drakesmith, H. (2002). Role of HFE in iron metabolism, hereditary haemochromatosis, anaemia of chronic disease, and secondary iron overload. Lancet *359*, 786-790.

Trowbridge, I. S., and Lopez, F. (1982). Monoclonal antibody to transferrin receptor blocks transferrin binding and inhibits human tumor cell growth in vitro. Proc. Natl. Acad. Sci. USA *79*, 1175-1179.

Truksa, J., Peng, H., Lee, P., and Beutler, E. (2006). Bone morphogenetic proteins 2, 4, and 9 stimulate murine hepcidin 1 expression independently of Hfe, transferrin receptor 2 (Tfr2), and IL-6. Proc. Natl. Acad. Sci. USA *103*, 10289-10293.

Tsunoo, H., and Sussman, H. H. (1983). Placental transferrin receptor. Evaluation of the presence of endogenous ligand on specific binding. J. Biol. Chem. *258*, 4118-4122.

van Weert, A. W., Dunn, K. W., Gueze, H. J., Maxfield, F. R., and Stoorvogel, W. (1995). Transport from late endosomes to lysosomes, but not sorting of integral membrane proteins in endosomes, depends on the vacuolar proton pump. J. Cell Biol. *130*, 821-834.

Vielmetter, J., Kayyem, J. F., Roman, J. M., and Dreyer, W. J. (1994). Neogenin, an avian cell surface protein expressed during terminal neuronal differentiation, is closely related to the human tumor suppressor molecule deleted in colorectal cancer. J. Cell Biol. *127*, 2009-2020.

Vogt, T. M., Blackwell, A. D., Giannetti, A. M., Bjorkman, P. J., and Enns, C. A. (2003). Heterotypic interactions between transferrin receptor and transferrin receptor 2. Blood *101*, 2008-2014.

Vulpe, C. D., Kuo, Y. M., Murphy, T. L., Cowley, L., Askwith, C., Libina, N., Gitschier, J., and Anderson, G. J. (1999). Hephaestin, a ceruloplasmin homologue implicated in intestinal iron transport, is defective in the sla mouse. Nat. Genet. *21*, 195-199.

Wallace, D. F., Pedersen, P., Dixon, J. L., Stephenson, P., Searle, J. W., Powell, L. W., and Subramaniam, V. N. (2002). Novel mutation in ferroportin1 is associated with autosomal dominant hemochromatosis. Blood *100*, 692-694.

Wallace, D. F., Summerville, L., Lusby, P. E., and Subramaniam, V. N. (2005). First phenotypic description of transferrin receptor 2 knockout mouse, and the role of hepcidin. Gut *54*, 980-986.

Wang, G. L., and Semenza, G. L. (1993). General involvement of hypoxia-inducible factor 1 in transcriptional response to hypoxia. Proc. Natl. Acad. Sci. USA *90*, 4304-4308.

Wang, R. H. *et al.* (2005). A role of SMAD4 in iron metabolism through the positive regulation of hepcidin expression. Cell Metab *2*, 399-409.

Ward, J. H., Jordan, I., Kushner, J. P., and Kaplan, J. (1984). Heme regulation of HeLa cell transferrin receptor number. J. Biol. Chem. *259*, 13235-13240.

Warren, R. A., Green, F. A., and Enns, C. A. (1997). Saturation of the endocytic pathway for the transferrin receptor does not affect the endocytosis of the epidermal growth factor receptor. J. Biol. Chem. *272*, 2116-2121.

Warren, R. A., Green, F. A., Stenberg, P. E., and Enns, C. A. (1998). Distinct saturable pathways for the endocytosis of different tyrosine motifs. J. Biol. Chem. *273*, 17056-17063.

Watts, C. (1985). Rapid endocytosis of the transferrin receptor in the absence of bound transferrin. J. Cell Biol. *100*, 633-637.

Weinstein, D. A., Roy, C. N., Fleming, M. D., Loda, M. F., Wolfsdorf, J. I., and Andrews, N. C. (2002). Inappropriate expression of hepcidin is associated with iron refractory anemia: implications for the anemia of chronic disease. Blood *100*, 3776-3781.

Welch, S. (1992). Transferrin: The Iron Carrier (Boca Raton: CRC Press).

West, A. P., Jr., Bennett, M. J., Sellers, V. M., Andrews, N. C., Enns, C. A., and Bjorkman, P. J. (2000). Comparison of the interactions of transferrin receptor and transferrin receptor 2 with transferrin and the hereditary hemochromatosis protein HFE. J. Biol. Chem. *275*, 38135-38138.

West, A. P., Jr., Giannetti, A. M., Herr, A. B., Bennett, M. J., Nangiana, J. S., Pierce, J. R., Weiner, L. P., Snow, P. M., and Bjorkman, P. J. (2001). Mutational Analysis of the Transferrin Receptor Reveals Overlapping HFE and Transferrin Binding Sites. J. Mol. Biol. *313*, 385-397.

Yang, F., Liu, X. B., Quinones, M., Melby, P. C., Ghio, A., and Haile, D. J. (2002). Regulation of reticuloendothelial iron transporter MTP1 (Slc11a3) by inflammation. J. Biol. Chem. *2*, 2.

Zhang, A. S., Davies, P. S., Carlson, H. L., and Enns, C. A. (2003). Mechanisms of HFE-induced regulation of iron homeostasis: Insights from the W81A HFE mutation. Proc Natl Acad Sci U S A *100*, 9500-9505.

Zhang, A. S., West, A. P., Jr., Wyman, A. E., Bjorkman, P. J., and Enns, C. A. (2005). Interaction of HJV with neogenin results in iron accumulation in HEK293 cells. J. Biol. Chem. *280*, 33885-33894.

Zhang, A. S., Xiong, S., Tsukamoto, H., and Enns, C. A. (2004). Localization of iron metabolism-related mRNAs in rat liver indicate that HFE is expressed predominantly in hepatocytes. Blood *103*, 1509-1514.

Appendix A

Regulation of Tf in HepG2 cells

Rationale

When characterizing lysates from HepG2 cells treated without or with Fe_2Tf (Chapter 2, (Johnson and Enns, 2004)), we detected by western blot an increase in Tf in lysates from cells treated with Fe_2Tf (Figure18A). We wondered whether the additional Tf derived from the exogenous Tf added to the culture medium or from a change in the metabolism of endogenous Tf.

Results

In order to discriminate between endogenous and exogenous Tf in western blot experiments, we treated cells with a non-glycosyated form of Fe_2Tf (ng-Fe_2Tf) that migrates at a lower molecular weight than the glycosylated endogenous form for 24 hr. The ng-Fe_2Tf is clearly visible in lysates from these cells (Figure 18B, lane 3) and, to a lesser extent, in cells washed with acid prior to lysis to strip surface-bound Tf (Figure 18B, lane 6). Thus, the increase in Tf in cells treated with Fe_2Tf is due, at least in part, to the binding and internalization of exogenous Fe_2Tf.

To assess whether Fe_2Tf treatment alters Tf metabolism in HepG2 cells, we assessed the affect of Fe_2Tf on Tf transcription, secretion, and synthesis. Levels of Tf transcript are similar in control and Fe_2Tf-treated cells (Figure 18C), indicating that Fe_2Tf does not alter the rate at which Tf transcript is synthesized or degraded. Treatment with Fe_2Tf does not alter the rate of Tf secretion from HepG2 cells (Figure 18D), either, though the overall level of Tf was lower in Fe_2Tf-treated cells. Finally, the rate of Tf synthesis decreases, rather than increases, in cells exposed to Fe_2Tf (Figure 18D).

Conclusions

From the preceding experiments we conclude that the increase in Tf protein observed in cells treated with Fe_2Tf is due to binding and internalization of exogenous Fe_2Tf. Exogenous ng-Fe_2Tf is easily distinguishable from endogenous Tf and is both bound and internalized by HepG2 cells. A change in the metabolism of endogenous Tf was not observed that could account for the observed increase in Tf.

In these experiments treatment with Fe_2Tf decreases the rate of Tf protein synthesis. Viewed from the perspective or iron regulation, this is consistent with a previous reports investigating the regulation of human Tf. Chimeric mice carrying the 5' untranslated region (UTR) of human Tf upstream of the chloramphenicol acetyl transferase (CAT) gene show decreased CAT enzyme activity correlating with decreased CAT protein but not mRNA levels 72 hours after interperitoneal injection of 10mg/kg body weight ferric ammonium citrate (FAC) (Adrian et al., 1990; Cox and Adrian, 1993). The response was mediated by a region in the 5' UTR of Tf containing an iron responsive element (IRE) that binds iron regulatory protein (IRP) (Cox and Adrian, 1993; Cox et al., 1995). The IRE in the 5' UTR of Tf is atypical in that IRP binding under low iron conditions increases Tf level. The Tf IRE thus behaves more like the IREs in the 3' UTR of TfR1 than the IRE in the 5' UTR of Ft. When bound by IRPs, the former stabilizes TfR1 transcript by blocking cleavage, thereby increasing TfR1 levels under low iron conditions (Casey et al., 1988). The latter blocks translation, thereby decreasing Ft levels under low iron conditions (Hentze et al., 1987; Rouault et al., 1988). The IRE-IRP mechanism that regulates Tf remains unclear. Our results support the conclusion that Tf protein synthesis is regulated through an IRE in response to iron level and complement results showing that desferioxamine (DFO) increases Tf

synthesis in HepG2 cells (Barnum-Huckins and Adrian, 2000). The regulation of Tf translation by iron may have physiological implications given that serum Tf levels are lowered in individuals with iron overload (Morgan, 1983).

Methods

Non-glycosylated Tf treatments Anne Brown-Mason generously provided 1 mg/mL ng-Fe_2Tf. This stock solution was concentrated to 35 mg/mL using a Centricon10 concentrator according to the manufacturer's instructions. HepG2 cells were seeded at 2 x 10^4 cells/cm^2 for 3 days prior to treatment with 6 μM Fe_2Tf or ng-Fe_2Tf for 24 hr. Lysates were collected and analyzed by SDS-PAGE as described in Chapter 2. Tf was visualized by western blot using goat anti-Tf serum (1:10,000) and swine anti-goat secondary antibody (1:10,000, Chemicon) followed by chemiluminescent detection.

Real-time qRT-PCR Tf transcript level was measured by real-time qRT-PCR following the method described in Chapter 2 (Johnson and Enns, 2004).

Immunoprecipitation Immunoprecipitation of metabolically-labeled Tf followed the the method described in Chapter 3 (Johnson et al., 2006). Goat anti-Tf serum (2 μL) was used to immunoprecipitate Tf.

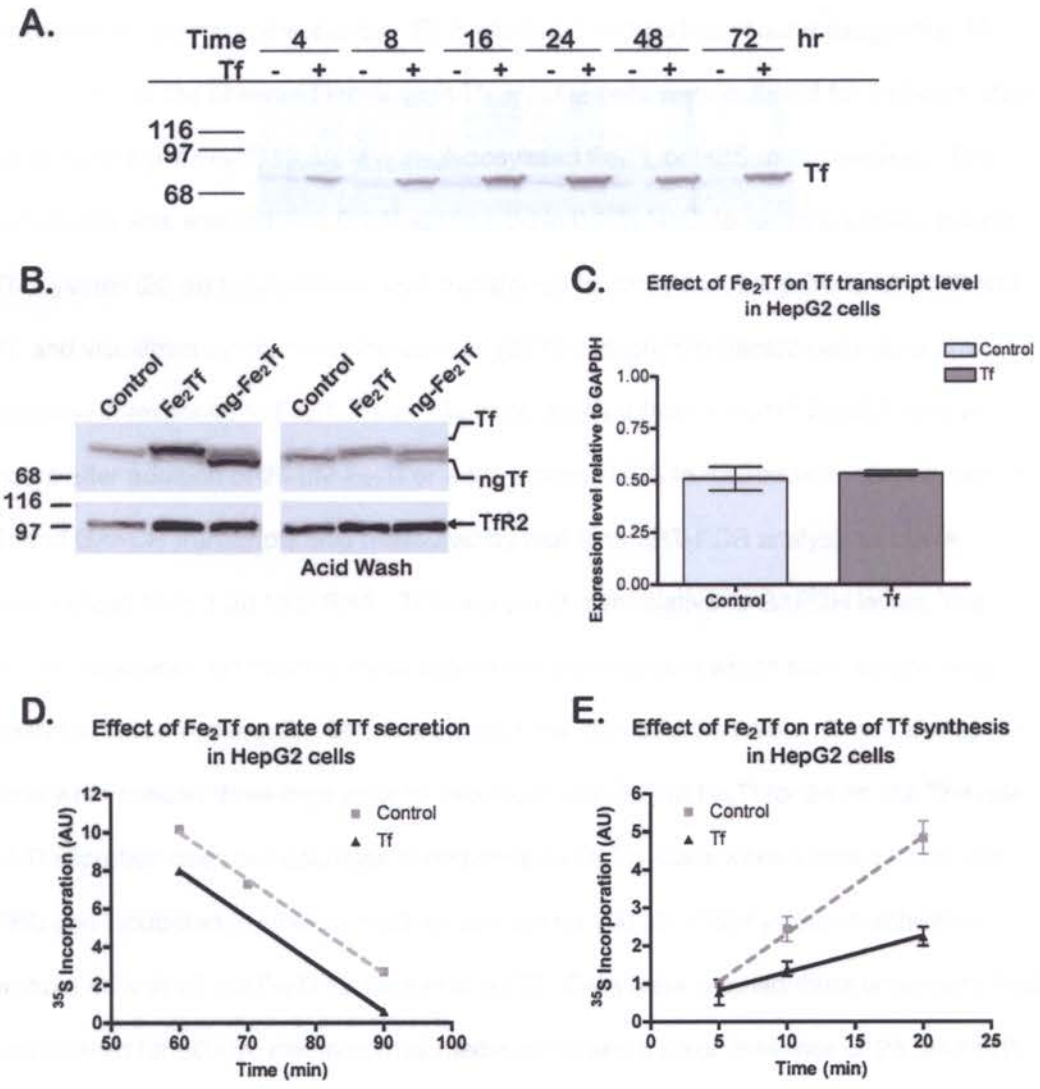

Figure 18. Effect of exogenous diferric transferrin on endogenous transferrin.

Figure 18. Effect of exogenous diferric transferrin on endogenous transferrin. (A) An increase in the amount of Tf is observed in cells treated with Fe_2Tf. HepG2 cells were cultured for 4 – 72 hours after addition of 25 μM Fe_2Tf or HBS to the medium. Lysates (20 μg total protein) were transferred to nitrocellulose, probed for Tf, and visualized by chemiluminescence. (B) Intracellular and surface-bound exogenous Tf contributes to the observed increase in Tf. HepG2 cells were cultured for 24 hours after addition of 6 μM Fe_2Tf, 12.5 μM non-glycosylated Fe_2Tf, or HBS to the medium. One set of cells was washed with 0.2 N acetic acid in 0.2 M NaCl to remove surface-bound Tf. Lysates (20 μg total protein) were transferred to nitrocellulose, probed for TfR2 and Tf, and visualized by chemiluminescence. (C) Tf transcript in HepG2 cells does not increase in response to Fe_2Tf. Total RNA was isolated from ~1 x 10^7 HepG2 cells 24 hours after addition of 25 μM Fe_2Tf or equal volume HBS to the medium. Expression of Tf and GAPDH transcripts was measured by real-time qRT-PCR analysis of cDNA synthesized from 2 μg total RNA. Tf levels are shown relative to GAPDH levels. The graph represents the mean of three separate experiments in which each sample was analyzed twice in triplicate. Error bars depict the standard deviation. (D and E) HepG2 cells were seeded three days prior to treatment with 25 μM Fe_2Tf for 24 hr. (D) The rate of Tf secretion does not decrease in response to Fe_2Tf. Cells were washed twice with PBS and incubated in labeling medium containing 100 μM [^{35}S]-cysteine/methionine without or with 25 μM Fe_2Tf for 60 min at 37°C. Cells were washed three times with PBS and chased for 60 - 90 min in normal media in the absence or presence of 25 μM Fe_2Tf. Lysates were collected and immunoprecipitated as described in Methods. (E) The rate of Tf synthesis decreases in response to Fe_2Tf. Cells were washed twice with PBS and incubated in labeling medium without or with 25 μM Fe_2Tf for 5 - 20 min at 37°C. Lysates were collected and immunoprecipitated as described in Methods.

Appendix B

Diferric transferrin does not induce hepcidin expression in human hepatoma cell lines

Rationale

We sought to identify a hepatoma cell line in which hepcidin responds to Fe_2Tf in order to study the relationship between Fe_2Tf concentration, TfR2 stability, and hepcidin expression and thereby define a mechanism by which TfR2 contributes to iron homeostasis. To this end, we used quantitative real-time PCR (qRT-PCR) to measure changes in the expression of hepcidin and other iron-related genes in response to Fe_2Tf.

Results

Profiles of iron-related gene expression were determined for HepG2, HepG2 cells stably transfected with TfR2 (HepG2/TfR2), Hep3B cells, and Hep3B cells stably transfected with TfR2 (Hep3B/TfR2). The relative expression levels of Cp, DMT1, Ft, and Tf were similar in HepG2 and Hep3B cells (Figure 19A and B; Table 1). Hepcidin expression was easily detected in HepG2 cells but near the limit of detection in Hep3B cells. Although TfR2 expression was slightly lower in Hep3B cells than in HepG2 cells, consistent with the finding that TfR2 protein is only detectable in the latter (Vogt et al., 2003). TfR1, HFE, Fpn1 expression were slightly higher in Hep3B cells than in HepG2 cells. Stable transfection of TfR2 increased TfR2 transcript level over 100-fold in both transfected cell lines. Hepcidin expression decreased by 18-fold upon overexpression of TfR2 in HepG2 cells but not in Hep3B cells. The change may be attributable to differences in culture condition or passage number. Otherwise, TfR2 expression had little effect on iron-related gene expression (Figure 19 C and D; Table 1) A significant decrease in TfR1 expression was not observed, despite an increase in intracellular iron that should accompany overexpression of TfR2, due to its internalization of bovine Tf

from the medium. Compensatory mechanisms might normalize changes in iron level over time. An effect of TfR2 on TfR1 expression might be more pronounced upon acute expression of TfR2, as in an inducible cell culture system.

The effect of Fe_2Tf on iron-related gene expression was initially assessed in HepG2 cells treated with Fe_2Tf for 24 hours (Figure 20A). Consistent with its iron-dependent regulation by the IRE/IRP system, TfR1 expression decreased slightly, but significantly (see also Figure 8), in cells treated with Fe_2Tf. No other significant changes were detected. Similar results were obtained with HepG2 (Figure 20B) and HepG2/TfR2 (Figure 20C) cells treated with Fe_2Tf for 2 and 6 hr and with Hep3B (Figure 20D) and Hep3B/TfR2 (Figure 20E) cells treated with Fe_2Tf for 2 and 24 hr.

Conclusions

Our results are consistent with other reports showing that iron fails to induce hepcidin expression *in vitro* as it does *in vivo.* Treatment of freshly isolated hepatocytes with ferric ammonium citrate (FAC) or the iron chelator desferrioxamine (DFO) does not elicit a change in hepcidin expression (Pigeon et al., 2001). Neither ferric ammonium citrate (FAC) nor Fe_2Tf affect hepcidin expression in hepatocytes cultured in serum-free medium, while in medium with serum, Fe_2Tf decreases, rather than increases, hepcidin expression (Nemeth et al., 2003). In HepG2 cells hepcidin decreases in response to iron nitrilotriacetate (FeNTA) and does not respond to Fe_2Tf (Gehrke et al., 2003). Since TfR2 is required for proper regulation of hepcidin, we had surmised that the low or undetectable levels of TfR2 protein in hepatoma cell lines might contribute to the unresponsiveness of hepcidin. Fe_2Tf did not induce hepcidin expression in HepG2 cells or Hep3B cells in which TfR2 was overexpressed (Figure 20C and E), however.

These results have prompted the hypothesis that molecules external to the hepatocyte, perhaps released by Kupffer cell macrophages or transported in the serum, relay iron signals to hepatocytes that regulate hepcidin expression. The role of cytokines IL-6 and IL-1, both released by macrophages, in regulating hepcidin in response to inflammation is well established (Nemeth et al., 2004b; Lee, 2005). IL-6 is not essential for iron signaling to hepatocytes, though, since IL-$6^{-/-}$ mice increase hepcidin expression when switched to a high-iron diet (Nemeth et al., 2004b). Hepcidin may not appropriately respond to iron in cell culture because culture conditions do not accurately reproduce physiological conditions. Culture conditions may alter the function, interactions, or signaling of proteins upstream from hepcidin. Alternatively, the absence of proper hepcidin regulation by iron in cell culture might be due to the expression profile of the hepatic cell itself. Hepatocytes dedifferentiate after a few days in culture, and thus may cease to express proteins needed to mediate the effect of iron on hepcidin. HepG2 cells express TfR1, TfR2, Tf, Fpn1, DMT1, Ft, HFE, Hepc, Hjv, and ceruloplasmin but in some cases at markedly different levels than hepatocytes in vivo. In HepG2, cells TfR2 and TfR1 transcript levels are similar (Figure 19A), but in hepatocytes, levels of TfR2 transcript are considerably higher than levels of TfR1 transcript (Zhang et al., 2004). Also in HepG2 cells, expression of HFE and Hjv is low (Figure 19A; Zhang et al., 2004). Thus, though the proteins that participate in iron regulation of hepcidin are present, the extent and stoichiometry of their expression may be inappropriate.

Methods

Stable transfection of HepG2 cells pcDNA3.1-flTfR2 HepG2 cells were seeded at 6.0 x 10^5 cells/cm^2 24 hr prior to transfection at which time their medium was replaced with fresh MEM containing 10% FBS. For each 35 mm dish transfected, FuGene6 transfection reagent (6 µL) was added to Opti-MEM (94 µL) in a sterile centrifuge tube without touching the wall of the tube. Plasmid DNA (1 µg) was then added. The mixture was incubated for 15 min at RT and then added dropwise to the dish of cells. The medium was replaced with fresh MEM/FBS 24 hr later. Cells were trypsinized 3.5 days later and replated to two 100 mm dishes in MEM/FBS containing 1 mg/mL G418. Medium was replaced every 5 days. Clones were picked approximately 2 weeks after transfection. HepG2/TfR2 cells were cultured in MEM supplemented with 10% FBS and 1 mg/mL G418.

Real-time qRT-PCR Transcript levels was measured by real-time qRT-PCR following the method described in Chapter 2 (Davies and Enns, 2004; Johnson and Enns, 2004; Zhang et al., 2004).

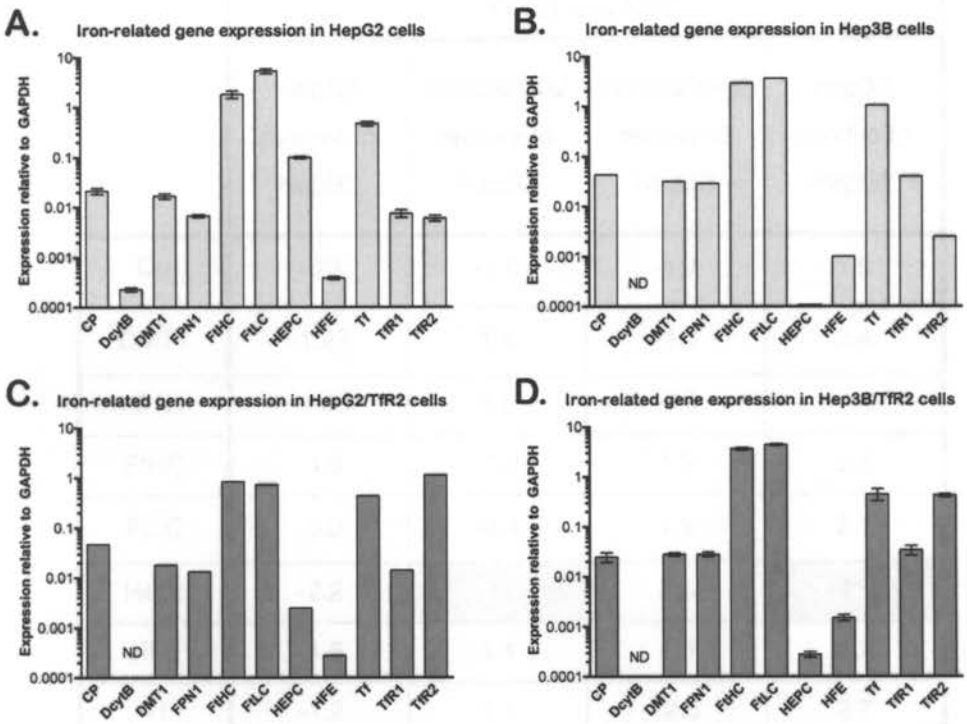

Figure 19. Profiles of iron-related gene expression in human hepatoma cell lines.

(A-D) Transcript levels were measured by real-time quantitative PCR as described in Chapter 2. (A and B) The expression of iron-related genes is similar in HepG2 and Hep3B cells. (C and D) Overexpression of TfR2 does not significantly alter the expression of iron related genes in HepG2 and Hep3B cells. HepG2 and Hep3B cells were stably transfected with plasmid encoding TfR2 as described in Methods and Chapter 3, respectively. ND indicates not determined.

Table 1. Relative expression of iron-related genes in hepatoma cells.

	FOLD-CHANGE			
	HepG2 relative to HepG2	HepG2/TfR2 relative to HepG2	Hep3B/TfR2 relative to Hep3B	Hep3B relative to HepG2
Cp	-.73	-1.6	-1.7	1.5
DMT1	-1.27	1.4	-1.1	2.4
FPN1	-1.03	2.0	-1.0	4.4
FtHC	-1.8	-1.2	1.2	2.8
FtLC	-3.0	-2.4	1.2	2.1
Hepc	-2.2	-18	2.6	-417
HFE	-1.6	1.1	1.5	4.2
Tf	-1.2	1.1	-2.3	2.7
TfR1	-0.7	1.4	-1.1	3.8
TfR2	-0.7	132	172	-3.5

The table shows the fold-difference in expression level of iron related genes in HepG2, Hep3B, HepG2/TfR2, and Hep3B/TfR2. The first column of figures compares expression levels in HepG2 cells measured in two different sets of experiments and provides a reference for variations that might be attributable to passage number, culture conditions, and cell line drift. The second and third columns of figures show the fold-change in gene expression upon transfection of HepG2 or Hep3B cells with TfR2. The final column compares the two hepatoma parent cell lines. Changes considered significant are highlighted.

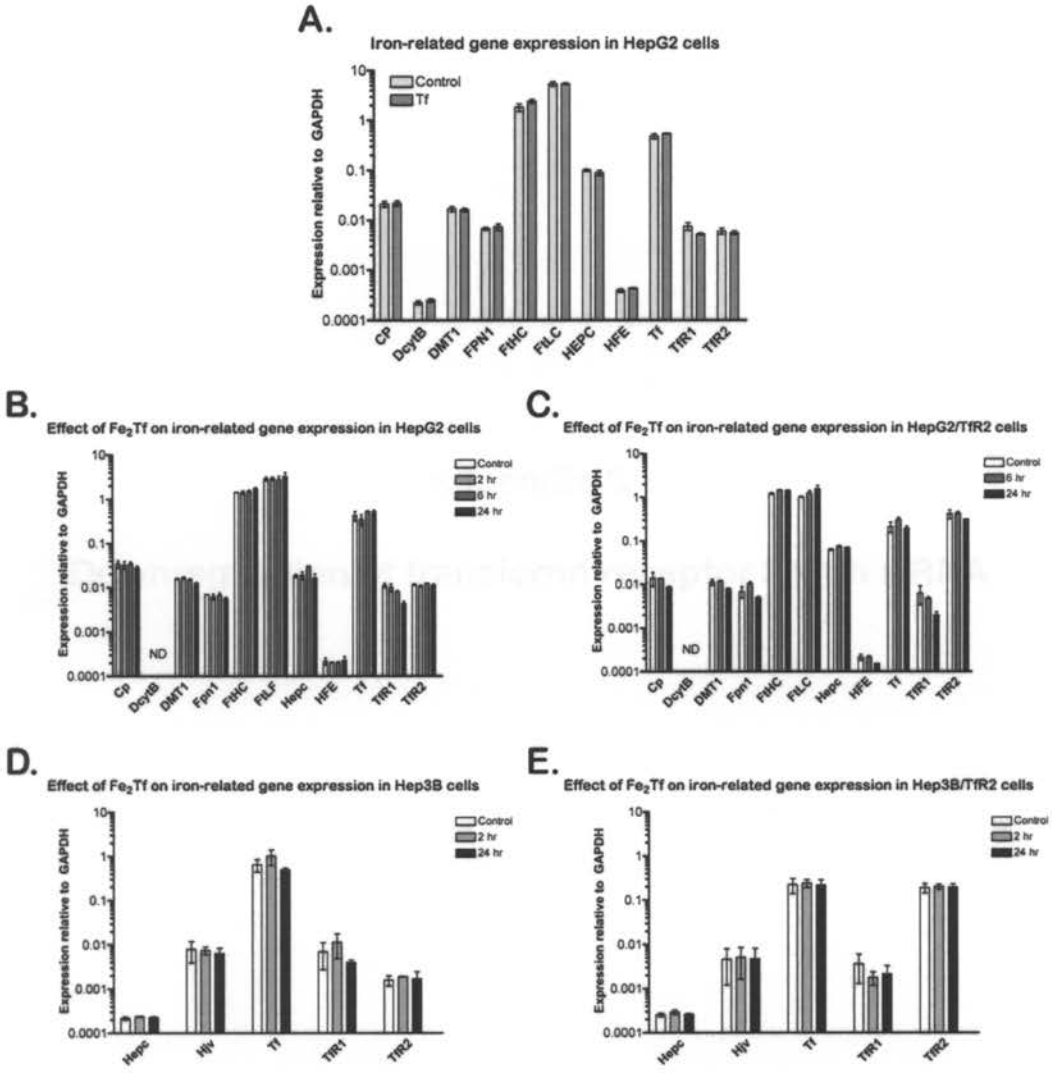

Figure 20. Effect of differic transferrin on expression of iron-related genes in human hepatoma cell lines. (A-E) Fe_2Tf does not alter iron-related gene expression in human hepatoma cell lines. HepG2 (A and B), HepG2/TfR2 (C), Hep3B (D) and Hep3B/TfR2 (E) cells were treated with 25 μM Fe_2Tf for the indicated lengths of time. Transcript levels were measured by real-time quantitative PCR as described in Chapter 2. ND indicates not determined.

Appendix C

Downregulation of transferrin receptor 2 with siRNA

Rationale

Trfr2^{Y245X} mice express lower levels of hepcidin transcript than wild-type mice. Unlike wild-type mice, These mutant mice also fail to induce hepcidin expression after injection with iron dextran (Kawabata et al., 2005). Thus, TfR2 positively regulates hepcidin expression. The mechanism by which it does so is not understood, however, and at the molecular level is more amenable to analysis in a cell culture system. To establish a method by which to study the effects of TfR2 knockdown in cell culture we used siRNA to downregulate endogenous TfR2 in HepG2 human hepatoma cells.

Results

Transfection of HepG2 cells with siRNA targeting TfR2 reduced TfR2 protein level by approximately 90% (Figure 21). No significant change in TfR2 protein level was observed in cells transfected without siRNA or transfected with various nonspecific siRNA duplexes.

Conclusions

One approach by which to study the requirement for TfR2 in mediating the effect of Fe_2Tf on hepcidin expression is to transfect TfR2 into a hepatoma cell line that does express endogenous TfR2, such as Hep3B cells, and compare the response of transfected and non-transfected cells to Fe_2Tf. Cell line variability is a major disadvantage to this approach, particularly in studying hepcidin expression, which is sensitive to culture conditions and numerous stimuli. Knockdown of TfR2 with siRNA is an alternative approach. A variety of nonspecific siRNA constructs are available to control for side effects of siRNA transfection. Knockdown and expressing cells can be

cultured under nearly identical conditions. Application of this approach, however, awaits identification of a cell culture system in which hepcidin responds to iron. Unlike mice fed an iron-rich diet, neither HepG2 cells, Hep3B cells, nor cultured hepatocytes upregulate hepcidin expression when treated with Fe_2Tf or non-transferrin bound iron (Figure 20; Pigeon et al., 2001; Gehrke et al., 2003; Nemeth et al., 2003) .

Methods

Control reagents and siRNA duplexes Control reagents and siRNA were obtained from Dharmacon (Lafayette, CO). Predesigned Standard si*Genome* siRNA duplexes (5 nmol) were dissolved in 250 µL 1x siRNA buffer to a final concentration of 20 µM (20 pmol/µL) and stored at -20° C in single use aliquots. Duplexes 01 and 04 were tested for efficacy. Duplex 01 used at 100 nM was found to be most potent and most specific in knocking down TfR2 expression and was used in subsequent experiments.

siRNA transfection HepG2 cells were seeded at 2 x 10^4 cells/cm^2 in 24-well plates 24 hr before transfection. From time of seeding to harvesting, the culture medium contained 12.5 µM Fe_2Tf in order to increase TfR2 protein level and thereby test the effectiveness of the siRNA procedure. Medium was refreshed just prior to transfection. For a single transfection, 50 pmol (5 µL of 20 µM stock) siRNA, was mixed with 50 µL Opti-MEM and 2.5 µL Oligofectamine (Invitrogen) was mixed with 10 µL Opti-MEM and added to 0.5 mL Opti-MEM to a final concentration of 100 nM. All treatments were performed in triplicate and reaction volumes were scaled appropriately. Mixtures were incubated 5 min at RT, combined, incubated an additional 20 min at RT, and added dropwise to cells. Medium was replaced 24 hr later. Cells were harvested 72 hr after transfection.

TfR2 protein expression was assessed by SDS-PAGE and western blot as described in Chapter 2 (Johnson and Enns, 2004).

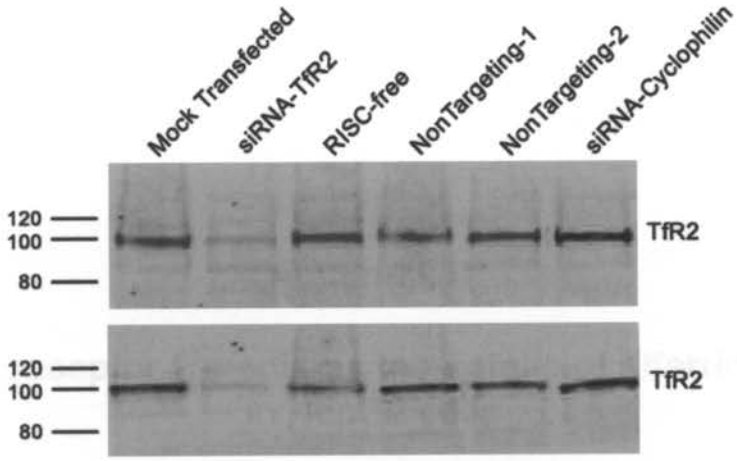

Figure 21. Downregulation of TfR2 in HepG2 cells with siRNA. Treatment of HepG2 cells with siRNA effectively reduces TfR2 protein level by approximately 90%. HepG2 cells were transfected with a short siRNA duplex targeting TfR2 (siRNA-TfR2, lane 2) as described in Methods. As control for non-specific effects, cells were transfected without duplex (Mock, lane 1); transfected with a siRNA duplex that does not interact with the RNAi machinery (RISC-free); transfected with siRNA duplexes that interact with the RNAi machinery but do not target a gene sequence (NonTargeting, lanes 4 and 5); or transfected with a siRNA duplex targeting a non-essential gene (siRNA-cyclophilin lane 6). Lysates were prepared 72 hr after transfection and assessed by SDS-PAGE and western blot. A significant reduction in TfR2 protein was only seen in cells transfected with siRNA targeting TfR2.

Appendix D

Transferrin receptor 2 mediates the uptake of diferric transferrin in HepG2 cells

Rationale

HepG2 cells express two transferrin receptors, TfR1 and TfR2, that bind Fe_2Tf with different affinities. TfR1 binds Fe_2Tf with ~1 nM affinity (Tsunoo and Sussman, 1983), endocytoses to early endosomes where iron is released for use by the cells, recycles to the cell surface, and releases apoTf. TfR2 binds Fe_2Tf with ~ 30 nM affinity (Kawabata et al., 2000; West et al., 2000), but its endocytosis has not been characterized in HepG2 cells. The extent to which TfR2 participates in Tf-mediated endocytosis in HepG2 cells was measured. We used the differential abilities of the receptors to bind Fe_2Tf and the ability of a poly IgA monoclonal antibody to downregulate TfR1 and block its interaction with Fe_2Tf (Trowbridge and Lopez, 1982; Taetle et al., 1986) to distinguish between TfR1- and TfR2-mediated Tf uptake.

Results

Pre-treatment with the 42/6 antibody reduced the uptake of 35 nM ^{125}I-Fe_2Tf by 80% (Figure 22, 35 nM+Ab, second set of bars), confirming that uptake of ^{125}I-Fe_2Tf is mediated by TfR1 at this concentration. The effectiveness of the 42/6 antibody enabled TfR2-mediated uptake of ^{125}I-Fe_2Tf to be assessed. Because the binding affinity of TfR2 for Fe_2Tf is low, washing removes Fe_2Tf bound to TfR2 at the cell surface (not shown). Thus, it was not possible to compare TfR1- and TfR2-mediated uptake of Fe_2Tf in a manner that takes into account receptor number. The absolute number of ^{125}I-Fe_2Tf molecules internalized by TfR2 and TfR1 within 6 min is approximately the same (white bars, 250 nM+Ab vs 35 nM-Ab). ^{125}I-Fe_2Tf levels are higher at steady state than during the initial uptake period when Fe_2Tf internalization is mediated by TfR1 (Figure 22, first

set of bars). By contrast, when Fe_2Tf internalization is mediated by TfR2, levels of ^{125}I-Fe_2Tf are the same after 6 and 30 min incubations (Figure 22, last set of bars).

Conclusions

The results indicate that TfR2 does mediate Fe_2Tf uptake in HepG2 cells. Downregulation of TfR1 by 80 - 90% inhibits 80% of Tf uptake at 35 nM, but only 60% of Tf uptake at 250 nM. The higher concentration of Tf required to observe TfR2-mediated uptake is consistent with previous studies reporting that TfR2 has a ~30-fold lower affinity for Fe_2Tf than does TfR1 (Kawabata et al., 2000; West et al., 2000).

Methods

^{125}I-Fe_2Tf uptake experiments HepG2 cells were seeded at 5.0 x 10^4 cells/cm^2 in six-well plates two days prior to the experiment. One set of cells, consisting of four plates with five wells seeded in each, was untreated; a second equivalent set of cells was treated with 25 µg/mL 42/6 anti-TfR1 antibody for 4 hr prior to uptakes. All subsequent media used with the second set of cells included 10 µg/mL 42/6 antibody. Cells were washed twice with serum-free MEM and incubated for 15 min at 37° C at 5% CO_2. Medium was then replaced with serum-free MEM supplemented with 35 nM or 250 nM ^{125}I-Fe_2Tf with (medium NS, 2 wells) or without (medium S, 3 wells) 12.5 µM Fe_2Tf. Cell were incubated at 37° C at 5% CO_2 for 6 min or 30 min to measure the initial rate of uptake or the steady-state level of Tf, respectively. Cells were placed on ice, washed for 2 min with 3 mL acid buffer (0.2 N acetic acid, 0.2 M NaCl) to remove surface-bound Fe_2Tf, washed four times with 2 mL final wash buffer (150 mM NaCl, 1 mM $CaCl_2$, 5 mM KCl, 1 mM KCl_2, and 200 mM HEPES, pH 7.4), collected in 1 mL solubilization buffer

(0.1 N NaOH, 0.1% Triton X-100), and transfered to plastic tubes. A second wash with 0.5 mL solubilization buffer was added to first. Counts, indicative of intracellular ^{125}I-Fe_2Tf levels, were measured with a γ-counter. Counts from wells incubated in medium NS were subtracted from counts from wells incubated in medium S to determine the specific binding.

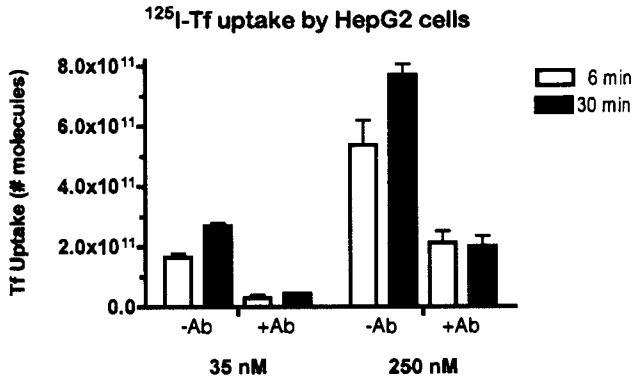

Figure 22. Internalization of diferric transferrin by TfR1 and TfR2 in HepG2 cells. Cell were incubated with 35 nM ^{125}I-Fe_2Tf (35 nM-Ab) to measure Tf binding to TfR1 or with 250 nM ^{125}I-Fe_2Tf to measure Tf binding to TfR1 and TfR2 (250 nM-Ab). To measure Tf binding to TfR2, cells were pre-incubated with 25 µg/mL 42/6 antibody (250 nM+Ab) for 4 hr to downregulate TfR1 and block ^{125}I-Fe_2Tf binding to TfR1 then incubated with 250 nM ^{125}I-Fe_2Tf. Incubations for 6 min (white bars) reflect ^{125}I-Fe_2Tf uptake (endocytosis), whereas incubations for 30 min (black bars) reflect steady state levels of ^{125}I-Fe_2Tf (endocytosis and exocytosis). Graph shows results from three separate experiments. Treatment with 42/6 effectively blocks ^{125}I-Fe_2Tf uptake by TfR1 (35 nM+Ab, second set of bars), indicating that uptake of 250 nM ^{125}I-Fe_2Tf in the presence of 42/6 antibody (250nM+Ab, last set of bars) is mediated predominantly by TfR2. TfR2 internalizes approximately the same absolute amount of ^{125}I-Fe_2Tf as TfR1 (white bars, 250 nM+Ab vs 35nM-Ab). Intracellular levels of ^{125}I-Fe_2Tf mediated by TfR2 uptake do not increase from 6 to 30 min as do those mediated by TfR1 uptake (first set of bars vs. last set of bars).

Appendix E

The endocytic pathway of transferrin receptor 2 is saturated in Hep3B/TfR2WT cells

Rationale

Hep3B/TfR2WT cells have a higher proportion of TfR2 at the cell surface (50%) than do HepG2 cells (30%) that express much less TfR2. This suggests that the higher level of TfR2 expression has saturated the endocytic machinery that mediates TfR2 internalization. To test this, we measured the rate of TfR2 internalization in Hep3B/TfR2 WT cells that were untreated or treated with Fe_2Tf. Fe_2Tf increases the expression of both surface and intracellular TfR2 proportionally (Figure 12). If the endocytic machinery is not saturated, a 3-fold increase in TfR2 expression should correlate with a similar 3-fold increase in the amount of TfR2 internalized.

Results

To measure the effect of Fe_2Tf on TfR2 internalization we used iodinated anti-TfR2 monoclonal antibody (^{125}I-mAb) to label TfR2. Use of ^{125}I-mAb also enabled us to distinguish TfR2 from TfR1 in hepatoma cells that express both receptors.

The affinity of ^{125}I-mAb for TfR2 was first measured by incubating Hep3B/ TfR2WT cells with 0 - 3 nM ^{125}I-mAb on ice for 90 minutes in the presence or absence of excess unlabeled 9F81C11 antibody. Specific binding was readily detectable (Figure 23A). Binding of ^{125}I-mAb was linear over this concentration range (Figure 23B) . Since titration to higher concentrations of ^{125}I-mAb was unfeasible, a competitive binding assay was used to determine the affinity of the 9F81C11 antibody for TfR2. Titrating 0 - 256 nM unlabeled Ab against 0.9 nM ^{125}I-mAb and fitting the data to a one-site competition model yielded an EC_{50} of 15 nM for the interaction of 9F81C11 antibody with TfR2 (Figure 23C). In subsequent experiments, cells were incubated with 90 nM

antibody, consisting of 9 nM ^{125}I-Ab and 81 nM unlabeled Ab (^{125}I-mAb/mAb), to saturate binding.

The effect of Fe_2Tf on ^{125}I-mAb/mAb binding was next assessed to ensure that Tf and the 9F81C11 antibody do not bind to overlapping sites on TfR2. Hep3B/TfR2WT cells were incubated with 90 nM ^{125}I-mAb/mAb in the absence or presence of 12.5 μM Fe_2Tf for 90 min on ice. The presence of Fe_2Tf did not significantly alter the binding of ^{125}I-mAb/mAb (Figure 23D), indicating that Tf does not interfere with the binding of 9F81C11 antibody to TfR2.

To measure the effect of TfR2 number on the rate of TfR2 internalization, Hep3B/TfR2WT cells were incubated without or with 12.5 μM Fe_2Tf, 24 hrs prior to and throughout the uptake experiment. Internalization was measured at 2, 3, 4, and 5 min. Uptake increased linearly over this time course, indicating that exocytosis was not yet occuring. The rate of TfR2 endocytosis per cell was similar in untreated cells and Tf-treated cells when Tf antibody uptake was assessed as nanograms of antibody internalized (Figure 23E). However, when antibody uptake was assessed relative to the number of binding sites, the rate of TfR2 endocytosis per surface TfR2 was slower in Tf treated cells than in untreated cells (Figure 23F).

Conclusions

The endocytosis of TfR2 can be saturated in Hep3B cells by treating cells with Fe_2Tf to increase TfR2 number. In uptake experiments the number of binding sites for antibody is higher in treated cells than in untreated cells. Consistently, Tf-treated cells internalize more antibody that untreated cells over the course of the experiment (Figure 23E). If endocytosis occurs efficiently, without saturation, and at the same rate in

treated and untreated cells, Tf-treated cells expressing more TfR2 (Figure 13A) should take up more antibody throughout the experiment. The relative rates of internalization, taking into account cell surface receptor number, should be the same. In this experiment, however, the absolute rate of internalization per cell is the same in treated and untreated cells (Figure 23E), whereas the relative rate of internalization per surface TfR2 is slower in treated cells. The results suggest that the expression level of TfR2 in Hep3B/TfR2WT cells has saturated the endocytic machinery such that internalization cannot occur in proportion to receptor number. This is consistent with the higher proportion of overexpressed TfR2 at the surface in Hep3B/TfR2WT cells (~50%, Figure 13) relative to endogenous TfR2 at the surface of HepG2 cells (~30%, Figure 12). We cannot completely exclude the possibility that treatment with Fe_2Tf slows the rate of TfR2 internalization. However, the steady state distribution of TfR2 between the cell surface and intracellular compartments is the same in treated and untreated HepG2 cells (Figure 12C) that endogenously express ~100-fold fewer TfR2 than Hep3B/ TfR2WT cells. Thus, if Fe_2Tf inhibited endocytosis it would have to inhibit exocytosis to a similar extent. The effect of Fe_2Tf on TfR2 endocytic rate can be tested by measuring the rate of ^{125}mAb uptake in hepatoma cells treated or not treated with Fe_2Tf. This was attempted using HepG2 cells that express TfR2 at a much lower level. Due to the low level of TfR2, however, specific binding was not sufficiently higher than background to permit analysis. The saturation of the endocytic machinery in Hep3B/TfR2 cells precludes any assessment of the effect of Fe_2Tf on TfR2 endocytosis.

Methods

Antibody preparation The IgG fraction of the mouse anti-TfR2 9F8C11 ascites was purified using a Protein A sepharose (Zymed/Invitrogen) column. Approximately 2 mL of unpurified ascites was centrifuged 2 x 15 min at 13,000 x g and diluted 1:2 into PBS. Half the diluted antibody was loaded onto a Protein A sepharose column with a 2 mL bed volume. The column was washed with 10 mL PBS, and protein was eluted with 500 µL 1.0 M glycine, pH 3.2 into 50µL 2.0 M Tris, pH 8.0. After washing the column with 20 mL PBS, the second half of the diluted antibody was loaded and eluted. Fractions were assayed for protein by measuring the absorbance at 280 nm. Fractions 3-5 from each purification were pooled, concentrated using Microcon100 concentrators (Millipore, Billerica, MA) according to the manufacturer's instructions, and buffer-exchanged into PBS using a BioSpin column (Bio-Rad, Hercules, CA). For iodination, 100 µL of the 11.36 mg/mL purified, concentrated antibody (mAb) was used.

Antibody binding and uptake experiments Hep3B/TfR2WT cells were seeded at 3.3 x 10^4 cells/cm^2 in six-well plates one day prior to the experiment and cultured in MEM/ 10%FBS without or with 12.5 µM Fe_2Tf, as indicated. Cells were washed twice with wash medium (MEM with 25 mM HEPES, pH 7.4). For all experiments three wells and two wells of a six well plate were incubated in medium S (wash medium + indicated concentration of ^{125}I-mAb or ^{125}I-m/mAb) or medium NS (medium S + indicated concentration of cold antibody), respectively. For uptake experiments, plates were incubated at 37° C and 5% CO_2, then placed on ice. Wells were washed with 2 mL acid buffer (0.2 N acetic acid, 0.2 M NaCl) for 2 min to remove surface-bound ^{125}I-mAb/ mAb and then washed four times with 2 mL final wash buffer (150 mM NaCl, 1 mM

$CaCl_2$, 5 mM KCl, 1 mM KCl_2, and 200 mM HEPES, pH 7.4). Cells were solubilized in 1 mL solubilization buffer (0.1 N NaOH, 0.1% Triton X-100). For binding experiments, plates were incubated on ice for 90 minutes. Wells were washed four times with final wash buffer and solubilized in solubilization buffer. For uptake and binding experiments, counts for each well were measured on a γ-counter. To determine the specific binding, counts from wells incubated in medium NS were subtracted from those incubated in medium S.

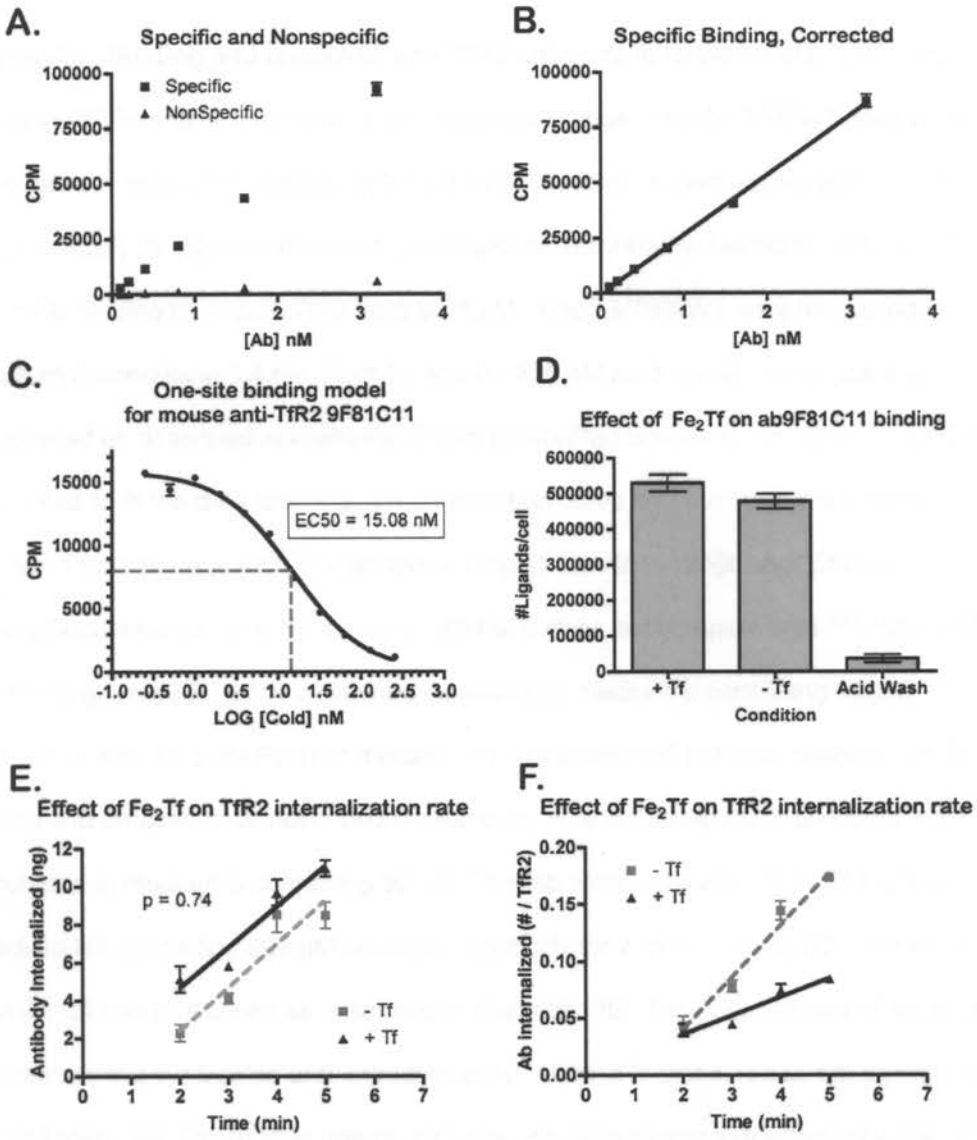

Figure 23. Binding and uptake of anti-TfR2 antibody in HepG2 cells.

Figure 23. Binding and uptake of anti-TfR2 antibody in HepG2 cells. (A and B) Binding of ^{125}I-mAb is linear over a low nanomolar range. Hep3B/TfR2WT cells were incubated in medium S containing 0.1 - 3.2 nM ^{125}I-mAb or medium NS with 300 nM cold antibody for 90 min onice and processed as described in Methods. (C) The EC_{50} for ^{125}I-mAb binding to Hep3B/TfR2 cells is 15 nM. Hep3B/TfR2WT were incubated in medium S containing 0.9 nM ^{125}I-mAb and 0 - 256 nM mAb for 90 min on ice and processed as described in Methods. Prism (GraphPad Software, Inc., San Diego, CA) was used to fit the data to a one-site competition curve and calculate the binding constant from the equation Y = Bottom + (Top-Bottom)/(1+10^(X-LogEC50)) where X=log(Concentration) and Y = binding. (D) Fe_2Tf does not compete with ^{125}I-mAb/mAb for binding. Hep3B/TfR2W cells were incubated in medium S containing 90 µM ^{125}I-mAb without or with 12.5 µM Fe_2Tf or medium NS containing 900 µM cold antibody for 90 min on ice and processed as described in Methods. (E and F) Hep3B/TfR2W cells were incubated in medium S containing 90 µM ^{125}I-mAb without or with 12.5 µM Fe_2Tf or medium NS containing 900 µM unlabeled antibody for 2 -5 minutes at 37° C or for 90 min on ice and processed as described in Methods. (E) The absolute rate of antibody uptake is similar in treated and untreated cells. Uptake is measured as nanograms of ^{125}I-mAb/Ab. (F) The relative rate of antibody uptake is slower in treated cells than in untreated cells. Uptake is measured relative to number of cell surface TfR2 molecules.

Appendix F

Colocalization of TfR2 with AP-3

Rationale

AP-3 is an adaptor protein complex that interacts with YXXØ-type tyrosine-based motifs in membrane proteins. Through its interactions with YXXØ motifs and clathrin, AP-3 recruits membrane protein into clathrin-coated pits for transport between endosomes and lysosome/lysosome-like compartments. Because TfR2 is degraded in the lysosome, AP-3 might mediate its trafficking to this compartment. If so, stabilization of TfR2 by Fe_2Tf might decrease its colocalization with AP-3. We assessed the colocalization of TfR2 with AP-3 and determined whether treatment with Fe_2Tf affected the extent of colocalization.

Results

A small fraction of TfR2 colocalized with AP-3 in the perinuclear region of cells (Figure 24). Treatment with Fe_2Tf did not alter the fraction of TfR2 that colocalized with AP-3.

Conclusions

A decrease in the association of TfR2 with AP-3-positive compartments does not appear to accompany the redirection of TfR2 to a recycling compartment. Our results do not rule out the possibility that AP-3 may play a role in TfR2 trafficking. Determining whether AP-3 interacts with TfR2 and whether AP-3 deletion alters TfR2 localization will provide additional insight.

Methods

Immunofluorescence The anti-δ SA4 supernatant recognizing the δ subunit of AP-3, developed by Andrew A. Peden, was obtained from the Developmental Studies Hybridoma Bank (Iowa City, Iowa) under the auspices of the NICHD. The colocalization of TfR2 with AP-3 was assessed by double-labeling immunofluorescent detection as described in Chapter 3 (Johnson et al., 2006). AP-3 was detected with a mouse monoclonal antibody (1:100). TfR2 was detected using the purified IgG fraction of the 16637 rabbit anti-TfR2 polyclonal anti-serum (8 µg/mL).

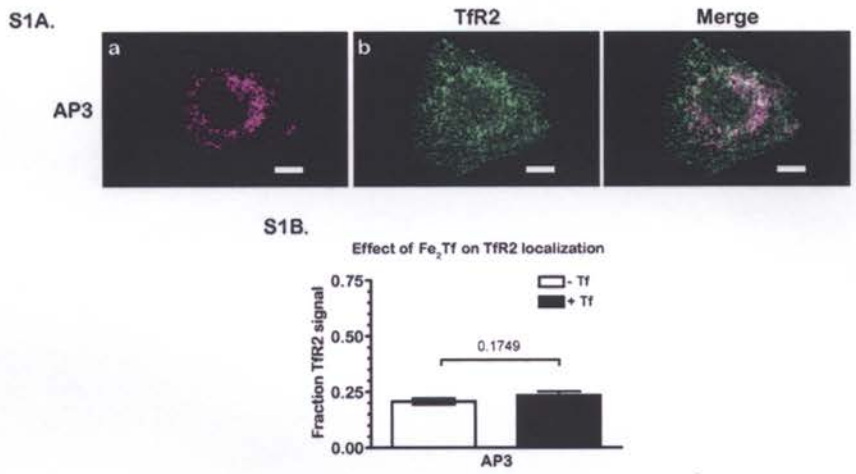

Figure 24. Colocalization of TfR2 with AP-3. (A) A small fraction of TfR2 colocalizes with AP-3. HepG2 cells were seeded at 6.25 x 10^3 cells/cm^2 on poly-L-lysine treated glass coverslips and cultured for 2 days prior to fixation, permeabilization, and labeling as described in Chapter 3. AP-3 is shown in magenta (a), TfR2 is shown in green (b), and colocalization is shown in white (c). (B) Fe_2Tf does not alter the fraction of TfR2 colocalizing with AP-3. Prior to the experiment, HepG2 cells were incubated for 48 hr ± 25μM Fe_2Tf. As in Figure 11, cells were double-labeled and visualized by scanning confocal microscopy. The effect of Fe_2Tf on the subcellular localization of TfR2 was assessed by quantitative colocalization analysis. The fraction of TfR2 signal colocalizing with AP-3 signal was analyzed in 40 images per condition acquired in 3 independent experiments. Data was evaluated by Student's t-test.